Journal of Architectural Research and Development

Honorary Editor-in-Chief

Pooya Lotfabadi

Eastern Mediterranean University, TRNC

Editors-in-Chief

Paolo Beccarelli

The University of Nottingham, UK

Rocio Maira Vidal

Spanish National Research Council, Spain

BIO-BYWORD SCIENTIFIC PUBLISHING PTY LTD
(619 649 400)
Level 10
50 Clarence Street
SYDNEY NSW 2000
Copyright © 2026. Bio-Byword Scientific Publishing Pty Ltd.
Complimentary Copy

ISSN (ONLINE): 2208-3537
ISSN (PRINT): 2208-3529

Journal of Architectural Research and Development

Focus and Scope

Journal of Architectural Research and Development is an international peer-reviewed and open access journal which is devoted to establishing a bridge between theory and practice in the fields of architectural and design research, urban planning and built environment research.

Topics covered but not limited to:

- Architectural design
- Architectural technology, including new technologies and energy saving technologies
- Architectural practice
- Urban planning
- Impacts of architecture on environment

About Publisher

Bio-Byword Scientific Publishing is a fast-growing, peer-reviewed and open access journal publisher, which is located in Sydney, Australia. As a dependable and credible corporation, it promotes and serves a broad range of subject areas for the benefit of humanity. By informing and educating a global community of scholars, practitioners, researchers and students, it endeavors to be the world's leading independent academic and professional publisher. To realize it, it keeps creative and innovative to meet the range of the authors' needs and publish the best of their work.

By cooperating with University of Sydney, University of New South Wales and other world-famous universities, Bio-Byword Scientific Publishing has established a huge publishing system based on hundreds of academic programs, and with a variety of journals in the subjects of medicine, construction, education and electronics.

Publisher Headquarter

BIO-BYWORD SCIENTIFIC PUBLISHING PTY LTD
Level 10
50 Clarence Street
Sydney NSW 2000
Website: www.bbwpublisher.com
Email: info@bbwpublisher.com

2026, Volume 10, Issue 5

Table of Contents

1 **Research on Compliance Risk Control and Optimization Strategies for the Whole-Process Bidding and Procurement of Road, Bridge and Tunnel Inspection Projects**
Zhou Zhang, Zonglin Zhou

8 **Research on AI-driven Intelligent Evaluation Model for the Renovation of Old Residential Communities**
Hongwei Zhu, Na Wang, Yanchao Wen, Huanghua Deng, Rui Hu, Hao Huang

18 **Teaching and Study of Artificial Intelligence-Driven Regional Architectural Design Courses**
Ding Ding, Ling Wang

25 **Research on Energy-Saving Structure Optimization and Carbon Reduction Technology of Building Doors and Windows in Cold Regions**
Meng Zhang

33 **Experimental Study on Dynamic Mechanical Properties of Layered Rock Under Cyclic Impact Loading**
Wenxin Jia, Yian Ma, Chong Xu, Jiaqi Guo

44 **Sensory Reconstruction Design Using Local Materials in Urban Renewal: A Case Study of the Reuse of Waste Bricks and Rubble in the Deji Alley Urban Renewal Project in Ningbo**
Ningyan Hu, Yuan Xiong

56 **Research on Subway Tunnel Construction Monitoring Technology for Complex Urban Environments**
Can Chen, Xi Ni

64 **Research on the Design of Central Median Opening During Expressway Reconstruction and Expansion**
Miaoqian Zhou, Mengdie Liu

72 **Study on Seepage and Deformation Responses during Tunnel Excavation and the Influence of Support Parameters**
Xizhen Wang

82 Soundscape Evaluation and Optimization Strategies for an Urban Riverside Wetland Park in Arid Northwest China: A Case Study of Yintan Wetland Park, Lanzhou
Yang Chao

92 Soundscape Creation of the Lanzhou Yellow River Waterwheel Garden from the Perspective of Historical Soundscape Restoration
Yichao Sun

Journal of Architectural Research and Development, 2026, Volume 10, Issue 5
https://bbwpublisher.com/journal/JARD
Online ISSN: 2208-3537
Print ISSN: 2208-3529

Research on Compliance Risk Control and Optimization Strategies for the Whole-Process Bidding and Procurement of Road, Bridge and Tunnel Inspection Projects

Zhou Zhang, Zonglin Zhou*

China Merchants Chongqing Testing Center for Highway Engineering Co., Ltd., Chongqing 400067, China

****Author to whom correspondence should be addressed.***

Copyright: © 2026 Author(s). This is an open-access article distributed under the terms of the Creative Commons Attribution License (CC BY 4.0), permitting distribution and reproduction in any medium, provided the original work is cited.

Abstract: Road, bridge, and tunnel inspection projects are critical to the quality and safety of transportation infrastructure. To ensure the effective implementation of inspection work, enterprises generally adopt bidding and procurement to select qualified and efficient inspection service providers, thereby reasonably controlling the procurement quality of engineering inspection services while improving the efficiency of stateowned assets. Considering the current bidding and procurement of road, bridge, and tunnel inspection projects, these processes are characterized by strong professionalism, high technical evaluation requirements, and dynamic performance management. Traditional risk supervision mechanisms can no longer meet the wholeprocess control requirements for the procurement of such inspection projects. Accordingly, this paper focuses on summarizing risk issues from four dimensions—preliminary preparation, announcement and bidding document issuance, bid opening and evaluation, and contract performance—and proposes compliance risk optimization measures, aiming to provide a reference for the highquality development of road, bridge and tunnel projects.

Keywords: Road, bridge and tunnel inspection projects; Bidding and procurement; Whole process; Compliance risk; Intelligent risk control

Online publication: October 28, 2026

1. Introduction

Under the influence of the strategy of building a transportation powerhouse, the number and scale of road, bridge and tunnel projects in China have shown a significant growth trend. In addition, with the rapid annual increase in transportation pressure, the state's supervision of transportation infrastructure construction has become noticeably stricter. This has greatly enhanced the emphasis of roadbridgetunnel construction

enterprises on engineering inspection, prompting them to abandon traditional inspection mechanisms and adopt bidding and procurement for inspection projects, engaging more professional third parties to provide project inspection services [1]. However, the implementation of bidding and procurement for road, bridge, and tunnel inspection projects still faces numerous compliance risks, which seriously constrain the safe and efficient operation of the procurement procedures. Therefore, construction enterprises should take the existing bidding and procurement risks as a reference, optimize the risk control mechanism, and safeguard the safety red line of transportation projects.

2. Characteristics of bidding and procurement for road, bridge and tunnel inspection projects

Bidding and procurement for road, bridge and tunnel inspection projects falls under service procurement and differs significantly from traditional procurement of engineering materials. First, the procurement subject matter is highly specialized. For example, roadbridgetunnel inspection includes safety testing and nondestructive quality inspection of structures, both of which demand extremely high levels of professional expertise from operators and precision from testing equipment. At the same time, the subject matter of inspection bidding is unique in that it does not take a visualizable physical form but is presented in the form of reports. Consequently, it is difficult for supervisory personnel to accurately quantify and evaluate the completion status of the subject matter, which may lead to a loss of control in supervision. Second, fragmentation is evident in the bidding and procurement of inspection projects [2]. Different project types—such as new construction, maintenance, and expansion—have different inspection requirements and standards, making it impossible to develop a standardized procurement template. Moreover, largescale inspection projects involve substantial volumes and numerous inspection items, necessitating fragmented, phased, and tiered implementation, which increases the procurement burden. Some enterprises may streamline procedures for convenience, thereby exposing themselves to compliance risks. Third, the bid evaluation system is complex. Compared with other engineering procurement tenders, inspection project bidding requires evaluation from multiple dimensions such as price, technical capability, and qualifications, making the evaluation process more intricate and demanding greater expertise from the evaluation experts [3]. However, the technical and qualification review dimensions include nonquantifiable evaluation indicators that are susceptible to subjective influence, potentially leading to improper evaluation practices. Fourth, contract performance management is challenging. In roadbridgetunnel construction inspections, some inspection projects have long implementation cycles, and construction progress or techniques may be adjusted during the process, requiring corresponding adjustments to the inspection plan. If a static contract management approach is adopted, this may result in inadequate control.

3. Compliance risk identification in the wholeprocess tendering and procurement of roadbridgetunnel inspection projects

3.1. Preliminary preparation risks

Inadequate risk control during the preliminary preparation phase of tendering and procurement for roadbridgetunnel (RBT) inspection projects can easily lead to massive and continuous outbreaks of risks in subsequent stages, thereby undermining the effectiveness of risk prevention and control. The compliance

risks at this stage are relatively complex. First, there is information omission in the procurement demand survey. The procurement information survey serves as the core reference for the preparation of tendering and procurement documents; if the information is incomplete, it will inevitably affect the integrity and accuracy of document preparation, resulting in a mismatch between the documented requirements and the actual procurement needs [4]. Second, the procurement method may be noncompliant. The most common risk issue is that the document preparers arbitrarily alter the procurement process, leading to the omission of certain critical review steps, which in turn prevents some noncompliant issues from being identified and rectified in a timely manner. Third, the tender documents may not meet the preparation requirements. The preparation of tender documents has clear standards, and the rights and obligations of all parties must be specified in detail and with precision. If the document preparation fails to define the division of responsibilities as required clearly, it will give rise to subsequent disputes and buckpassing.

3.2. Announcement and issuance risks

The announcement and issuance phase is a critical link in ensuring openness and fairness in the tendering and procurement of RBT inspection projects. Improper handling at this stage can trigger numerous risks. First, the announcement may be nonstandard. For example, the platform, content, or duration of the announcement for some projects may not comply with the standards, thereby affecting bidders' comprehensive and accurate access to tender information and disrupting the tendering market. Second, the prequalification review of the announcement may not be rigorous. In RBT inspection projects, the procuring entity's prequalification process may be oversimplified, failing to conduct a comprehensive review of the enterprise's qualifications, performance, credit status, etc., thus allowing noncompliant enterprises to enter the bidding scope and potentially giving rise to subsequent inspection risks [5]. At the same time, there may be covert manipulation during the review process, thereby undermining the fairness of the tendering process. Third, the clarification and addendum procedures within the announcement process may be unreasonably designed. If the clarification mechanism of the project's tendering and procurement agency is unfair, it can lead to asymmetric bidding information among bidders, which is inequitable. In addition, improper publication of addendum documents, resulting in frequent changes to the scope of services and technical standards, can easily cause compliance disputes.

3.3. Bid opening, evaluation, and review risks

Bid opening, evaluation, and review are key phases throughout the tendering and procurement process. The compliance risks at this stage are mainly reflected in inadequate process control and integrity issues. First, inadequate control over the bid opening process—leading to superficial registration, inspection, and supervision of bid documents—may result in the loss or substitution of bid documents and consequently cause bid failure. Second, insufficient competency of the bid evaluation experts may affect the quality of evaluation and trigger compliance risks. For instance, RBT inspection projects are highly specialized; if the evaluation experts are not proficient in the project's technical aspects, the accuracy of their evaluation of bid documents will be compromised [6]. Moreover, some experts may face integrity challenges during the evaluation process; once they fail to uphold professional ethics, integrity risks may arise. Finally, loopholes in the implementation of evaluation criteria can give rise to compliance risks. If evaluators arbitrarily change the evaluation criteria during the performance of their duties, or fail to review abnormally low-priced bid documents promptly, this may breed the risk of malicious lowprice bidding, leading the winning bidder to

lower service standards to increase profits during subsequent service delivery, thereby compromising the quality of the inspection project.

3.4. Contract performance risks

In the tendering and procurement of RBT inspection projects, the contract performance phase is prone to compliance risk outbreaks, as specifically manifested in the following two aspects: First, there is a serious lack of awareness among both contracting parties regarding contract signing control. For example, if the contract signing time limit exceeds the compliance scope but the parties fail to negotiate on this issue, the contract may subsequently become invalid. Alternatively, there may be arbitrary modifications to the technical standards, payment agreements, and other clauses of the tender documents during contract signing, which severely weakens the binding force of the contract on both parties and may lead to the risk of noncompliant changes. Second, there are supervisory loopholes during contract performance. Contract performance is not merely a unilateral execution of contract terms by the winning bidder; the tendering company must also participate in supervision throughout the process. The tendering party may establish a dedicated contract performance supervision team to carry out oversight in parallel with the inspection unit, focusing on the inspection unit's inspection items, methods, personnel qualifications, inspection equipment, and other dimensions throughout the process, so as to avoid noncompliant operational risks during inspection.

4. Countermeasures for optimizing compliance risk management in the wholeprocess tendering and procurement of RBT inspection projects

4.1. Improving the compliance management system

The key to controlling compliance risks throughout the wholeprocess tendering and procurement of RBT inspection projects lies in relying on a specialized compliance management system to address process and standard loopholes in traditional inspection management, ensuring the compliant implementation of the entire tendering and procurement process. First, optimize the industryspecific procurement management mechanism [7]. Construction enterprises may, in accordance with the Tendering and Bidding Law of the People's Republic of China, the Regulations for the Implementation of the Tendering and Bidding Law of the People's Republic of China, the Guidelines for Fulfilling the Primary Responsibilities of Tenderers, and other relevant laws, regulations, and industry rules, select an appropriate procurement method based on project scale and requirements, formulate standardized evaluation rules, and ensure their proper implementation, thereby effectively avoiding the risk of noncompliant procurement. Second, establish a "technology + compliance + legal affairs" tripartite integrated audit system. This system introduces technical departments into compliance procurement risk prevention and control, enabling joint review of tender documents from multiple dimensions—technical, legal, and compliance—to ensure the precision and comprehensiveness of compliance control, prevent ambiguous rights and responsibilities in control provisions, and effectively eliminate hidden noncompliance risks. Third, establish a comprehensive accountability system. The system should clearly define the authority, responsibilities, and compliance standards of all parties, including evaluators, construction entities, and agencies, and compile these into a task checklist. Designate the handling officers and approving officers as primary responsible parties; once any noncompliant issue occurs, accountability can be promptly assigned to the primary responsible parties, thereby eliminating compliance risks such as inadequate performance and noncompliant procurement.

4.2. Refining standardized wholeprocess control

During project tendering and procurement, a wholeprocess closedloop management mechanism should be adopted to standardize the procurement procedures. First, strengthen the optimization of the preliminary procurement process [8]. Before procurement and tendering commence, staff should conduct a comprehensive and indepth survey of procurement needs to ensure information completeness. At the same time, during document preparation and procurement approval, procurement procedures and approval standards should be established based on the specific project circumstances, so as to ensure that the inspection unit's qualifications and technical standards meet the procurement requirements. In addition, establish a graded approval system that, through multiple layers of review and procedural regulation, builds a safety defense line from the very beginning, effectively blocking loopholes for noncompliant operations. Second, reinforce announcement issuance and qualification review. Announcement issuance must be conducted on statutory media platforms, with the publication period meeting legal requirements and the content conforming to legal and industry provisions, so as to ensure the symmetry of procurement information and the fairness of procurement tendering. Moreover, enterprise review should cover a comprehensive scope, including corporate qualifications, equipment performance, credit records, personnel qualifications, etc., and a uniform review standard should be applied to all enterprises to avoid issues such as qualification namelending and covert manipulation that undermine market fairness. Third, during bid opening, evaluation, and review, a standardized onsite management mechanism should be developed to ensure that each step—including bid document inspection, information disclosure, and confirmation of objections—is guided by clear procedural norms, and that staff keep thorough records of all work activities. At the same time, to ensure the professionalism of evaluation experts, enterprises or their entrusted agencies should establish an expert database, comprehensively collect expert information, and improve the alignment between experts and the evaluation work. More importantly, uniform evaluation and scoring standards should be adopted during review to prevent inconsistencies that compromise the fairness of tendering and procurement. Meanwhile, optimize the clarification and addendum process to safeguard the impartiality of evaluation fully. Finally, contract performance control should be optimized from the perspectives of template standardization and clear rights and responsibilities [9]. Strictly investigate issues such as dual contracts and unauthorized modification of clauses. In addition, during contract performance, a dedicated followup review team should be established to conduct regular or unscheduled inspections of equipment performance, process implementation, personnel attendance, and other aspects.

4.3. Establishing a sound wholeprocess supervision and assessment mechanism

The problem of "emphasizing tendering while neglecting performance" remains prevalent in the tendering and procurement of RBT inspection projects, which severely affects the comprehensive and indepth implementation of risk prevention and control measures for such projects. Accordingly, construction enterprises need to place greater emphasis on the performance of tendering contracts and establish a wholeprocess supervision and assessment mechanism covering pre, during, and postcontract stages to strengthen performance oversight. First, the management department should participate in precontract signing control from the very beginning, focusing on the review of procurement and tender documents to ensure their compliance and completeness, thereby strengthening source control of compliance risks. Second, the management department should support the rigorous and compliant implementation of

tendering and procurement work through professional teams. Specifically, based on the characteristics and requirements of each procurement and tendering project, select professional supervisory personnel to form a dedicated supervision team, which is responsible for continuously following up and overseeing the contract performance process and maintaining visual and written records of each performance phase to ensure traceability [10]. Finally, establish postperformance accountability and evaluation systems. The completion of contract performance does not signify the end of risk control work; management personnel should conduct a comprehensive review of the entire contract performance process, archive the review results in a resource database, and simultaneously include the cooperative enterprise's performance, service quality, creditworthiness, and other information in the database list. This control approach facilitates stricter screening of future partner qualifications.

4.4. Building an industrywide intelligent risk control system

Given the numerous shortcomings of manual control in the tendering and procurement of RBT inspection projects, enterprises may adopt intelligent risk control platforms to establish a fully automated earlywarning and traceability mechanism, with platform modules set up as referenced in **Table 1**. First, construct an online tendering and procurement review platform, creating online review modules for each phase of the procurement process, so that relevant departments and personnel can operate through the online platform to complete the review. This model can overcome geographical and time constraints, enabling multidepartmental simultaneous review and supervision, thereby ensuring comprehensive and timely implementation of oversight. In addition, the construction of an online review mechanism allows for full recording of all work implementation processes, and any modifications can be traced, which not only facilitates the traceability of each work phase but also effectively prevents the risk of offline arbitrary modifications to document clauses. Second, adopt intelligent risk control earlywarning mechanisms to identify potential risks in a timely manner. Based on the project characteristics, enterprises may set reasonable earlywarning thresholds in the warning module, enabling the system to quickly identify risks by comparing contract performance status against the earlywarning standards, and promptly send alert notifications to supervisory personnel, thereby enhancing the efficiency of risk warning.

Table 1. Technical parameter table of the intelligent risk control system for roadbridgetunnel inspection projects

System module	Functional indicator	Technical parameter
Online review platform	Multi-department collaborative review	Review coverage 100%, traceability retention 100%
	Process tracing	Retention period ≥ 5 years
Risk warning module	Anomaly identification	Warning time ≤ 2 hours
	Risk level classification	Threelevel warning

5. Conclusion

In summary, compliance prevention and control in the tender and procurement of highway, bridge, and tunnel inspection projects is a critical link for effectively mitigating procurement risks. However, given the current status of such procurement activities, numerous hidden compliance risks exist throughout the entire procurement process, undermining regulatory compliance and failing to meet the demands of procurement

control. Through the optimization of risk prevention and control strategies, it is possible to build a solid defense line via institutional frameworks, standardize operational behaviors through streamlined procedures, ensure implementation via closedloop management, and strengthen supervision using intelligent technologies. This enables precise identification of compliance risks, eliminates potential hazards at the source, and ensures order in the inspectiontender procurement market. In the future, transportation infrastructure entities should, from the perspective of smart and digital transformation, develop riskcontrol models to enhance the efficiency and quality of risk management, thereby ensuring the safety of highway, bridge, and tunnel projects.

Disclosure statement

The authors declare no conflict of interest.

References

[1] Lian B, 2024, Prevention and Handling of Bidding and Procurement Risks in State-Owned Enterprises. China Market, 2024(4): 84–87.

[2] Pei J, 2024, Discussion on Risks and Optimization Strategies of Construction Project Bidding and Procurement. North-South Bridge, 2024(10): 124–126.

[3] Li S, 2024, Risk Identification and Response Strategies for Construction Project Bidding and Procurement. Construction and Decoration, 2024(1): 129–131.

[4] Shang H, 2024, Construction of Risk Prevention and Supervision System for Bidding and Procurement. Bidding and Procurement Management, 2024(12): 19–21.

[5] Gao Y, 2024, Analysis of Risk Control and Supervision Mechanisms for State-Owned Enterprise Bidding and Procurement in the Digital Age. China Science and Technology Investment, 2024(32): 98–100.

[6] Chang C, 2025, Analysis of Municipal Engineering Bidding and Procurement Risks and Optimization Strategies. China Real Estate Industry, 2025(28): 42–45.

[7] Zhang Y, 2021, Problems and Countermeasures in Bidding Management of Construction Projects in China. China Strategic Emerging Industries, 2021(40): 160–162.

[8] Luo H, 2021, Problems and Optimization Measures in Construction Project Bidding. Construction Engineering Technology and Design, 2021(18): 1574.

[9] Huang J, 2025, Cost Control and Pathway Selection for Project Bidding and Procurement Management. Shandong Transportation Science and Technology, 2025(4): 136–138.

[10] Zhao H, Wang H, 2025, Study on Quality Defects and Improvement Measures in Highway, Bridge and Tunnel Construction. China Brand and Anti-Counterfeiting, 2025(4): 238–240.

Publisher's note

Bio-Byword Scientific Publishing remains neutral with regard to jurisdictional claims in published maps and institutional affiliations.

Journal of Architectural Research and Developmentn, 2026, Volume 10, Issue 5
https://bbwpublisher.com/journal/JARD
Online ISSN: 2208-3537
Print ISSN: 2208-3529

Research on AI-driven Intelligent Evaluation Model for the Renovation of Old Residential Communities

Hongwei Zhu, Na Wang, Yanchao Wen, Huanghua Deng, Rui Hu, Hao Huang

Chongqing Institute of Engineering, Chongqing 400056, China

Copyright: © 2026 Author(s). This is an open-access article distributed under the terms of the Creative Commons Attribution License (CC BY 4.0), permitting distribution and reproduction in any medium, provided the original work is cited.

Abstract: Addressing the industry bottlenecks of low efficiency, strong subjectivity, and difficulty in integrating multi-source data in the preliminary assessment of old residential community renovations, this paper proposes a fuzzy comprehensive evaluation model based on multi-modal data fusion and AI-driven technology. The model establishes an evaluation system covering 17 indicators across seven dimensions: safety, livability, sustainability, economy, sociality, technology, and resilience. The Analytic Hierarchy Process (AHP) is used to determine indicator weights, and a multi-modal feature extraction module is designed to process image data, text data, and structured data separately. Building on this, the evaluation output is linked to renovation cost estimation, forming an integrated "evaluation-cost" output. This paper elaborates on the model's overall architecture, the construction of the indicator system and weight calculation methods, multi-source data fusion strategies, and cost association mechanisms. Typical computational examples validate the feasibility of the model process and the rationality of its decision-making logic. The results indicate that the model can effectively integrate multi-source information, output comprehensive scores and renovation grades, and provide corresponding cost range recommendations, offering an engineering-ready intelligent tool for scientific decision-making in old residential community renovations.

Keywords: Old residential community renovation; Multi-modal data fusion; Fuzzy comprehensive evaluation; AI evaluation model

Online publication: Oct 13, 2026

1. Introduction

As of 2025, there are 219,000 old residential communities built before 2000 in China, involving more than 300 million residents, with over 60% exhibiting structural safety hazards and aging infrastructure. Both the 2025 government work report and the "14th Five-Year Plan" of the Ministry of Housing and Urban-Rural Development call for accelerating renovations, with basic renovations to be implemented comprehensively, reflecting unprecedented policy urgency.

However, the preliminary assessment phase of old residential community renovations still heavily relies on traditional manual inspection methods. The current evaluation process typically requires organizing professionals to conduct building-by-building inspections and item-by-item scoring, taking 2–4 weeks per community and costing approximately 120,000 yuan. Moreover, manual judgments are highly subjective, with error rates as high as 30%. Additionally, renovation assessments of old residential communities involve various heterogeneous data types, including building structures, underground pipelines, public spaces, resident demands, and dynamic monitoring. Existing evaluation systems struggle to effectively integrate these data, often resulting in a disconnect between "physical space assessments" and "social demand assessments". In recent years, breakthroughs have been made in image recognition and natural language processing (NLP) through CNNs, Transformers, and pre-trained models, with multi-modal fusion demonstrating excellent performance in smart healthcare, autonomous driving, and other scenarios. In the construction field, there have been single-modal applications such as crack detection and engineering report classification, but a multi-modal fusion solution for comprehensive evaluation of all elements in old residential communities has yet to be developed.

This paper proposes an intelligent evaluation model for old residential community renovations based on multi-modal data fusion and fuzzy comprehensive evaluation (referred to as "the model"). The main contributions are as follows:

(1) A comprehensive evaluation indicator system for old residential community renovations is constructed, covering seven evaluation dimensions and 17 specific indicators. The Analytic Hierarchy Process (AHP) is used to allocate weights from the criterion level to the indicator level, ensuring the systemicity and quantifiability of the evaluation framework.

(2) A multi-modal feature extraction and fusion architecture tailored to old residential community scenarios is designed to process image data (building facade defect detection), text data (resident renovation demand extraction), and structured data (building age, pipeline material, and other attributes), achieving unified representation of multi-source information.

(3) A module linking evaluation results to renovation costs is established, mapping comprehensive scores and renovation grades to cost estimation ranges, providing direct reference for subsequent plan generation and fund allocation.

(4) The feasibility of the model process is validated, and its potential for engineering practice is demonstrated through the development of a prototype system and computational examples.

2. Models and methods

2.1. Overall architecture

The overall architecture of this model is illustrated in **Table 1**, encompassing four core layers: Data Acquisition Layer:

Utilizing an integrated air-space-ground data collection approach, this layer gathers multimodal data, including building facade images captured through unmanned aerial vehicle (UAV) oblique photography (with a resolution of ≤ 2 cm), building structural point clouds obtained via 3D laser scanning (with an accuracy of ± 3 mm), underground pipeline detection using ground-penetrating radar and sonar imaging, resident demand texts collected through questionnaires and community discussion platforms, and dynamic monitoring data acquired through Internet of Things (IoT) sensors.

Feature Extraction and Fusion Layer: This layer incorporates specialized feature extraction modules tailored to different data types. The visual branch employs convolutional neural networks for defect detection and classification, while the text branch utilizes pre-trained language models to extract keywords and sentiment tendencies from resident demands. The structured branch standardizes numerical values of building attributes and pipeline parameters.

Evaluation and Computation Layer: The fused feature vectors are input into a fuzzy comprehensive evaluation engine. This engine incorporates a 7-dimensional, 17-item indicator weighting system determined by the Analytic Hierarchy Process (AHP) method. It maps the evaluation values of each indicator to a unified scale using membership functions and ultimately computes sub-scores for each dimension and an overall renovation score for the residential area through weighted comprehensive calculations.

Output and Correlation Layer: Based on the comprehensive score, the renovation priority level (high/medium/low) is determined, and the score is correlated with the renovation workload. The cost estimation module outputs an estimated cost range, generating an assessment result in the form of "one report per residential area". See **Table 1**.

Table 1. System architecture diagram

User Interaction Interface (UI Layer)		
Data Management (Data Mgmt)	**Multi-source Acquisition AI Evaluation (Modeling) (Evaluate)**	**Digital Twin Decision-Making (Decision)**
	Core Business Logic Layer	
Data CRUD Module	-Data Addition, Deletion, Modification, and Retrieval - Data Validation - Dynamic Table Rendering	
AI Evaluation Engine Module	- Safety Score (Year → Aging Coefficient) - Livability Score (User-inputted Score) - Multi-dimensional Weighted Summation - Grade Determination and Recommendation of Solutions	
Backup/Export Module	- Export in JSON Format - Data Clear and Reset	
	Data Persistence Layer	
	localStorage(Browser Local Storage) Key Name: "xiaoqu_list" Format: JSON Array	

2.2. Construction of the evaluation index system

The evaluation index system serves as the framework of the model. Based on references to current national standards, relevant literature, and expert consultations, this paper sets the comprehensive evaluation of renovation needs in old residential areas as the objective layer, divides it into seven evaluation dimensions as the criterion layer, and further refines it into 17 quantifiable indicators as the indicator layer [1,2]. The structure of the evaluation index system is shown in **Table 2**.

The definitions and measurement methods for each indicator are as follows: Structural

Damage Degree (C1): AI identifies the crack width and deflection angle of load-bearing components from UAV images, combined with an aging coefficient for comprehensive assessment.

Fire Safety (C2): Statistics on the unobstructed rate of fire lanes (%), coverage rate of firefighting facilities (fire extinguishers, fire hydrants) (%), and quality inspection pass rate.

Facility Completeness (C3): Includes the coverage rate of barrier-free facilities (ramps, handrails, elevators, etc.) and the per capita area of public space (m^2/person).

Environmental Comfort (C4): Green coverage rate combined with the NDVI index and noise pollution index.

Service Convenience (C5): Based on a 15-minute living circle radius, statistics on the completeness rate of daily life facilities such as garbage collection stations, fitness plazas, and convenience stores.

Energy Efficiency (C6): Utilization rate of renewable energy and heat transfer coefficient of the building envelope.

Water Resource Recycling (C7): Installation rate of water-saving appliances (%) and coverage rate of rainwater collection systems (%).

Solid Waste Management (C8): Configuration rate of garbage classification facilities (%) and recycling rate of construction waste (%).

Cost Controllability (C9): Budget deviation degree of renovation cost per unit area (yuan/m^2).

Return on Investment (C10): Operational cost savings rate (%) and expected magnitude of property value appreciation (%).

Resident Participation (C11): Participation rate of residents in collecting opinions on renovation plans (%).

Community Cohesion (C12): Average monthly usage frequency of community public spaces (plazas, activity centers, etc.).

Cultural Continuity (C13): Preservation rate of historical features (%).

Digital Facilities (C14): Coverage rate of intelligent security systems (cameras, smoke detectors, etc.) and density of IoT sensing devices.

Intelligent Operation and Maintenance (C15): Average response time to facility failures (min).

Disaster Resilience (C16): Measured by the percentage of accumulated water drained within a specified time, reflecting drainage and flood prevention capabilities (%).

Adaptive Renovation (C17): Proportion of reserved space for capacity expansion of various pipelines (water supply, power supply, gas, communication) (%).

Table 2. Hierarchical structure diagram of the evaluation index system

Evaluation dimension	Evaluation indicator	Detailed design
(1) Safety dimension (building structural safety)	① Structural damage degree	Crack width of load-bearing components
		Material aging coefficient
		Foundation settlement rate
	② Fire safety	Unobstructed rate of fire lanes
		Coverage rate of firefighting facilities
(2) Livability dimension (quality of residential environment)	③ Facility completeness	Coverage rate of barrier-free facilities
		Per capita area of public activity spaces
	④ Environmental comfort	Greening rate
		Noise pollution index
	⑤ Service convenience	Completeness rate of facilities within a 15-minute living circle

	⑥ Energy efficiency	Heat transfer coefficient of building envelopes
		Utilization rate of renewable energy
(3) Sustainability dimension (resource utilization efficiency)	⑦ Water resource recycling	Coverage rate of rainwater collection systems
		Installation rate of water-saving appliances
	⑧ Solid waste management	Configuration rate of garbage classification facilities
		Recycling rate of construction waste
	⑨ Cost controllability	Renovation cost per unit area
(4) Economic dimension (cost-effectiveness of renovation)	⑩ Return on investment	Expected property value appreciation
		Operational and maintenance cost savings rate
	⑪ Resident participation	Participation rate in collecting opinions on renovation plans
(5) Social dimension (community governance efficacy)	⑫ Community cohesion	Usage frequency of public spaces
	⑬ Cultural continuity	Preservation rate of historical features
	⑭ Digital facilities	Coverage rate of intelligent security systems
(6) Technical dimension (level of smart technology)		Density of IoT sensing devices
	⑮ Intelligent operation and maintenance	Response time to facility failures
	⑯ Disaster resilience	Drainage and flood prevention capability
(7) Resilience dimension (risk resistance capability)		Drainage and flood prevention capability
	⑰Adaptive renovation	Reserved space for pipeline capacity expansion

2.3. Determination of weights based on AHP

The Analytic Hierarchy Process (AHP) is employed to determine the weights of indicators at each level, with the following steps [3,4]:

2.3.1. Step 1: Construct the hierarchical structure

The objective level is "Comprehensive Evaluation of Renovation Needs for Old Residential Areas (A)"; the criterion level comprises seven dimensions (Safety B1, Livability B2, Sustainability B3, Economy B4, Sociality B5, Technicality B6, Resilience B7); and the indicator level includes specific indicators (C1—C17) under each dimension.

2.3.2. Step 2: Construct the judgment matrix

Domain experts are invited to conduct pairwise importance comparisons of the seven dimensions at the criterion level using Saaty's 1–9 scale method. The constructed judgment matrix is denoted as $A = (aij)_{7\times7}$, where aij represents the relative importance of dimension i to dimension j, and satisfies the condition $aij \cdot aji = 1$.

2.3.3. Step 3: Calculate the weight vector

Calculate the geometric mean for each row of the judgment matrix:

$$g_i = \sqrt[n]{\prod_{j=1}^{n} a_{ij}}$$

Then, normalize to obtain the weights wi for each dimension:

$$w_i = \frac{g_i}{\sum_{k=1}^{n} g_k}$$

2.3.4. Step 4: Consistency check

Calculate the maximum eigenvalue λmax:

$$\lambda_{\max} = \frac{1}{n} \sum_{i=1}^{n} \frac{(Aw)_i}{w_i}$$

Calculate the Consistency Index (CI) and the Consistency Ratio (CR):

$$CI = \frac{\lambda_{\max} - n}{n - 1}$$

Look up the Random Consistency Index (RI) in **Table 3**.

Table 3. Random consistency index (RI)

Matrix order	1	2	3	4	5	6	7
RI	0	0	0.58	0.90	1.12	1.24	1.32

Calculation of Consistency Ratio (CR):

$$CR = \frac{CI}{RI}$$

When n = 7, the Random Consistency Index (RI) is 1.32. If CR < 0.1, the judgment matrix passes the consistency check; otherwise, the scale needs to be adjusted.

2.3.5. Step 5: Calculation of comprehensive weights

Repeat the above steps for the specific indicators under each dimension to calculate the weights at the indicator level. The final comprehensive weight is equal to the weight at the criterion level multiplied by the weight at the indicator level.

2.4. Multimodal feature extraction and fusion

The data sources targeted by this model can be categorized into three types:

Image modality: Images of building facades captured by unmanned aerial vehicle (UAV) oblique photography, point cloud maps generated by 3D laser scanning, etc. The overall detection mean Average Precision (mAP) of this module can reach above 0.85 on public datasets. For structural deformation analysis of point cloud data, the PointNet++ network is employed for deformation region segmentation, and offsets are extracted by comparing with design drawings.

Text modality: Open-ended opinion texts submitted by community residents through the Wenjuanxing platform and community meeting records. A Chinese pre-trained language model is used for semantic encoding to extract keywords (such as “elevator installation”, “additional parking spaces”, “pipeline replacement”, “barrier-free renovation”, etc.) and calculate sentiment polarity scores. The output consists of frequency and intensity vectors for each demand category.

Structured modality: Attribute data such as building year, structural type, building area, number of

floors, pipeline material, number of historical repairs, and settlement monitoring rate. After numerical encoding, this type of data is normalized using Min-Max normalization to unify the dimensions.

2.5. Fuzzy comprehensive evaluation and score calculation

The operation of the fuzzy comprehensive evaluation engine consists of three steps [5,6]:

Membership Degree Calculation: Set grade evaluation criteria (e.g., "excellent/good/fair/poor") for each indicator. Calculate the membership degree of each indicator for each grade based on its actual value.

Weighted Aggregation within Dimensions: According to the weights at the indicator level, perform weighted summation of the membership degree vectors of each indicator under the same dimension to obtain the grade membership degree distribution for each dimension.

Comprehensive Calculation at the Criterion Level: Multiply the membership degree matrix of the seven dimensions by the weight vector at the criterion level to obtain the final comprehensive evaluation membership degree vector. Take the weighted average and convert it to a percentage-based comprehensive score.

2.6. Evaluation-cost correlation mechanism

The evaluation-cost correlation module is one of the core features that distinguish this model from general evaluation models.

Its principle is as follows: For each renovation dimension, its score status can be mapped to a typical range of engineering renovation projects and unit cost intervals. For example:

(1) When the score of the "safety" dimension falls below the threshold, it triggers the renovation items of "structural reinforcement + pipeline replacement", and the unit area cost and its allowable fluctuation range are estimated based on building characteristics.

(2) When the score of the "livability" dimension is low, and the "age-friendly" sub-item is insufficient, it triggers the renovation items of "installation of handrails/ramps/elevators".

(3) When the score of "sustainability" is insufficient, it triggers the renovation items of "external wall insulation + energy-efficient window replacement + rainwater harvesting".

3. Example calculation and model validation

To verify the feasibility and logical rationality of this model's process, this paper conducts a simulation using a typical old residential area (built in 1985, with a 6-story brick-concrete structure, a total building area of approximately 5000 m², and 280 households) as the example object. The relevant data are constructed based on public information and typical characteristics of residential areas, aiming to test the model's full-link operation capability from data input to evaluation output and then to cost correlation.

3.1. Example setting and data input

The key input parameters for the example residential area are set as shown in **Table 4**.

Table 4. Input parameters for the example residential area

Indicator	Value	Description
Year built	1985	40+ years of building age
Structural type	Brick-concrete	No seismic columns

Facade crack rate	23%	Simulated AI recognition result
Fire protection facility coverage rate	35%	Only configured in some buildings
Barrier-free facility coverage rate	10%	Severely lacking
Green coverage rate	12%	Below the lower limit of the standard
15-minute living circle completeness rate	70%	Basic functions acceptable
Residents' demand intensity for elevator installation	0.82	NLP text analysis result
Pipeline replacement demand ratio	76%	Estimated based on pipeline material
Base cost per unit area	850 yuan/m²	Average value of similar renovation projects

3.2. Evaluation results

After inputting the aforementioned example data into the model, the scores for each dimension and the overall comprehensive score are presented in **Table 5**.

Table 5. Dimension-specific scores and comprehensive results for the example residential area

Evaluation dimension	Weight	Dimension score	Weighted contribution
Safety	0.28	48	13.44
Livability	0.22	55	12.1
Social	0.18	70	12.6
Resilience	0.15	62	9.3
Technical	0.1	65	6.5
Sustainability	0.05	40	2
Economic	0.02	78	1.56
Overall score	—	57.5	—
Renovation grade	—	High priority	Score <60

In this example, the safety dimension scored the lowest (48 points), which aligns with the actual conditions of the community, such as its early construction year, poor seismic performance of the brick-concrete structure, and a high crack rate of 23% on the building facades. The sustainability dimension also scored relatively low, reflecting the common weaknesses of old residential areas in terms of energy conservation and resource recycling.

3.3. Cost correlation output

Based on the evaluation results, the renovation priority level for this community is determined to be "high priority". The model automatically triggers cost estimates for the following renovation items [7]. See **Table 6**.

Table 6. Renovation projects and cost estimates

Renovation item	Triggering basis	Estimated unit cost (yuan/m²)	Estimated total cost (10,000 yuan)
Structural reinforcement	Safety index < 60	280–350	140–175
Comprehensive pipeline replacement	Pipeline demand rate 76%	180–220	90–110
Fire-fighting facility supplementation	Coverage rate 35%	40–55	20–27.5
Accessibility renovation + elevator installation	Coverage rate 10%, demand 0.82	200–280	100–140
Greening and sponge city renovation	Greening rate 12%	50–70	25–35
Total	—	750–975	375–487.5

The final estimated total renovation cost range for the residential area is 3.75 to 4.88 million yuan (equivalent to 750 to 975 yuan/m²), which falls within a comparable range to the actual settlement costs of similar renovation projects in the same region (approximately 4 to 5.2 million yuan). This verifies the engineering rationality of the cost correlation mapping logic.

3.4. Ablation comparison and discussion

To validate the advantages of multimodal fusion over single-modality methods, a simplified ablation comparison was conducted for this example, with the results presented in **Table 7**.

Table 7. Ablation comparison results

Model configuration	Score difference	Description
Image-only modality	Overall score 65	Obvious facade defects severely underestimating the impact of residents' demands
Text-only modality	Overall score 68	Unable to reflect building ontology; disease score is relatively high
Structured-data-only modality	Overall score 62	Lack of residents' demands and defect image support
Multimodal fusion (our model)	Overall score 57.50	Comprehensively reflects physical defects and social needs

The ablation comparison indicates that evaluation results from single modalities exhibit significant deviations (either being too high or deviating from the actual urgency of renovation). After multimodal fusion, the information from various dimensions mutually corrects each other, resulting in a lower comprehensive score that is closer to the actual urgency of renovation, and providing more comprehensive renovation recommendations.

4. Conclusion

This paper proposes an AI evaluation model based on multimodal data fusion and fuzzy comprehensive evaluation to address issues such as low efficiency in preliminary evaluations of old residential areas, difficulties in integrating multi-source information, and disconnections between evaluations and costs. The model focuses on 17 indicators across seven major dimensions, employs AHP for weight assignment, designs feature extraction and attention fusion strategies for image, text, and structured data, and establishes an evaluation-oriented cost correlation module to achieve a complete chain of "data input—feature fusion—comprehensive evaluation—cost estimation" [8].

The value of the model lies in transitioning evaluations from manual experience to data-driven approaches, making evaluations traceable and interpretable. It unifies building inspections, public opinion collection, and cost calculations, directly linking to costs and providing continuous support for decision-making. Current limitations include: reliance on expert judgment for AHP weights, which requires dynamic adjustments with policy changes; the cost module is based on case rules, with accuracy that needs improvement; and the example uses non-measured data, requiring engineering validation for real-world performance. Subsequent efforts will focus on accumulating actual data to fine-tune the model, introducing reinforcement learning to optimize renovation combinations, and developing a digital twin visualization platform to form a closed-loop lifecycle. This study provides a feasible technical solution for intelligent evaluation of old residential areas and offers a new perspective for the integration of engineering management and AI.

Funding

Chongqing Undergraduate Innovation and Entrepreneurship Training Program, under the project "An AI-Driven Rapid Evaluation Model for the Upgrading and Renovation of Old Residential Communities" (Project No.: S202512608007); Science and Technology Research Program of the Chongqing Municipal Education Commission, "Research on Rapid Assessment of the Upgrading and Renovation of Old Residential Communities Based on 'AI + Smart Measurement'" (Project No.: KJQN202501901)

Disclosure statement

The authors declare no conflict of interest.

References

[1] Zhang H, 2026, Research on the Comprehensive Benefit Evaluation of Green Renovation in Old Residential Areas. Low Temperature Architecture Technology, 2026(2): 17–21.

[2] Research on Renovation Strategies for Old Residential Areas Under the "Dual Carbon" Goals, 2024, Sustainable Development, 14(8): 1984–1995.

[3] Li R, Fan P, Mao R, et al., 2024, Research on Post-Occupancy Evaluation of Old Residential Area Renovation Based on the AHP Method. Architecture & Culture, 2024(7): 170–173.

[4] Liu W, Zhao X, 2022, Evaluation of Green Renovation Potential in Existing Buildings Based on the AHP-FUZZY Method. Green Science and Technology, 2022(22): 234–238.

[5] Peng W, 2025, Fuzzy Comprehensive Evaluation of Green Construction in Old Residential Area Renovation Based on AHP. Green Science and Technology, 2025(20): 272–275.

[6] Research on Performance Evaluation of Old Residential Area Renovation Projects—Taking the Renovation Projects in Hengyang City as an Example, 2023, Project Management Technology.

[7] Research and Practical Validation on Construction Cost Estimation for Old Renovation Housing Projects Based on Fuzzy Mathematical Modeling, 2023, Construction Supervision, Detection & Cost.

[8] Research on Influencing Factors of Cost Management in Old Residential Area Renovation Projects Based on AHP-DEMATEL, 2023, Journal of Engineering Management.

Publisher's note

Bio-Byword Scientific Publishing remains neutral with regard to jurisdictional claims in published maps and institutional affiliations.

Journal of Architectural Research and Development, 2026, Volume 10, Issue 5
https://bbwpublisher.com/journal/JARD
Online ISSN: 2208-3537
Print ISSN: 2208-3529

Teaching and Study of Artificial Intelligence-Driven Regional Architectural Design Courses

Ding Ding*, Ling Wang

School of Architecture and Civil Engineering, Xihua University, Chengdu 610039, Sichuan, China

***Corresponding author:** Ding Ding, dd@mail.xhu.edu.cn

Copyright: © 2026 Author(s). This is an open-access article distributed under the terms of the Creative Commons Attribution License (CC BY 4.0), permitting distribution and reproduction in any medium, provided the original work is cited.

Abstract: In the process of digitization and globalization, traditional regional architectural design education faces certain limitations. Although AI technology offers a new pathway for the innovation of architectural education, the integration of the two still encounters multiple challenges. To explore the compatibility between AI technology and the teaching of regional architectural design, this study proposes an approach for the teaching system that integrates technological empowerment, cultural restructuring, and capability development. Combining teaching cases, this work constructs a multi-level modular curriculum system that progresses from foundational empowerment to core practice and then to expansive innovation. Additionally, the study introduces a multi-dimensional evaluation mechanism that emphasizes both process and outcomes, along with a multi-type supporting resource development system.

Keywords: Artificial intelligence; Architecture; Style imitation; Text-to-image generation; Image-to-image generation

Online publication: October 23, 2026

1. Introduction

As globalization and digitalization are intertwined and evolving together, architectural education is confronting unprecedented challenges and opportunities. For a long time, traditional architectural design education has had certain limitations in terms of information exchange, divergent thinking, and the integration of theory with practice [1]. The introduction of artificial intelligence (AI) technology offers new ways to overcome these limitations. In particular, generative AI tools, such as Midjourney and Stable Diffusion, have dynamically entered the field of architecture, providing more possibilities for rapid image generation and inspiration for students [2]. In addition, these tools can not only be used for visual concept generation but also play a crucial role in design aspects such as architectural structural analysis, spatial planning, parametric modeling, and performance analysis [3].

However, as an important vehicle for inheriting and promoting local culture, regional architectural design education still faces challenges in its integration with AI. First, the complexity, diversity, and tacit

knowledge of regional architecture are difficult to fully quantify and encode, resulting in a potential lack of depth and accuracy when AI models handle regional specificity. Second, most deep learning models lack interpretability, with opaque decision-making processes and the so-called "black box" problem, which may lead students to overly rely on AI-generated results while neglecting critical thinking about design principles and regional context [3]. Without reliable human intervention, AI-generated results may sometimes lack originality and depth, and even exhibit a certain degree of mediocrity. Third, there is currently a lack of unified and effective standards for evaluating the teaching effectiveness of AI-assisted design, especially in measuring students' creativity, regional adaptability, and the development of critical thinking. How to assess the correctness, creativity, and regional relevance of designs assisted or generated by AI remains a question worthy of discussion. Fourth, many practitioners in traditional architectural education lack professional knowledge and teaching experience in AI technology, making it difficult for them to effectively integrate AI tools into the curriculum or guide students in deeply understanding and utilizing AI tools [4]. Correspondingly, the rapid development of AI tools also places pressure on teachers for continuous learning [5]. Fifth, AI models are trained based on existing data. If the training data itself contains biases or lacks diversity, the designs generated by AI may further solidify these biases and even produce designs that are unethical or insensitive to regional culture [6].

Based on the above situation, this paper aims to explore the compatibility between AI technology and regional architectural design teaching and propose ideas for reconstructing a teaching system with an integrated framework of technology, culture, and competence. Through an analysis of the mechanisms of AI in terms of technological empowerment, cultural reconstruction, and competence cultivation, combined with specific teaching cases, this paper will construct a multi-level, modular curriculum system, providing a new paradigm for the living inheritance of regional architectural culture and the cultivation of innovative architectural talents in the digital age.

2. Compatibility between AI and regional architectural design education

At a time when the wave of digitalization is sweeping across the globe, the deep integration of AI technology with regional architectural design teaching has emerged as a pathway to drive innovation in architectural education. This adaptability is not only manifested in the optimization of traditional teaching processes by technological tools but also lies in its reconfiguration of the interactive relationship among humans, technology, and culture, providing a brand-new paradigm for the inheritance and innovation of regional architectural culture.

2.1. Technological empowerment: Breaking through traditional teaching bottlenecks

The teaching of traditional regional architectural design has long faced three major dilemmas. First, the refinement of cultural symbols relies heavily on extensive field research and manual drawing, requiring students to spend months combing through unstructured data such as local chronicles and oral histories from craftsmen. Second, design practice is constrained by geographical space, making it difficult for students to intuitively grasp the profound impacts of complex terrain, landforms, and climatic conditions on architectural forms. Third, knowledge transfer is unidirectional, with teachers acting as "authorities on knowledge", struggling to accommodate the individualized needs of each student in understanding regional culture. The intervention of AI technology offers possibilities for resolving these challenges [7].

Taking the research on traditional Thai architectural teaching as an example, the temple complexes along the Chao Phraya River in Bangkok embody unique aquatic cultural genes. In traditional teaching, students are required to sort out the connections between spatial layouts and decorative symbols through on-site mapping and consulting ancient texts. With the introduction of AI, a multimodal database encompassing architectural floor plans, historical images, and videos of religious ceremonies can be constructed. This database enables students to rapidly generate three-dimensional models of temple main halls in virtual environments and utilize computer vision technology to identify the evolutionary patterns of eave decorations across different historical periods. The combination of data-driven approaches and scenario simulation can condense the data collection and form verification tasks that traditionally take weeks into just a few days, allowing students to devote more energy to cultural interpretation and conceptual deliberation.

2.2. Cultural reconstruction: Activating the modern translation of regional genes

The core of regional architectural design lies in the creative transformation of local knowledge; AI technology provides a unique cognitive framework for this endeavor. In traditional teaching, students often fall into the trap of superficial imitation of architectural forms, struggling to grasp the underlying cosmic and ethical structures of regional culture. The intervention of AI, through a bidirectional process of decoding and re-encoding, can facilitate the revitalization and regeneration of cultural symbols.

In a teaching case (**Figure 1**) that integrates architectural styles from Sichuan-Chongqing and Southeast Asia, there exists cultural resonance between the stilted building morphology of Chongqing's Hongya Cave and the wooden structures of traditional dwellings in Chiang Mai, Thailand [8]. However, achieving an organic fusion of these two styles had previously posed a significant challenge in teaching. By analyzing spatial scales, material properties, and climate adaptability data from buildings in both regions, the AI system generated a model library of new stilted buildings tailored to Chongqing's mountainous terrain and humid climate. Building upon this foundation, students utilized parametric design tools to adjust the depth of eave projections and the connection methods of wooden components, thereby creating hybrid-style solutions that not only retained the ecological wisdom of Sichuan-Chongqing architecture in adapting to mountainous terrain but also incorporated the transparent and light spatial qualities of Thai architecture. Evidently, the collaborative creative mode between humans and machines breaks the mental set of "region as a single culture", enabling students to understand that regionality does not equate to the solidification of a particular style but rather involves the dynamic recombination of different cultural genes through technological mediation.



Figure 1. Architectural design case integrating styles from Sichuan-Chongqing and Southeast Asia.

2.3. Goal-driven approach: Cultivating composite competencies in future architects

The integration of AI into the teaching of regional architectural design, driven by the digital age, represents a paradigm shift in education. This transformation manifests itself on three levels. First, the role of teachers evolves from that of knowledge transmitters to learning facilitators, with their core responsibility being the design of thought-provoking question chains that stimulate deep thinking. Second, there is a fundamental change in students' skill sets. In addition to mastering traditional design skills, they must also possess digital literacy encompassing data governance, algorithm optimization, and critical filtering. Third, the evaluation system shifts from being outcome-oriented to process-oriented, capturing every parameter adjustment and conceptual iteration made by students on AI platforms to generate visual maps of their thought processes. For instance, in the teaching practice of industrial architectural design, students utilized AI tools for structural simulations to analyze the load-bearing characteristics of traditional brick arches and the connection methods with modern steel structures, thereby designing new industrial building solutions that not only meet the requirements of brewing processes for space humidity and temperature but also comply with modern seismic standards [9]. This teaching model, oriented towards real-world problems, mediated by technology, and rooted in culture, embodies the core value of regional architectural design education in the AI era.

3. Reconstruction approach for the teaching system

The reconstruction of the AI-driven teaching system for regional architectural design (**Figure 2**) centers on constructing an integrated framework that combines technology, culture, and capacity. Through systematic reorganization of the curriculum structure, dynamic optimization of teaching processes, in-depth innovation of evaluation mechanisms, and collaborative development of supporting resources, this system aims to break down disciplinary barriers and the one-way transmission model inherent in traditional architectural education. This model facilitates a paradigm shift from knowledge transfer to the cultivation of higher-order capabilities, ultimately achieving the dual objectives of preserving the vitality of regional architectural culture and nurturing innovative talents in the digital age.

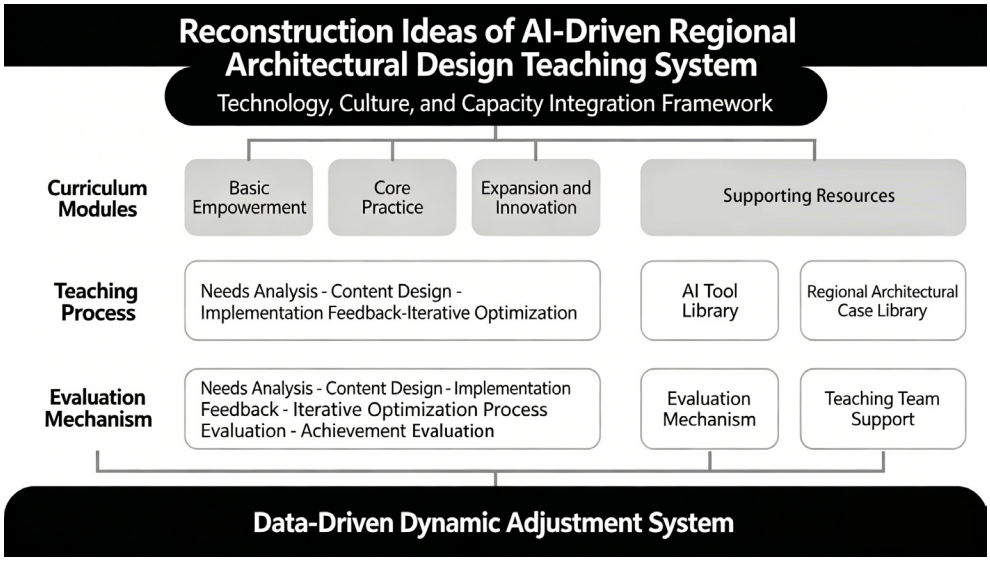

Figure 2. Conceptual framework for the reconstruction of the teaching system.

The reorganization of curriculum modules follows a logical sequence of basic empowerment—core practice—extension and innovation, forming a multi-tiered, modular knowledge and skill system. First, the basic empowerment module focuses on mastering technological tools and establishing cultural awareness. On one hand, through courses such as Introduction to Architectural AI Technologies and Data Collection and Processing, students are helped to grasp the operational logic of tools like text-to-image, image-to-image, and parametric design, as well as methods for collecting, cleaning, and visualizing architectural big data, thereby establishing a fundamental understanding of "technology serving design". On the other hand, traditional courses on regional architecture are optimized by introducing AI-assisted teaching for cultural symbol extraction. By constructing a multimodal database of regional architectural cultures across multiple regions, students are guided to systematically extract core symbols, spatial prototypes, and ecological wisdom from regional architecture using AI image recognition and text analysis tools. Second, the core practice module, as a pivotal component of the teaching system, should be driven by real-world projects, deeply integrating AI technology throughout the entire design process. In the preliminary design phase, AI geographic information analysis tools are employed to rapidly complete site suitability analysis and concept generation. During the schematic design phase, generative AI tools are used to refine details, parametric design optimizes performance, and AI structural simulations validate feasibility. In the presentation phase, AI visualization techniques are fused with traditional presentation methods to enhance the cultural appeal of design proposals. Finally, the extension and innovation module emphasizes interdisciplinary collaboration and cutting-edge exploration. Interdisciplinary courses are offered to guide students from architecture, computer science, environmental studies, cultural heritage, and other disciplines to collaboratively complete complex design projects. Simultaneously, elective courses on cutting-edge topics are set up to cultivate students' critical thinking and innovative exploration spirit. Throughout this process, a student-centered, AI-mediated, and teacher-guided closed loop of human-machine collaboration needs to be established.

For such a curriculum, evaluation dimensions should encompass multiple aspects, including technological application, cultural translation, design capability, collaboration, and reflection. The weighting of each dimension can be dynamically adjusted according to the curriculum module, considering not only students' mastery and rational application of AI technologies but also the depth of understanding and innovative translation of regional culture in their design proposals, as well as their comprehensive design performance and communication contributions in interdisciplinary collaboration. Evaluation methods should emphasize the combination of formative and summative assessments, complementing quantitative scoring with qualitative evaluations. Utilizing an AI teaching management platform to record students' learning trajectories and incorporating qualitative evaluations from teachers and opinions from industry experts ensures the scientific rigor and comprehensiveness of the evaluation results as much as possible.

Furthermore, the development of teaching resources is crucial for the efficient operation of this system. The application of multimodal databases on regional architectural cultures provides data support for teaching in terms of regional architectural resources, AI design cases, and tool algorithms. The development of teacher resources primarily focuses on training and enhancing the AI teaching capabilities of existing architecture faculty, supplemented by the recruitment of professional teachers from related fields or the hiring of industry experts to participate in curriculum design and practical guidance. This approach facilitates the construction of a composite faculty team, ensuring that teaching content closely aligns with industry demands and cultural heritage preservation requirements.

4. Conclusions

This study explores AI-driven teaching in regional architectural design, clarifying the compatibility between AI technology and regional architectural design education at the levels of technological empowerment, cultural reconstruction, and competency development. The work proposes a framework for restructuring the teaching system. Through the design of curriculum modules encompassing basic empowerment, core practice, and extension and innovation, combined with an evaluation mechanism that emphasizes both process and outcomes, as well as the construction of multi-type supporting resource development system, this study offers a pathway to address bottlenecks in traditional regional architectural design education. Additionally, this study establishes a human-machine collaborative teaching paradigm for the dynamic preservation of regional architectural culture and the cultivation of architectural innovation talents in the digital era.

However, while this study has constructed an overall teaching system framework, it still lacks more detailed practical validation in areas such as the adaptability of AI tools across diverse regional architectural cultural contexts and the tiered development of digital literacy for students at different academic levels. Moreover, a standardized approach for controlling the translation accuracy of regional cultural symbols in AI technology applications has yet to be established. Future research could further engage in localized teaching practices by incorporating the architectural cultural characteristics of different regions, refine application standards and operational procedures for AI tools across various teaching stages, and delve deeper into exploring long-term mechanisms for integrating AI with regional architectural design education. Through university-enterprise collaboration and interdisciplinary cooperation, continuous improvements can be made to teaching resources and faculty development. By balancing the application of technological tools with the expression of regional cultural essence, this research aims to propel AI-driven regional architectural design education toward greater precision, systematization, and innovation, ultimately cultivating a new generation of architectural talents equipped with cultural preservation awareness, digital technological proficiency, and innovative design thinking.

Author contributions

D.D. conceived the idea of the study. D.D. performed the experiments. D.D. and L.W. analyzed the data and wrote the paper.

Funding

Sichuan Provincial Research Institute of Thai Studies (Project No.: SPRITS202518); Engineering Research Center of Chuanxibei Rural Human Settlements Construction in Sichuan Provincial College (Project No.: RSH2025ZC03); Project of First-Class Postgraduate Teaching Team of Xihua University “Landscape Planning and Design Teaching Team” (Project No.: YTG202606)

Disclosure statement

The authors declare no conflict of interest.

References

[1] Du S, Lu X, Chen Z, et al., 2024, Research Into a Stable Diffusion-Based Human-Machine-Human Teaching Model for Architectural Design Courses. Journal of Green Building, 19(3): 299–318.

[2] Donduran G, Kasali A, Dogan F, 2024, Artificial Intelligence as a Pedagogical Tool for Architectural Design Education. Journal of Design Studio, 6(2): 219–229.

[3] Albukhari N, 2025, The Role of Artificial Intelligence (AI) in Architectural Design: A Systematic Review of Emerging Technologies and Applications. Journal of Umm Al-Qura University for Engineering and Architecture, 16(4): 1457–1476.

[4] Liu C, Sun Z, 2024, Empirical Study on the Efficacy of Engineering Education via an AI-Driven Adaptive Learning Environment for Architectural Structural Analysis. Journal of Computational Methods in Science and Engineering, 25(2): 1417–1431.

[5] Dong N, 2025, Advantages and Challenges of Generative Artificial Intelligence Technology in Teaching Design Professionals. Academis Notes. Series: Pedagogical Sciences, 14: 182–187.

[6] Cheung L, Dall'Asta C, 2024, Human-Computer Interaction (HCI) Approach to Artificial Intelligence in Education (AIEd) in Architectural Design. Eídos, 17(23): 109–131.

[7] Tu H, Zhang T, Li J, et al., 2025, Exploring the Integration of Generative Artificial Intelligence in Architectural Programming and Design Education: A Case Study of Tongji University's International Graduate Course. Architectural Journal, 2025(S2): 119–124.

[8] Jacob S, 2017, Charoenpong Kindergarten. Design, 2017(6): 30–31.

[9] Wang C, 2020, Research on the History of Industrial Heritage in Sichuan During the Period of "The First Five" Value Analysis, thesis, Southwest University of Science and Technology.

Publisher's note

Bio-Byword Scientific Publishing remains neutral with regard to jurisdictional claims in published maps and institutional affiliations.

Journal of Architectural Research and Developmentn, 2026, Volume 10, Issue 5
https://bbwpublisher.com/journal/JARD
Online ISSN: 2208-3537
Print ISSN: 2208-3529

Research on Energy-Saving Structure Optimization and Carbon Reduction Technology of Building Doors and Windows in Cold Regions

Meng Zhang*

East University of Heilongjiang, Harbin 150066, Heilongjiang, China

***Corresponding author:** Meng Zhang, 452182382@qq.com

Copyright: © 2026 Author(s). This is an open-access article distributed under the terms of the Creative Commons Attribution License (CC BY 4.0), permitting distribution and reproduction in any medium, provided the original work is cited.

Abstract: The heat loss of the building envelope system, doors and windows, is the component with the weakest thermal insulation performance, and the proportion of heat dissipation is much higher than that of other envelope structures such as walls and roofs. In China's high-latitude cold zone, the extreme low temperature can drop below -40 ℃ in winter, and there is a huge temperature difference between indoor and outdoor for a long time. The continuous cold and heat exchange behavior of doors and windows continues to aggravate the heating load of buildings and promote the continuous growth of carbon emissions during the operation stage of buildings. Traditional building doors and windows generally have various problems, such as the excellent thermal conductivity of profiles, simple sealing structures, and weak thermal insulation of glass. The joint gap between the window frame matrix, the glass edge, the doors and windows, and the wall will form a continuous thermal bridge channel, which will lead to building diseases such as frosting and mildew on the indoor wall, which will directly affect the building function and living comfort. The long-term high-load operation of heating equipment has caused a lot of inefficient loss of fossil energy, and the pressure of regional carbon emission control has intensified. In this paper, the various channels of heat loss of building doors and windows in cold regions are studied, and the thermal insulation short boards of four structural systems, namely profile structure, sealing system, glass material, and installation nodes, are systematically combed, and targeted structural optimization schemes are formulated for various technical defects. This paper studies the carbon reduction path covering the whole process of building materials production, engineering construction, building operation, and component scrap recycling, and quantitatively analyzes the practical application value of various optimization technologies by combining the measured data of temperature monitoring, energy consumption statistics, and carbon emission accounting at the construction site.

Keywords: Severe cold area; Building doors and windows; Energy-saving structure; Thermal bridge blocking

Online publication: Oct 16, 2026

1. The traditional door and window structures in cold regions have double defects of heat preservation and carbon emission

1.1. Defect of profile thermal bridge structure

The thermal conductivity of ordinary aluminum alloy substrate can reach 237 W/(m k). The traditional aluminum alloy door and window profiles are not provided with closed thermal insulation cavities, and the inner and outer metal structures form a through thermal conduction channel [1]. The heat loss in the window frame area accounts for more than 30% of the total heat loss of the whole window, and the heat dissipation problem of the thermal bridge is particularly prominent. In the early stage, the aluminum profile with a broken bridge only adopted a simple single-cavity thermal insulation structure; the width of the thermal insulation strip was less than 24 mm, and the cavity was not filled with thermal insulation foam material [2]. The low-temperature environment will accelerate the air convection movement in the cavity, which will cause the overall thermal insulation performance of the profile to be greatly attenuated. Conventional PVC plastic-steel profiles are only provided with two to three cavities, and the wall thickness of the profiles is designed to be thin. At -30 ℃ low temperature, it is easy to shrink and deform, and the joint gap between the sealing strip and the profile continues to expand, and the cold air permeability shows an obvious growth trend [3]. A large number of petroleum-based additives will be mixed in the production process of ordinary wood-plastic composite profiles, and the overall implicit carbon of the components is at a high level. Long-term freeze-thaw cycles will induce surface cracking and peeling of profiles, and the thermal insulation performance will continue to decline with the increase of service life [4].

1.2. The short board of sealing system structure

The traditional door and window sealing system is only equipped with a single layer of rubber sealing strip, and the low-temperature resistance of ordinary rubber materials is obviously insufficient. Long-term freeze-thaw cycles will cause problems such as hardening, shrinkage, and aging of rubber strips, and a continuous ventilation gap will be formed between the window sash and the window frame. The airtightness of this kind of doors and windows can only reach the third to fourth standards, which cannot meet the requirements of the design code for energy-saving buildings in cold regions. The conventional sealing structure is not equipped with an isobaric drainage cavity, and outdoor snowmelt water can penetrate into the profile cavity through the gap. In the low-temperature environment, the accumulated water freezes and expands, and the extruded sealing strip is deformed, so the problems of leakage and air leakage are aggravated [5]. The gap between the window frame and the hole of the wall is only filled with ordinary foaming agent, and the outside is simply blocked by cement mortar. The thermal conductivity of mortar material is high, and an annular thermal bridge structure is formed around the wall, and the window sill area is in a low-temperature frosting state for a long time. After the wall insulation layer is wetted, the thermal insulation performance is greatly attenuated, and the building heating energy consumption is significantly increased.

1.3. The lack of carbon emission control in the whole cycle

Traditional door and window manufacturing links use a large amount of primary electrolytic aluminum materials, and the electrolytic process is highly dependent on thermal energy; the raw material mining and smelting processes will release a lot of greenhouse gases. The equipment in the processing workshop is not equipped with an energy-saving frequency conversion control system, and the surface spraying process adopts high-VOC organic solvent coatings, so the power consumption and total carbon emissions in the

production process remain high for a long time [6]. In the service stage of doors and windows, only heating equipment is used to make up for the heat loss, and the abundant solar radiation resources in winter have not been effectively developed and utilized, and the carbon emissions of buildings in long-term operation continue to expand. After the doors and windows reach the designed service life, they are mostly disposed of directly, and the utilization rate of recyclable materials such as aluminum and glass is low. The application of recycled materials in secondary processing accounts for less than 10%, and the problem of resource waste is prominent. The new raw material mining and smelting operation will produce an additional increase in carbon emissions.

2. Systematic optimization technology of energy-saving structure of doors and windows in severe cold area

2.1. Structural upgrade of profile thermal insulation cavity

(1) Structural optimization of multi-cavity widened broken bridge aluminum profile.

The optimized broken-bridge aluminum profile adopts the special base material of 6063-T5 and the PA66GF25 glass fiber nylon thermal insulation strip with a width of 35 mm or more. The thermal conductivity of the thermal insulation base material is as low as 0.3W/(m k), which can effectively block heat conduction through the metal. Five to six groups of independent closed cavities are set on the section of the profile, and the cavities are filled with low-density polyurethane thermal insulation foam materials, thus eliminating the heat exchange problem caused by air convection in the cavities. The internal and external structures of the profile are separated by staggered heat insulation strips, which effectively prolong the heat conduction path, and the heat transfer coefficient of the whole frame can be controlled within 1.8 W/(m 2 k) at low temperature. In view of the special working conditions of strong wind and frost heaving in cold areas, the wall thickness of the profile is thickened to 2.0mm, and the overall deformation resistance of the structure is significantly improved, effectively avoiding the sealing failure caused by low-temperature deformation.

(2) Improvement of special multi-cavity PVC composite profile for low temperature.

Improved PVC profiles are prepared based on low temperature-resistant modified substrates, and special antifreeze polymer additives are added, which can keep the structure stable in the extremely low-temperature environment of -40 ℃ without brittle cracking and shrinkage deformation. The profile is designed with six or more layered closed structures. The inner and outer cavities are isolated from each other, completely blocking the internal air convection heat exchange channel. Glass fiber-reinforced ribs are embedded in the profile to improve the overall structural stiffness. Exclusive thermal insulation layers are added in the splicing area of window frames and window sashes to prevent local thermal bridge defects caused by splicing gaps. Compared with the traditional single-cavity plastic-steel profile, the heat transfer coefficient of the improved profile is reduced by 40%, and the carbon emissions in the production stage are much lower than those of the original aluminum alloy material, which is suitable for the low-cost energy-saving renovation project of affordable housing in severe cold areas.

2.2. Structural optimization of multilayer isobaric sealing system

(1) Three-way EPDM weatherproof sealing structure

The traditional single-layer rubber sealing structure was abandoned, and three independent EPDM sealing systems were used to upgrade the structure. The outer rubber strip is responsible for preventing wind

and water; the middle cavity balances the internal and external air pressure; the inner rubber strip ensures airtightness and heat-preservation performance; and the three sealing members can be attached to the surface of the sash profile in all directions. EPDM rubber strip adopts a low-temperature, weather-resistant modified formula, which can still maintain good elasticity at -45 ℃, and has no issues such as hardening, shrinkage, or deformation after 300 freeze-thaw cycles, ensuring the stability of building airtightness to reach the Grade 8 standard. A special drainage diversion channel is reserved in the middle isobaric cavity, so that the snowmelt water can be discharged outward along the cavity and will not penetrate into the indoor side structure, thus thoroughly solving the leakage and air leakage diseases caused by the freezing of accumulated water to open the sealing gap.

(2) No thermal bridge attached frame structure at the entrance of the wall

In the construction stage of doors and windows, the graphite polystyrene thermal insulation frame is embedded in advance, and the thermal conductivity of the frame is controlled at 0.032 W/(m k), effectively isolating the annular thermal bridge between the concrete structure of the wall and the metal window frame. The outer side of the attached frame is flush with the external wall insulation layer, the splicing gap is filled with low thermal conductivity insulation mortar, and the surface layer is coated with weather-resistant waterproof sealant to complete the sealing treatment. The gap inside the hole is filled with high-density closed-cell foaming agent, which has extremely low thermal conductivity and will not form a heat conduction channel. The window sill area is designed with an outward-leaning, water-covered structure, which effectively avoids the problem of rain and snow accumulation and infiltration, and eliminates the frosting thermal bridge disease on the window sill from the installation node level.

2.3. Optimization of thermal insulation structure of high-performance glass

(1) High-light-transmission three-glass two-cavity Low-E insulating glass

The combination of three layers of tempered glass and two layers of 12mm inert gas cavities is adopted, and the inner glass is plated with a high light transmittance and low radiation film, so that the visible light transmittance can be maintained above 62%, ensuring that solar radiation can be fully received indoors in severe cold winter. The hollow cavity is filled with argon, which inhibits the convection heat transfer of air inside the cavity. The glass edge replaces the traditional metal aluminum strip, and the glass fiber warm edge spacer strip is used to eliminate the thermal bridge effect of the glass edge. The temperature of the inner surface of the glass can be increased by 6–8 ℃, so as to prevent large-scale condensation and freezing in winter. The whole set of glass combination can reduce the heat transfer coefficient of the whole window to 1.2w/(m^2 k), which is suitable for the construction requirements of various energy-saving buildings in cold regions.

(2) Application of vacuum glass integrated structure

The vacuum degree in the vacuum glass is kept within 0.1Pa, which eliminates the heat dissipation path of gas conduction and convection heat transfer. The thermal insulation performance of a single piece of vacuum glass is equivalent to that of a 1.5 m thick brick wall, and the minimum heat transfer coefficient of the whole window can reach 0.4 w/(m 2 k). The inner side of the glass is coated with an infrared barrier coating, and the micro stainless steel support points are arranged in the vacuum cavity, which is suitable for the complex working conditions of long-term temperature difference deformation in cold areas. The overall thickness of vacuum glass is reduced by 70% compared with that of conventional three-glass insulating glass,

and the cross-section size of the window frame profile can be simultaneously optimized and narrowed, thus reducing the consumption of profile raw materials and the implied carbon emission of components. Vacuum glass with multi-cavity broken bridge aluminum profiles can meet the design index of zero-carbon building doors and windows in cold regions.

2.4. Composite structure of passive heat collection and sunshade

The south-facing doors and windows of the building are equipped with a manually retractable built-in louver structure. In winter, the louver components are put away to maximize the reception of solar short-wave radiation, and the indoor base temperature is improved by solar energy, thus reducing the overall running time of heating equipment. In summer, the louver members are deployed to block direct sunlight indoors, reduce the indoor heat storage temperature, and reduce the energy consumption of refrigeration equipment. No sunshade component is added to the north-facing doors and windows, so as to reserve the heat intake channel in winter to the maximum extent. The sunshade louver adopts a lightweight recycled aluminum substrate, and the cavity of the blade is filled with thermal insulation cotton. The whole sunshade system does not need a continuous power supply and relies on passive solar energy resources to achieve energy saving and carbon reduction.

3. Innovative technology for carbon reduction in the whole process of supporting doors and windows in severe cold areas

3.1. Low-carbon raw material selection technology

Recycled aluminum materials are preferred in the production of door and window profiles. The energy consumption of smelting recycled aluminum materials is only 30% of that of primary aluminum, and the carbon dioxide emissions in the smelting process are greatly reduced [7]. The application ratio of recycled aluminum is increased to over 70%, which can reduce nearly half of carbon emissions in the raw material production stage. Thermal insulation materials replace traditional petroleum-based polyurethane, and solid wastes such as straw-based and mineral wool are used to regenerate thermal insulation base materials, so the preparation process of raw materials does not need to consume fossil energy. In the glass production process, Shi Ying tailings and other industrial solid wastes are used to replace some natural Shi Ying ores, and the melting furnace is equipped with photovoltaic power supply equipment to reduce the carbon increment caused by thermal power consumption. Waterborne solvent-free environmental protection products are selected for sealant, high-carbon organic solvent raw materials are eliminated, and the carbon footprint of door and window components in the whole life cycle is controlled from the source [8].

3.2. Low-energy processing and manufacturing technology

The door and window processing workshop is fully equipped with energy-saving equipment such as frequency conversion cutting and numerical control drilling to reduce the power loss caused by the no-load operation of the equipment [9]. The profile cutting process adopts precision simulation typesetting technology, and the waste rate of raw materials can be controlled within 5%, thus reducing the indirect carbon emissions caused by material waste. The surface treatment of components abandons high-temperature oily spraying technology and adopts electrostatic powder circulating spraying technology. Powder coating can be recycled, no liquid waste pollutants are discharged, and the overall energy consumption of the spraying process is

reduced by 40%. The production plant is equipped with wind power and distributed photovoltaic generator sets, and the production electricity depends entirely on clean energy, so as to eradicate carbon emissions from thermal power in the processing link. The hardware fittings for doors and windows are made of lightweight and high-strength recycled materials to reduce the overall input of metal raw materials.

3.3. Passive carbon reduction control in the operation stage

Passive sunshade and heat collection composite structure can fully tap solar energy resources in winter and reduce the consumption scale of heating energy such as gas and coal. The doors and windows are equipped with intelligent micro-ventilation components, which can realize small ventilation on low-temperature, sunny days and avoid large-scale heat loss caused by window opening in the whole house. In extreme cold weather, the ventilation gap can be automatically closed to stably accumulate indoor heat [10]. The building is equipped with an intelligent energy consumption monitoring module, which can collect the heat loss data of doors and windows in real time, and dynamically adjust the operating power by linking heating equipment to avoid the energy waste caused by excessive heating and continuously reduce the carbon emission level in the operation stage of the building.

4. Comparative analysis of application effect of severe cold engineering

4.1. Application data of newly built ultra-low energy consumption residential buildings

A passive residential project in Mohe, Heilongjiang Province, adopts a complete set of optimized structures of five-cavity broken-bridge aluminum profiles with a 35 mm-wide heat-insulation bar, vacuum glass, EPDM three-way seal, graphite-framed thermal bridge, recycled aluminum profiles, and built-in sunshade blinds. The measured heat transfer coefficient of the whole window is 0.68 W/(m^2 k), the airtightness reaches the Grade 8 standard, and there is no frost or ice on the inner surface of the glass in winter. The annual heating gas consumption of a single-family residence decreased by 32%, and the carbon emissions of doors and windows in the whole life cycle decreased by 46% compared with those of traditional single-layer aluminum windows. The profiles of the project are all made of recycled aluminum, and the production workshop relies on a photovoltaic power supply, and the carbon emission reduction rate of raw material preparation and component processing reaches 38%.

4.2. The measured benefits of the renovation of doors and windows in old residential areas

The original doors and windows of an old residential area in northern Inner Mongolia are single-layer ordinary plastic-steel structures. In the reconstruction project, six-cavity modified PVC profiles and three-glass Low-E hollow sealed doors and windows were replaced, and the construction treatment of a non-thermal bridge-attached frame at the entrance of doors and windows was completed simultaneously. Before the renovation, the average monthly consumption of coal for heating in winter was 1.2 tons, and after the renovation, the average monthly consumption decreased to 0.73 tons, and the annual coal-fired carbon emission of single-family houses decreased by about 1.1 tons. The doors and windows used in the renovation are made of low-carbon profiles, which can be completely recycled after being scrapped, and the renovation cost of the project can be fully recovered by saving energy consumption in heating within four years.

4.3. Summary of comprehensive benefits of various technologies

The multi-cavity thermal insulation profile structure can reduce the heat transfer coefficient of the whole window by 40% to 65%, and block the heat dissipation channel of the profile metal thermal bridge from the source. A multi-layer sealing structure with an attached non-thermal bridge frame can reduce cold air infiltration by more than 70% and effectively reduce the building heating load. Vacuum glass and triple-glass Low-E insulating glass can inhibit the loss of infrared radiation heat, and the annual energy-saving range of a single window can reach more than 30%. Low-carbon renewable raw materials and photovoltaic energy-saving processing technology can reduce nearly half of the hidden carbon in door and window components. Passive solar shading and heat collection structures rely on natural energy to reduce the consumption of fossil fuel for heating. The closed-loop recovery system can reduce carbon emissions in the component scrapping treatment stage. The synergistic application of multiple technologies can simultaneously achieve the dual construction goals of improving the thermal insulation performance of doors and windows and reducing carbon emissions in the whole cycle. Different types of buildings in severe cold areas can match different technical schemes. Vacuum glass with recycled broken bridge aluminum profiles is preferred for new zero-carbon buildings, and a modified multi-cavity PVC triple-glass structure can be adapted for low-cost renovation of old houses. A wood-aluminum composite low-carbon profile system can be adopted for high-end passive houses. All kinds of schemes can adapt to the complex working conditions of severe cold, low temperature, strong wind, and freezing and thawing, and their engineering practical value is more prominent.

5. Conclusion

In summary, the energy-saving and carbon-reducing technologies for doors and windows in severe cold areas will continue to be iteratively upgraded around two dimensions: material innovation and intelligent empowerment. The low-temperature and high-performance composite substrate is the core direction of material research and development in the future. With the popularization and application of photovoltaic-integrated intelligent doors and windows, the deep integration of transparent photovoltaic modules and glass structures can be realized. In winter, photovoltaic power generation can supplement building heating electricity and achieve the effect of reducing carbon in the independent production capacity of doors and windows. In the future, the industry will continue to improve the unified standard of carbon accounting for doors and windows in severe cold areas, build a regional recycling and processing industrial chain for recycled doors and windows, promote the deep integration of energy-saving structures for doors and windows and low-carbon technologies, and help comprehensively promote the near-zero carbon renovation of buildings in severe cold areas in the north.

Funding

Heilongjiang Provincial Natural Science Foundation Project: “Application Research on Key Technologies for Low-Energy Consumption and Carbon Reduction in Building Doors and Windows in Severely Cold Regions” (Project No.: LH2022E101)

Disclosure statement

The author declares no conflict of interest.

References

[1] Luo H, Liu N, 2026, Research on the Application of Energy-Saving Technologies for Green Buildings in Severe Cold Regions. Petrochemical Technology, 33(6): 463–464.

[2] Xin D, 2026, Research on Energy-Saving Renovation of Campus Buildings and Heating Systems at a University in Daqing City, thesis, Bayi Agricultural University, Heilongjiang Province.

[3] Ge M, Zhang Y, Zhou C, et al., 2026, Research Progress on the Application of Phase Change Materials in Building Structures in Extremely Cold Regions. New Materials for Chemical Engineering, 1–7.

[4] Ma Z, 2026, Research on Exterior Wall Insulation Construction Techniques and Frost Crack Prevention Measures for Building Structures in Severe Cold Regions. China Building Decoration & Renovation, 2026(3): 154–156.

[5] Zhuang H, 2025, Research on the Optimization of Thermal Performance of Building Envelope Structures in Severe Cold Regions. New Construction Science & Technology, 34(10): 31–33.

[6] Lu X, Kong Q, Ma L, 2025, Thermal Insulation Design and Research of Modular Building Structures in Severe Cold and Cold Regions. China Residential Facilities, 2025(8): 34–36.

[7] Wang L, Wang C, 2025, Research on Technological Innovation of Building Envelope for Near-Zero-Energy Buildings in Severe Cold Regions. Science & Technology Innovation & Application, 15(23): 89–92.

[8] Wang Y, 2025, Research on Optimization of Energy-Saving Retrofitting of Existing Residential Buildings in Severe Cold Regions, thesis, Shenyang Jianzhu University.

[9] Yu M, 2025, Research on Carbon Reduction Optimization and Multi-Parameter Sensitivity Analysis of Ultra-Low Energy Buildings in Severe Cold Regions, thesis, Shenyang Jianzhu University.

[10] Cui W, Li Y, Zhang N, et al., 2024, Research on Heat Recovery-Based Energy-Saving Retrofitting of Aging Office Buildings in Severe Cold Regions. Building Energy Efficiency (Chinese & English Edition), 52(12): 130–135.

Publisher's note

Bio-Byword Scientific Publishing remains neutral with regard to jurisdictional claims in published maps and institutional affiliations.

Journal of Architectural Research and Developmentn, 2026, Volume 10, Issue 5
https://bbwpublisher.com/journal/JARD
Online ISSN: 2208-3537
Print ISSN: 2208-3529

Experimental Study on Dynamic Mechanical Properties of Layered Rock Under Cyclic Impact Loading

Wenxin Jia[1], Yian Ma[2], Chong Xu[3], Jiaqi Guo[1]

[1]School of Civil Engineering, Henan Polytechnic University, Jiaozuo, Henan, China
[2]Xi'an-Chengdu Passenger Dedicated Line Shaanxi Co., Ltd., Xi'an, Shaanxi, China
[3]China Railway First Survey and Design Institute Group Co., Ltd., Xi'an, Shaanxi, China

Copyright: © 2026 Author(s). This is an open-access article distributed under the terms of the Creative Commons Attribution License (CC BY 4.0), permitting distribution and reproduction in any medium, provided the original work is cited.

Abstract: Bedding planes impart pronounced anisotropic mechanical behavior to layered rock masses, and their deformation and failure modes are also governed by these planes. Consequently, tunnels excavated in layered rock masses are susceptible to asymmetric large deformations, collapses, and other disasters, directly threatening the safe construction of nationally significant projects. Currently, the drilling and blasting method remains the dominant construction technique for mountain tunnels, during which the layered surrounding rock is inevitably subjected to repeated blasting dynamic loads, substantially affecting its stability. In light of this, this study focuses on layered rock masses and employs a combination of laboratory experiments and theoretical analysis to investigate the effects of bedding plane angle, number of impacts, and impact load amplitude on the dynamic mechanical properties of layered rock masses. The principal findings are as follows: Split Hopkinson pressure bar (SHPB) cyclic impact tests reveal that the dynamic stress–strain curves of layered rock masses exhibit a distinct "rebound" phenomenon as the number of impacts increases, followed by a transition to a "semi-open" loop shape.

Keywords: Layered rock; Cyclic impact loading; Dynamic mechanical properties; Stress-strain curve; Dip angle

Online publication: Oct 16, 2026

1. Introduction

During tunnel excavation, layered rock masses, as the most common type of surrounding rock structure, are subjected not only to static loads such as in-situ stress but also to cyclic impact disturbances induced by blasting excavation. Owing to the presence of bedding planes, such rock masses exhibit pronounced anisotropy, and their mechanical behavior and failure modes are considerably more complex than those of homogeneous rock masses. Under cyclic impact loading, the interaction between bedding planes and stress waves can trigger abrupt changes in the dynamic mechanical properties of layered rock masses, easily leading to instability and failure of the surrounding rock. Therefore, investigating the dynamic mechanical

properties of layered rock masses with different bedding plane inclinations under cyclic impact loading holds significant theoretical importance and engineering value for ensuring the safety of underground projects.

In recent years, researchers worldwide have conducted extensive studies on the dynamic mechanical behavior of rocks. Advancements ranging from experimental technique development to the revelation of mechanical properties have laid a foundation for understanding the performance evolution of rock masses under complex loading conditions. Regarding dynamic testing methods for rocks, Li Xibing and Zhang et al. have provided systematic reviews of dynamic testing techniques and mechanical behavior of rocks [1,2]. Fan Chao et al. summarized the application achievements of the split Hopkinson pressure bar (SHPB) in testing the dynamic mechanical properties of rocks [3]. Ren Wenke et al. and Wang Jiangbo et al. investigated SHPB incident wave shaping techniques and similarity laws, respectively, providing a basis for improving test accuracy [4,5]. In terms of cyclic impact studies on homogeneous rocks, Jin Jiefang et al. conducted research on stress–strain curves and stress wave characteristics of rocks under cyclic impact, establishing a data acquisition and analysis framework for cyclic impact tests [6]. With respect to the dynamic mechanical properties of layered rock masses, scholars have carried out explorations targeting different bedding structures and loading conditions. Yang Renshu et al. prepared layered composite rock masses and performed SHPB dynamic compression tests, finding that differences in wave impedance lead to significantly different mechanical responses and failure patterns under different propagation directions [7]. Ma Qinyong et al. performed SHPB tests on deep roadway sandstone containing joints with varying inclinations, revealing the influence of joint inclination on the dynamic strength of sandstone rock masses [8]. Fan Zhao and Zhang Jing conducted impact tests on rock masses with different bedding plane inclinations and analyzed the anisotropic effects of bedding inclination on dynamic mechanical parameters [9,10]. Furthermore, Yin Zhiqiang et al. revealed the influence of static load on the dynamic mechanical properties and stress wave propagation in jointed coal-rock masses, while Zhang Xiaowu et al. systematically analyzed the anisotropy of mechanical properties and energy evolution in layered rocks [11,12]. For composite rock masses, Shang Hui studied the dynamic mechanical properties of concrete–sandstone composite specimens, revealing the influence of interface inclination on the dynamic strength of the composites [13]. Wu Jianyang and Wu Baolin investigated the mechanical properties of composite layered rocks and soft–hard interbedded rock masses under dynamic loading [14,15]. Wang Zhide et al. carried out impact tests on filled jointed rock masses and soft–hard interbedded rock masses, respectively, revealing the significant influence of joint inclination and soft–hard layer combination on the dynamic bearing capacity [16,17]. These studies have enriched the understanding of the dynamic mechanical behavior of complex layered structures.

Currently, research on the dynamic mechanical properties of layered rock masses mostly focuses on single-impact conditions, whereas studies on dynamic properties under cyclic impact are relatively scarce. Existing cyclic impact research primarily addresses homogeneous rocks. Although some scholars have conducted cyclic impact tests on layered slate with different bedding inclinations and identified stage characteristics of damage evolution, studies that comprehensively consider the influence of multiple factors, such as impact velocity and bedding inclination, on the dynamic mechanical behavior of layered rock masses remain very limited. Hence, conducting multi-level velocity cyclic impact tests on layered rock masses with different bedding inclinations to reveal their dynamic stress–strain response characteristics as well as strength and deformation evolution laws can not only enrich the theory of layered rock mass dynamics but also provide an important basis for the stability assessment and support design of layered surrounding rock engineering. In view of this, this study employs an electromagnetically driven split Hopkinson pressure bar (SHPB) apparatus to prepare layered rock mass specimens with four bedding plane inclinations (0°, 30°, 60°, and 90°) using rock-like materials such as cement, quartz sand, and gypsum. Constant-velocity cyclic impact tests are

conducted at impact velocities of 3, 3.35, 3.65, and 4 m/s. This research aims to reveal the dynamic mechanical properties of layered rock masses with different bedding inclinations under cyclic impact loading, with a view to providing a theoretical basis and technical support for optimizing blasting parameters and controlling surrounding rock stability in the drill-and-blast construction of tunnels in layered surrounding rock.

2. Cyclic impact tests on layered rock

2.1. Layered rock specimen

At present, many scholars commonly employ rock-like materials such as cement, gypsum, diatomite, and quartz sand to prepare rock-like specimens. The physical and mechanical properties of these materials (e.g., density, strength, elastic modulus, Poisson's ratio, and failure characteristics) are similar to those of natural rocks, while also offering good workability and controllability. In view of these advantages and the requirements of the intended experiments, the present tests, based on the research achievements of our university, use C42.5 ordinary Portland cement, 80–120 mesh quartz sand, gypsum, and tap water to fabricate layered rock mass specimens [18]. The constituent materials are shown in **Figure 1**, and the mix proportion of cement, quartz sand, gypsum, and water is 1:0.6:0.1:0.5 by weight.



Figure 1. Materials for synthesis.

According to the standard suggested by the International Society for Rock Mechanics (ISRM), the drilled cores were cut and ground into cylindrical specimens with a diameter of 50 mm and a height of 50 mm, as shown in **Figure 2** [10,19].

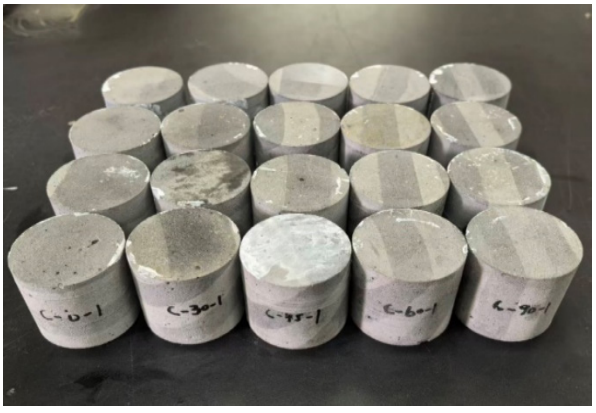

Figure 2. Layered rock mass specimen.

2.2. SHPB test apparatus

The cyclic impact tests on layered rock mass specimens with different bedding plane inclinations were

conducted using an electromagnetic-driven split Hopkinson pressure bar (SHPB) apparatus, developed independently by Henan Polytechnic University, in conjunction with acoustic monitoring equipment. The apparatus consists of three parts: a driving system, a loading system, and a data acquisition system. The driving system comprises a control cabinet and an electromagnetic coil. The loading bar system is composed of a striker bar (400 mm), an incident bar (2000 mm), a transmitted bar (1400 mm), and an absorber bar (400 mm). All bars are made of 40Cr alloy steel with a diameter of 50 mm, an elastic modulus of 210 GPa, a density of 7.93 g/cm^3, and a longitudinal wave velocity of 5190 m/s. The data acquisition system includes strain gauges, a dynamic strain meter, and an optical velocimeter. Additionally, a high-speed camera (resolution 1920 × 1980, frame rate 22000 fps, exposure time 3 μs) and an LED fill light were positioned beside the specimen to record the entire deformation process. During testing, the layered rock mass specimen was placed between the incident bar and the transmitted bar, with a thin layer of petroleum jelly applied to the end faces to minimize friction [8]. The electromagnetic coil drives the striker bar to impact the incident bar, and the amplitude of the generated incident wave is controlled by the striker velocity. Due to the wave impedance mismatch at the bar–specimen interfaces, reflected and transmitted waves are formed and recorded by the strain gauges mounted on the respective bars, then acquired in real time by the dynamic strain meter. To suppress wave oscillation and facilitate constant strain rate loading, a 1-mm-thick annealed copper disk was used as a pulse shaper, which absorbs energy through plastic deformation and reduces the peak slope of the stress wave [4,5]. See **Figure 3**.

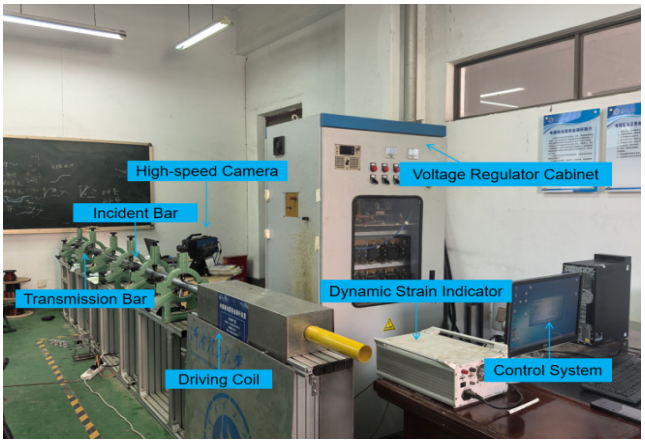

Figure 3. SHPB experimental apparatus.

2.3. Experimental scheme

To investigate the mechanical properties and damage evolution of layered rock masses subjected to cyclic disturbance by stress waves, cyclic impact dynamic tests were carried out on layered rock mass specimens using the electromagnetic-driven SHPB apparatus. In this test, four impact velocities were preset, ranging from low to high as 3 m/s, 3.35 m/s, 3.65 m/s, and 4 m/s. Constant-amplitude cyclic impact tests were performed on layered rock mass specimens with four different bedding plane inclinations (0°, 30°, 60°, and 90°). At a given impact velocity, the test for a group was terminated once the specimen underwent complete failure. The specific impact scheme is presented in **Table 1**. For each impact velocity, three parallel specimens were tested, and the final results were taken as the average to ensure data stability. Furthermore, to ensure that the peak intensity of the incident wave remained identical during each cyclic impact, the charging voltage of the control cabinet and the position of the striker bar within the driving coil were kept constant at a given velocity. In addition, during each cyclic impact test, a high-speed camera was used to record the crack initiation, propagation, and coalescence processes on the surface of the layered rock mass specimen, as well as to capture its final failure pattern.

Table 1. Experimental scheme for cyclic impact tests on layered rock mass

Loading mode	Specimen number	Impact velocity
Cyclic impact	C-β-1	3.00m/s
	C-β-2	3.35m/s
	C-β-3	3.65m/s
	C-β-4	4.00m/s

3. Analysis of testing results

3.1. Dynamic stress equilibrium

The SHPB impact test procedure is based on two fundamental assumptions. First, during the test, the striker bar is driven by electromagnetic force to impact the incident bar, and the resulting stress waves propagate in both the incident bar and the transmitted bar as one-dimensional elastic stress waves, with the bars maintained in a one-dimensional stress state. Second, after the stress wave undergoes several round-trip reflections between the two end faces of the specimen, the stress distribution across any cross-section of the specimen and the loads at both ends of the specimen reach a dynamic equilibrium, thereby placing the specimen in an approximately uniform one-dimensional stress state [20]. Based on these assumptions, the s tress, strain, and strain rate of the specimen can be calculated using the following formulas:

$$\sigma(t)=\frac{E_c A_e}{2A_s}\left(\varepsilon_I(t)+\varepsilon_R(t)+\varepsilon_T(t)\right) \quad (1)$$

$$\varepsilon(t)=\frac{c_e}{L_s}\int_0^t\left[\varepsilon_I(t)-\varepsilon_R(t)-\varepsilon_T(t)\right]dt \quad (2)$$

$$\dot{\varepsilon}=\frac{c_e}{L_s}\int_0^t\left[\varepsilon_I(t)-\varepsilon_R(t)-\varepsilon_T(t)\right] \quad (3)$$

where E_c denotes the elastic modulus of the bars, A_e and A_s denote the cross-sectional areas of the bars and the specimen, respectively, c_e denotes the longitudinal wave speed of the one-dimensional stress wave in the bars, L_s denotes the specimen length, and $\varepsilon_I(t)$, $\varepsilon_R(t)$, and $\varepsilon_T(t)$ denote the strain signals corresponding to the incident, reflected, and transmitted waves, respectively. See **Figure 5**.

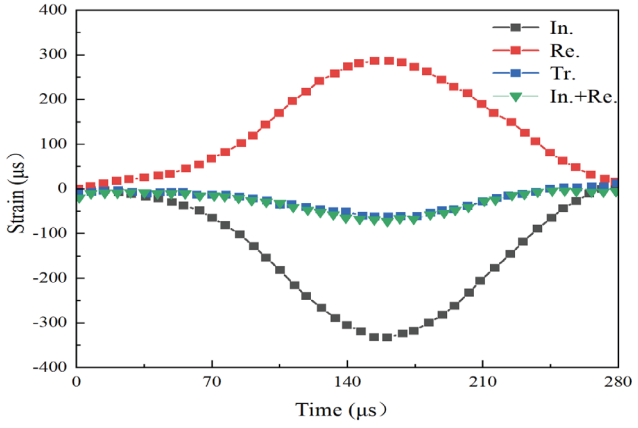

Figure 5. Dynamic stress equilibrium curve.

Taking the dynamic stress equilibrium of the layered rock mass specimen at an impact velocity of 4 m/s as an example, as shown in **Figure 5**, it can be observed that the superimposed curve of the incident and reflected waves agrees well with the transmitted wave curve, indicating that the dynamic stresses at both ends of the specimen are nearly identical during the impact process and simultaneously demonstrating the accuracy of the test results obtained in this study.

3.2. Dynamic mechanical properties

The stress–strain curves of rock mass specimens with different bedding plane inclinations (0°, 30°, 60°, and 90°) under cyclic impact at different velocities of 3 m/s, 3.35 m/s, 3.65 m/s, and 4 m/s are presented in **Figures 6** and **7**. As can be seen from **Figures 6**, **7**, **8**, and **9**, the dynamic mechanical properties of the layered rock mass specimens exhibit a significant correlation with both the cyclic impact velocity and the bedding plane inclination angle.

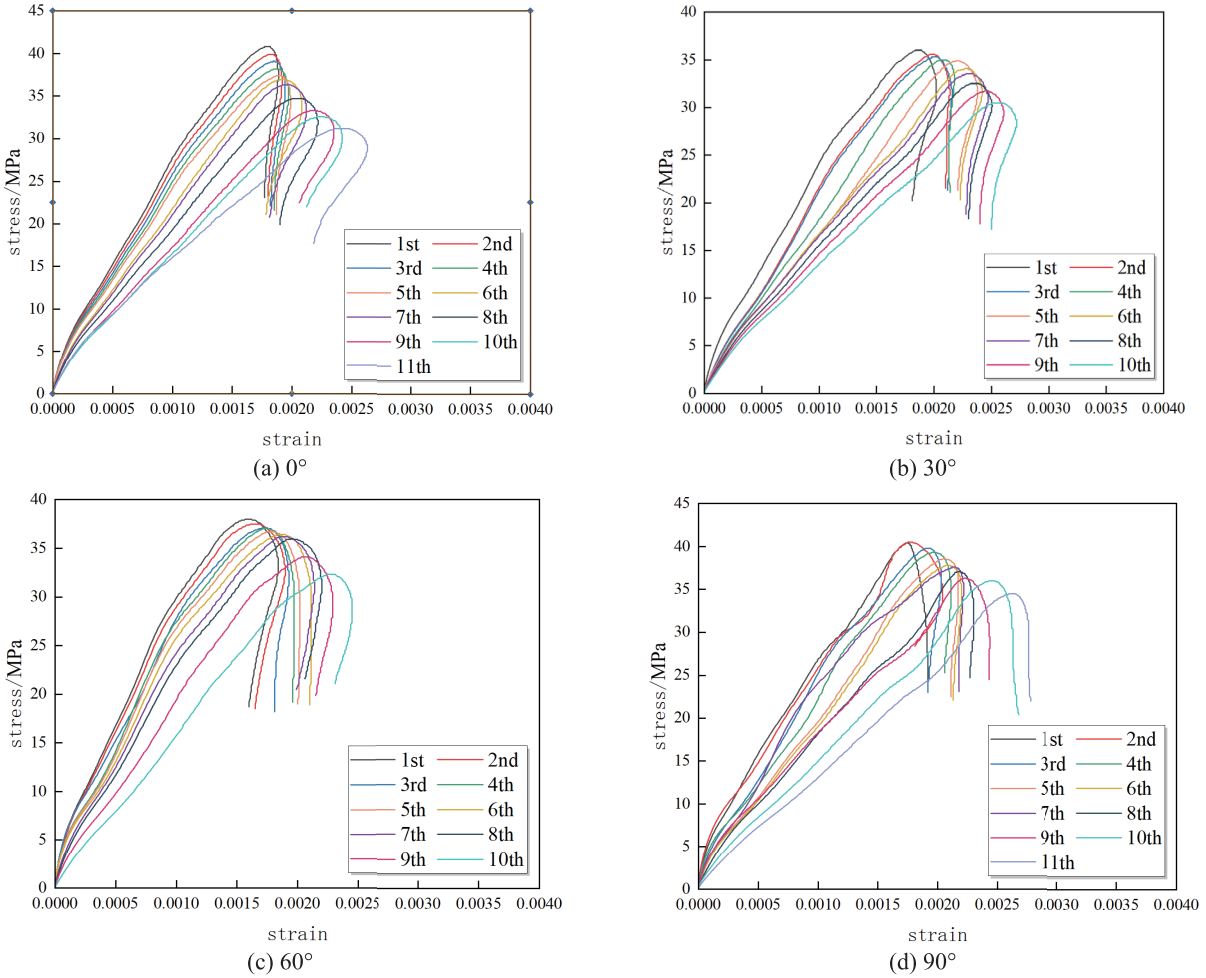

Figure 6. Stress-strain curve of layered rock mass at an impact velocity of 3 m/s.

At an impact velocity of 3 m/s, the layered rock mass specimens with different bedding plane inclinations sustained the greatest number of impacts, and their peak stress and peak strain exhibited no significant changes during the early stage of cyclic loading. This indicates that under low-velocity impact loading, the damage induced

within the rock specimen is relatively minor. The reason is that under this stress wave loading condition, the specimen remains in the linear response stage and has not yet reached its damage threshold.

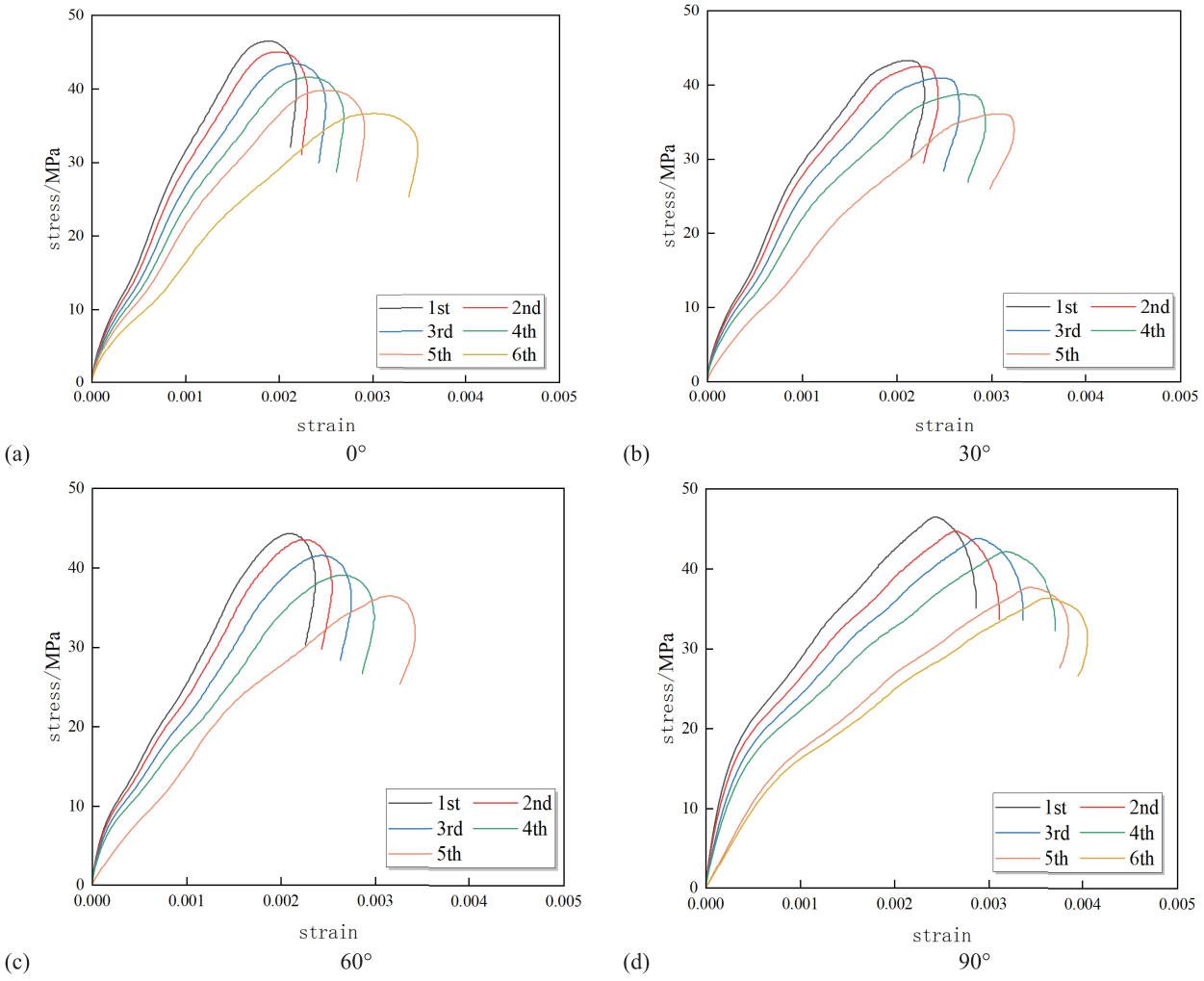

Figure 7. Stress-strain curve of layered rock mass at an impact velocity of 3.35 m/s.

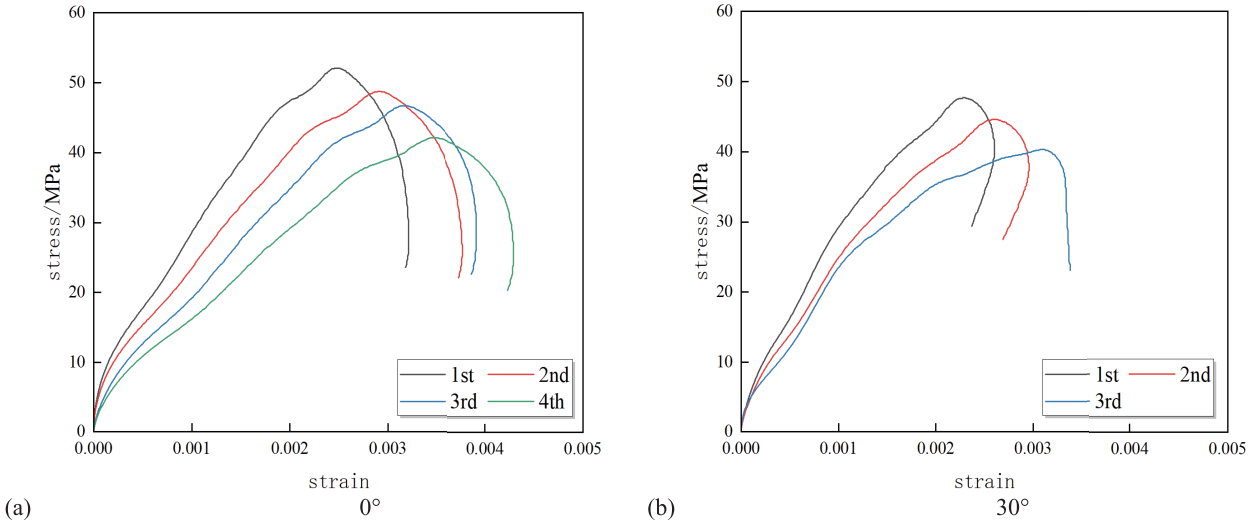

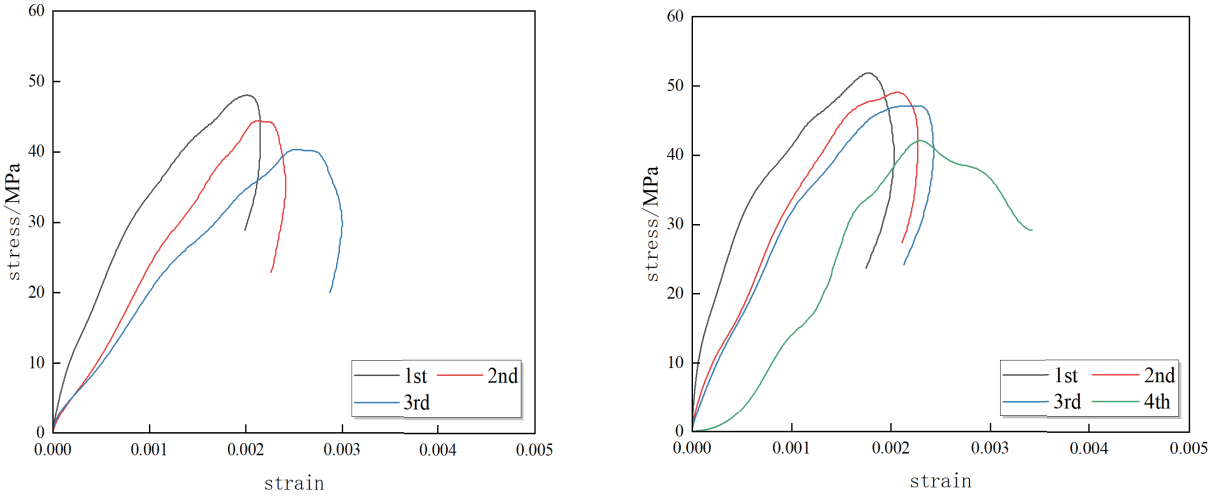

Figure 8. Stress-strain curve of layered rock mass at an impact velocity of 3.65 m/s.

As the impact velocity increases, the number of impacts required to cause failure of the layered rock mass specimens gradually decreases; at an impact velocity of 4 m/s, the number of cyclic impacts sustained by the rock specimens drops to two. This indicates that under high-velocity impact loading, the resistance of the layered rock mass specimens to external loading decreases substantially, demonstrating the mechanical characteristic whereby the specimens undergo continuously increasing deformation and progressive strength deterioration under cyclic impact loading.

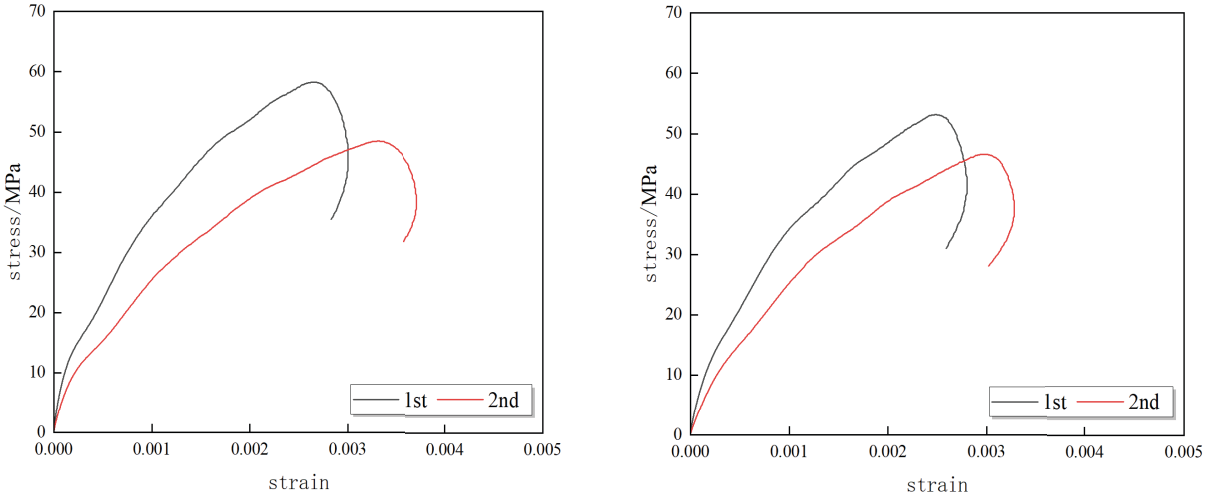

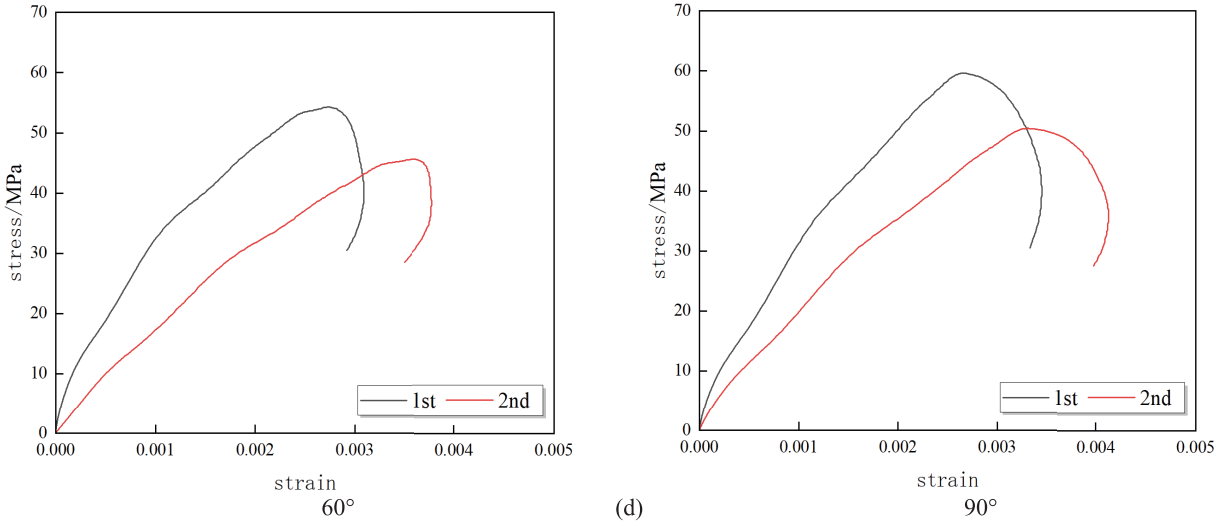

(c) 60° (d) 90°

Figure 9. Stress-strain curve of layered rock mass at an impact velocity of 4 m/s.

From the perspective of the same cyclic impact velocity, the stress–strain curves of layered rock mass specimens with different bedding plane inclinations exhibit similar characteristics. In the early stage of cyclic impact, the stress–strain curves display a distinct "rebound" phenomenon. As the number of impacts increases, the peak stress gradually decreases, the peak strain gradually increases, and the stress–strain curves show a tendency to shift progressively to the right; concurrently, the rebound behavior disappears, and the curves transition to a "semi-open" type.

Comparing specimens with different bedding plane inclinations under the same cyclic impact velocity reveals clear differences in the dynamic mechanical properties. Specimens with inclinations of 0° and 90° require the greatest number of impacts to reach failure, whereas those at 30° and 60° require the fewest. Correspondingly, in terms of peak stress, the 0° and 90° specimens possess the highest dynamic stress strength, while the dynamic mechanical strength of the 30° and 60° specimens is relatively lower. The primary reason is that inclined bedding planes disperse the concentration of the stress wave, causing energy attenuation and reducing the effective stress within the layered rock mass specimen. Moreover, at the endpoints or irregularities of the bedding planes, dynamic stress concentration is prominent; intermediate inclination angles facilitate the coalescence of stress concentration effects within the specimen, thereby inducing macroscopic fracture. It is worth noting that when conducting blasting excavation in tunnels within rock masses exhibiting bedding plane inclinations of 30–60°, the intensity of blasting vibration should be controlled and the layout of blasting holes optimized to prevent excessive propagation of stress waves along the bedding planes.

4. Conclusions

Under cyclic impacts, the dynamic mechanical properties of layered rock are jointly governed by impact velocity and bedding angle, exhibiting a significant synergistic control effect of rate and structure.

(1) Impact velocity determines the rate of damage accumulation and the failure process. At low velocities, the specimen sustains minimal damage, and the stress–strain curve exhibits a "rebound" phenomenon in the early stage while remaining in the linear phase. As the velocity increases, the number of impacts

required for failure drops sharply, and the curve gradually shifts to the right, transitioning to a "half-open" shape, reflecting intensified deformation and continuous strength deterioration.

(2) Bedding angle controls the strength and failure mode of the rock mass. Specimens with 0° and 90° bedding angles exhibit high strength and require more impacts to fail. In contrast, specimens with 30° and 60° bedding angles show lower strength and fail more quickly, because the inclined bedding planes tend to induce stress concentration and form through-going fractures, leading to energy attenuation and reduced effective stress.

(3) The combination of high impact velocity and moderate bedding angles is the most destructive. At bedding angles of 30–60°, the stress wave concentration effect is prominent, and the load-bearing capacity of the specimen decreases significantly. During tunnel blasting excavation under such conditions, special attention should be paid to controlling vibration intensity and optimizing blast-hole layout to prevent excessive propagation of stress waves along the bedding planes.

Funding

Key Project of the Key Project of the Science and Technology Research and Development Program of China State Railway Group Co., Ltd. (Project No.: N2024G049)

Disclosure statement

The author declares no conflict of interest.

References

[1] Li X, Gu D, Lai H, 1993, On the Reasonable Loading Stress Waveforms Determined by Dynamic Stress-Strain Curves of Rocks by SHPB. Explosion and Shock Waves, 1993(2): 125–130.

[2] Zhang B, Zhao J, 2014, A Review of Dynamic Experimental Techniques and Mechanical Behaviour of Rock Materials. Rock Mechanics and Rock Engineering, 47(4): 1411–1478.

[3] Fan C, Yu K, Meng Q, et al., 2018, Stability Evaluation of Weak Slopes Under Heavy Precipitation. Soil Engineering and Foundation, 32(5): 552–558.

[4] Ren W, Li W, Wang J, et al., 2021, Quantitative Study on Influence of Pulse Shaper on Split Hopkinson Pressure Bar (SHPB) Incident Waveform. Transactions of Beijing Institute of Technology, 41(9): 901–910.

[5] Wang J, Li W, Ren W, et al., 2022, Experimental and Numerical Study on the Incident Pulse Similarity Law and Pulse Shaping Technique in SHPB Test. Journal of Vibration and Shock, 41(6): 169–176 + 221.

[6] Jin J, Li X, Chang J, et al., 2013, Stress-Strain Curve and Stress Wave Characteristics of Rock Subjected to Cyclic Impact Loadings. Explosion and Shock Waves, 33(6): 613–619.

[7] Yang R, Li W, Fang S, et al., 2019, Experimental Study on Impact Dynamic Characteristics of Layered Composite Rocks. Chinese Journal of Rock Mechanics and Engineering, 38(9): 1747–1757.

[8] Ma Q, Su Q, Ma D, et al., 2020, SHPB Experimental Study on Dynamic Characteristics and Failure Behaviors of Sandstone Containing Weakly Filled Joints With Various Angles in Deep Roadways. Chinese Journal of Rock Mechanics and Engineering, 39(6): 1104–1116.

[9] Fan Z, 2021, Experimental Study on Dynamic Mechanical Properties of Layered Purple Sand Rock Under Uniaxial Impact, thesis, Xiangtan University.

[10] Zhang J, 2024, Mechanical Properties and Crack Propagation Characteristics of Layered Rock Mass Subjected to Coupled Static-Dynamic Compression, thesis, Shijiazhuang Tiedao University.

[11] Yin Z, Wang J, Zhang Z, et al., 2022, Influence of Static Load on Dynamic Mechanical Properties and Stress Wave Propagation of Jointed Coal Rock Masses. Chinese Journal of Rock Mechanics and Engineering, 41(S2): 3152–3162.

[12] Zhang X, Xu J, Liu Z, et al., 2023, On Mechanical Properties and Energy Evolution Anisotropy of Layered Rocks. Journal of Hunan University of Science and Technology (Natural Science Edition), 38(2): 1–9.

[13] Shang H, 2025, Research on the Dynamic Mechanical Characteristics of Concrete-Sandstone Variable-Angle Composites Under Impact Loading, thesis, Anhui University of Science and Technology.

[14] Wu J, 2024, Study on Mechanical Properties and Failure Mechanism of Composite Layered Rock Under Dynamic Load, thesis, Anhui University of Science and Technology.

[15] Wu B, 2023, Experimental Study on Mechanical Properties of Soft and Hard Composite Rock Mass Under Impact Load, thesis, Xi'an University of Science and Technology.

[16] Wang Z, Zhou Q, Qian M, et al., 2026, Dynamic Characteristics of Hard-Soft Interbedded Rock Mass Under Impact Loading. Blasting, 1–20.

[17] Wang Z, Xing Y, Wu Y, et al., 2026, Research on the Mechanism of Impact Failure of Rock Mass With Different Inclination Filling Joints. Journal of Wuhan University of Technology, 48(1): 58–65.

[18] Wang Z, Guo J, Gao F, et al., 2024, Acoustic Emission Characteristics and Crack Types Evolution of Soft and Hard Interbedded Rock-Like Specimens Under Uniaxial Compression. Chinese Journal of High Pressure Physics, 38(6): 37–51.

[19] Shi Y, Guo Y, Feng G, et al., 2025, Effect of Different Rock Strength on the Uniaxial Compression Bearing Characteristics of Rock-Backfill Body-Rock Combination. Chinese Journal of Rock Mechanics and Engineering, 44(5): 1326–1339.

[20] Wang S, Cheng C, Gong J, et al., 2025, Dynamic Mechanical Properties of Magnesium Oxychloride-Based Titanium Gypsum Concrete After High-Temperature Exposure. Construction and Building Materials, 472: 140841.

Publisher's note

Bio-Byword Scientific Publishing remains neutral with regard to jurisdictional claims in published maps and institutional affiliations.

Journal of Architectural Research and Developmentn, 2026, Volume 10, Issue 5
https://bbwpublisher.com/journal/JARD
Online ISSN: 2208-3537
Print ISSN: 2208-3529

Sensory Reconstruction Design Using Local Materials in Urban Renewal: A Case Study of the Reuse of Waste Bricks and Rubble in the Deji Alley Urban Renewal Project in Ningbo

Ningyan Hu, Yuan Xiong*

Faculty of Innovation and Design, City University of Macau, Macau 999078, China

****Author to whom correspondence should be addressed.***

Copyright: © 2026 Author(s). This is an open-access article distributed under the terms of the Creative Commons Attribution License (CC BY 4.0), permitting distribution and reproduction in any medium, provided the original work is cited.

Abstract: Demolition and relocation of Chinese cities produce considerable construction waste, and old bricks and tiles, as well as the community's memories attached to them, are often discarded, resulting in a loss of place identity. This paper explores the sensory resources in local waste materials and proposes the concept of sensory and material reconstruction based on tactile, auditory and visual experiences. Based on the above research, this paper studies the renewal project of the Deji Alley Historic and Cultural District in Ningbo. Post-completion surveys, sensory attribute tests and user interviews were carried out at some material-reuse sites. The four material-reconstruction strategies in this paper are stacking, collage, vertical masonry and cage-filling. Findings reveal that the original traces retained on reclaimed materials serve as distinctive sensory resources that evoke residents' place-based memories. Moreover, the four strategies require no specialized equipment and are readily applicable to micro-renewal projects in older communities. This study offers a low-cost, low-carbon, and human-centered approach to material reuse in urban renewal.

Keywords: Urban renewal; Local waste materials; Sensory reconstruction; Material grammar; Sense of place

Online publication: Oct 13, 2026

1. Introduction

1.1. Research background

As China's urban development enters a phase of renewal of the existing urban stock, large-scale demolition and relocation associated with urban renewal have improved living conditions while also generating substantial volumes of construction waste. According to statistics from the Ministry of Housing and Urban-Rural Development, China generated approximately 3.5 billion metric tons of construction waste in 2022,

of which more than 40% was reportedly associated with urban renewal and demolition activities. But the percentage of recycling and reuse is less than 10% and much less than the figures given by some countries (70–90%), as it is not yet high enough to be considered as high as possible. The costs of transportation and landfill disposal are estimated to reach up to CNY 100,000 to remove the waste that has been left behind after the demolition of every 10,000 m 2 built-up area. Meanwhile, there are old bricks, tiles, and slabs of bluestone used by the community to remember the community, which are cleared off and substituted with granite paving, aluminum windows and doors, and pressure-treated wood benches. This results in making the city homogenized and the local identity and sense of place eroded. To those who have lived in the region for a long time, the new environment can become alienating, and the material remains of the memories of generations may be forgotten.

Christian Norberg-Schulz is one of the most prominent theorists of architectural phenomenology, and he believed that a place is not just an object, but also has a genius loci, or a character, which is the spirit of the place. The presence of such objects can be seen in the fact that when they are completely removed, it would have been difficult to create a new identity of a place by using the old materials. The quality of open space in cities is also becoming more focused on as urban renewal projects are being implemented with the focus on regenerating the existing neighborhoods rather than creating new ones. The role of open spaces of the city should be taken into consideration not only as a part of the city environment, but also as the space where the local population remembers its own history and preserves its identity. The state of urban public open spaces is quite important because it contributes to the image of the city and the life quality of its citizens. In the context of the reproduction of the urban space, the process of urban renewal does not necessarily mean the restoration of the urban space itself, but the creation of social relations and the distribution of their benefits.

1.2. Research objectives and significance

This study aims to develop design methods for the sensory reconstruction of locally-sourced reclaimed materials in urban regeneration, addressing two deficiencies in contemporary material reuse practices: a focus on material attributes at the expense of sensory experience, and a preference for visual qualities over tactile engagement. This paper has three specific aims. First, an analytical system will be established to describe and evaluate the tactile, auditory and visual sensory characteristics of reclaimed materials, thus complementing engineering-driven mechanical-property research and vision-centered landscape design. Second, it establishes a material-reconstruction grammar of practical, replicable strategies based on field investigations of the completed Deji Alley project, such as stacking, collage, vertical masonry and cage-filling. Each strategy has a particular sense of perception: touch, sound, light and shadow, etc. Third, based on the “Tactile Memory” project in Deji Alley, after the project, post-project surveys, sensory evaluations and user interviews were conducted to explore how the sensory qualities of reclaimed materials shape place memory, and it was investigated whether locally sourced materials with original textures and traces trigger residents’ site-related memories and emotional attachments.

The two types of theoretical contributions are: First, it expands the scope of application for spirit-of-place theory in practice by transforming its conceptual ideas into a material-oriented design approach. Christian Norberg-Schulz’s phenomenological theory proposes a “character” for place identity but provides little methodological guidance on its material application. Through the intermediate concept of sensory reconstruction, this study operationalizes abstract place character into a usable material grammar and

provides a methodological path for phenomenology-oriented design research. Second, it adds an experience-based definition of sustainable design. Existing sustainable-design scholarship prioritizes quantifiable metrics such as carbon output, recyclability and material lifecycles while neglecting user sensory experience. This paper proposes that the concept of sustainability should also include waste reduction and tactile-auditory material experience, integrating material recycling with cultural experience. Practically, the research benefits three urban-renewal stakeholder groups. It offers designers a small-scale, low-technology tool set. The four reconstruction methods do not require special equipment and can be carried out by masons using wire mesh and cement mortar for budget-limited micro-renovation of old areas. Local people can join in waste-material identification, collection, and sorting, create community-accessible designs, and foster a sense of collective ownership. Urban authorities can reduce transport costs, landfill pressure, and carbon emissions at the source to protect the community's memory and social cohesion. Provide evidence-based alternatives to traditional waste disposal for construction waste governance.

2. Literature review

2.1. Current state of domestic research

Recently, research at home on material reuse in urban renewal has been developing rapidly. From an engineering standpoint, Jin Jiangying (2026) has shown that reclaimed brick and tile materials are technically feasible, with a compressive strength of 18 MPa, 32% lower thermal conductivity than traditional clay bricks, and a 72% solid-waste utilisation rate [1]. Fan Tiankui (2026) and Tang Huifang (2026) have examined the system of China's urban renewal policies at the institutional and policy levels and proposed strengthening the top-level design and multidimensional evaluation system [2,3]. In terms of social-risk governance, Li Qiong (2026) and Zhang Zimeng (2026) have used social network analysis to study the development of actual risk, perceived risk and strategic behavior in Shanghai's old-city renewal, and pointed out that perceived risk is central to group polarization and residents' behavioral responses [4,5]. Tang Yan and Hao Ting (2026) studied the implementation of sustainability through the "Shanghai Shangshengxin" project and provided research methods for this study. Wang Weili et al. (2023) proposed using recycled materials as physical catalysts for incremental activation of old urban spaces in the field of renewal design strategies [6]; Wu Yi et al. (2026) developed five strategic categories for existing bridge landscape renewal [7]; Liu Wanhua (2026) put forward three principles for industrial heritage residential renewal that emphasize the retention of spatial context and functional improvement; and Yan Jing and Zhang Tiantian (2026) applied the Analytic Hierarchy Process to evaluate social restoration results in Suzhou Old City [8,9].

In short, all these studies have expanded the knowledge base in many areas: optimization of material performance, institutional construction, social risk management, sustainable design, catalytic renewal, infrastructure renovation, heritage protection and assessment methods. However, a serious deficiency still exists: in engineering, policy, risk governance and spatial planning, most of the discussions have focused on the "material" side—improving durability, standardizing processes, resolving social conflicts and enhancing sustainability—and have paid little attention to the sensory experience of reclaimed materials on people's bodies.

Internationally, the conscious reuse of reclaimed materials in architecture can be traced back to the mid-20th century, and Carlo Scarpa's renovation of the Verona Castle Museum is a typical case. Scarpa embedded damaged stone fragments in the new floors and walls, using a "display-oriented" method to turn ruins into

readable historical materials and prompting later generations to focus on displaying rather than hiding waste materials. Zhang et al. (2026) used spatial syntax to enhance the function of historic districts and optimize pedestrian and bicycle systems, providing quantitative support for waste reuse design [5]. Qin et al. (2025) considered the problem of multi-stakeholder governance and proposed institutional design that balances the demands of residents, public interests and efficiency to achieve renewal [10]. Together, these foreign studies have provided a strong interdisciplinary foundation for historic district renewal and material reuse, but they have also failed to address the sensory dimension that this paper aims to explore.

3. Shortcomings of existing research

Based on the above review, the existing research has three main deficiencies. First, existing research remains predominantly engineering-oriented, with limited attention to sensory experience. Current research on the reuse of construction waste is largely concentrated in engineering and technical fields such as material mechanics, mix design, and durability testing. Research in the field of design studies is relatively weak and primarily focuses on visual aesthetic analysis (color, texture, form), while systematic research on bodily senses such as touch and hearing remains virtually nonexistent.

Second, existing research emphasizes macro-level strategies while providing limited guidance at the methodological and operational levels. When discussing the reuse of waste materials, existing literature often remains at the level of advocating that "reuse should occur" or presents "portfolio-style" showcases of case studies, while providing limited operational guidance on how reclaimed materials can be reused in practice. When faced with a pile of waste materials, designers lack methodological tools that can be referenced, combined, and critically evaluated.

Third, visual-centrism dominates evaluation criteria. Current practices evaluate designs using reclaimed materials primarily in terms of their visual effects, including aesthetic appeal and formal coherence. There is a lack of systematic assessment methods and evaluation criteria for the user's physical experience (such as whether it is comfortable to sit on, whether it makes noise when walked on, or whether it feels cool to the touch).

According to the above weaknesses, this research will help in the following aspects: treating the topic in a sensory aspect, simplifying action-oriented reconstruction syntax, and relying on body experience as the evaluation point. This view should not be seen as a substitute of engineering studies of reclaimed materials or studies of visual aesthetics but it is supposed to complement them in the dimension of the sensory-bodily.

4. Research subjects and methods

4.1. Research site

This research chose the Deji Alley Historical and Cultural Block Renewal Area in Jiangbei District, Ningbo City, Zhejiang Province as the case study site. Deji Alley was constructed in the late Qing dynasty and early Republic of China era, and it is one of the best-preserved traditional alley communities in the old city of Ningbo, with a total area of about 1.2 ha. The area preserves a large number of traditional residential houses built from the late Qing dynasty to the Republic of China era, featuring blue-gray bricks, black tiles, Shikumen gatehouses, and wooden structures. In 2023, this area was included in the pilot project of old urban area renovation and micro-renovation in Jiangbei District. It plans to renovate public space in the partially

collapsed courtyards and idle corner plots while retaining the main structure of historical buildings.

During the renewal process, the demolition of illegal structures and some dilapidated buildings generated a large amount of construction waste. In March 2024, the research team conducted a systematic collection, sorting, and statistical analysis of the on-site waste. The results showed that the total volume of debris was approximately 62 metric tons. Of this, intact or partially intact blue bricks (240 × 115 × 53 mm) accounted for about 35% of the total; fragments of red bricks accounted for about 20%; fragments of small blue roof tiles and cylindrical roof tiles accounted for about 18%; broken ceramic tiles (primarily from old kitchens and bathrooms) accounted for about 10%; concrete fragments accounted for about 12%, and other mixed waste accounted for about 5%. Notably, the surfaces of a large number of bricks and tiles retained their original traces: the blue bricks showed traces of mortar, soot-stained black spots, and signs of weathering and spalling; moss grew on the surfaces of the roof tiles, and their edges showed chips and chips; some broken ceramic tiles still retained their blue-and-white patterns. These are the main sources of material that will be used in the future sensory design.

It must be noted that the paper is a retrospective research study and not a design practice. The project of the actual renewal of the area of Deji Alley was contracted by the Jiangbei District Housing and Urban-Rural Development Bureau of Ningbo City, and the author of this work did not take part in the design or building process of the project itself. Rather, as an independent scientist, the researcher conducted the field survey, material testing, sensory examination, and interviews with the users after the completion of the project (May 2026) to gain general knowledge about the design and methodology of current practices.

4.2. Research methods

This paper is a case study in nature that will involve the analysis of the subject matter, field research, and sensory evaluation, as well as interviews with the users. It involves a literature review of the domestic and foreign literature on architectural waste reuse, place memory, and sensory design, which is necessary to understand the essence of local waste and the concept of reconstruction of the senses, to identify the existing gap in knowledge, and to create the theoretical basis. The survey was then done in the field after the Deji Alley project had been completed, where the materials of the waste were documented by photographing them, categorizing them, estimating their quantity, and how they are distributed in space in terms of location, density, and availability of every node. Moreover, the dimensions, color, integrity, and surface marks of the waste were also recorded. This would be an initial dataset of this survey to conduct further sensory studies and to formulate the grammar of material reconstruction.

The analysis is the core of the project, which includes the case study of four waste nodes already constructed, namely a cage wall at the entrance, a tile pathway on a vertical plane, a mosaic ceramic bench and a low wall made up of broken bricks. The research team did not interfere with the design process in any way but rather recorded and examined the composition of materials, construction processes, sensory experience, spatial relationships of the nodes and then inferred a general reconstruction grammar that can be used to describe the nodes. In order to investigate the relationship between the perception of the material characteristics of wastes and the memory of the place, the physical samples were brought to the potential users, such as long term residents and those who are close by to the place, during the conceptualization stage. Then it was possible to conduct semi-structured interviews to get subjective comments on the recognition of the materials, comfort of the senses, and effects on memory.

5. Analysis of the sensory properties of waste materials and development of a material reconstruction grammar

5.1. Analysis of the sensory properties of waste materials

The research team has been working on the properties of the waste material samples that were taken in the field, at Deji Alley and a property profile was established in three different dimensions: touch, sound and sight.

Tactile Dimension: The blue bricks were tested for surface touch, and 20 samples were taken to measure their thermal conductivity, roughness, and texture. The mean value of the roughness of the surfaces of the blue bricks was much higher than that of the newly produced blue bricks because of the long-term exposure and the remaining mortar. It is possible to sense a small amount of projecting mortar particles on the surface of the brick when it was run by fingers, as well as indentations caused by weathering. This sensation of being both coarse and cozy was reported in the test as similar to the feeling of touching the wall of an old house. The roof tile fragments had sharp edges and moss-covered surfaces which were slightly wet and slippery to the touch. There were also sharp ends of the porcelain pieces, but they were not too hot because they were glazed, which made the contrast of tactile feelings very impressive.

Auditory: When the waste materials are tested in a tapping and stomping test, the whole blue bricks give a dull thud-thud when they come together, and when they hit the red brick pieces, they produce a sound that is much sharper. The sound of the roof tiles crushed by foot pressure sounds like a crackling and it can be heard very well in the alleyways which are old and not so noisy. When rubbed against each other, the porcelain fragments will make a small rustle noise as opposed to the acoustic qualities of the traditional wood-fired porcelain.

Visual Dimensions: The reclaimed materials have mainly bluish-gray, brick red and off-white colors, which constitute a low-saturation warm gray color palette. Surface marks are as follows: mortar residue (irregular white or light grey patches), soot stains (dark brown to black), mossy green spots and weathering cracks. These marks record the history of the use of the building; e.g. the dark brown to black spots with soot show that the brick was formerly situated near a stove or flue.

5.2. Refining the design syntax for sensory reconstruction

This paper has been conducted on the basis of the field survey and analysis of materials of the important nodes in the Deji Alley project that were completed; as a result, four grammars of reconstruction have been discovered with universal applications. The broken bricks are stacked in either a regular or irregular pattern to build volumes and boundaries. In the case of header courses and herringbone patterns, regular stacking is used to create an orderly appearance and tactile rhythm of low walls and the base of feature walls; but in the case of irregular stacking, there is more diversity in texture and relief, which is more suited to natural-style bordering. This was the technique applied in the Deji Alley project where it was used to construct dry-laid low walls using broken bricks, the gaps between the bricks allow the passage of light through them so that they appear to be dappled with light and shadow.

The mosaic art is a way of inserting the shattered ceramic pieces and tiles into the surface of benches or walls in order to create some sort of spots of touch. The ceramic fragments have been glazed and their surfaces are smooth as opposed to the roughness of the cement base, which has blue-and-white patterns randomly distributed on it. Practically, the sharpness of the pieces should be removed by sanding to avoid any chance of scratches.

The vertical laying technique is used to place whole or half tiles vertically and make permeable paving. The arched form of the tiles enables minor elastic distortion when subjected to pressure, creating a wave-like undulation underfoot, and the spaces between tiles allow rainwater to pass through. Therefore, it is particularly suitable for memory trails and small plazas, and even a slight sway and the soft sound of footsteps can be part of a multi-sensory experience.

Lastly, the cage-filling technique involves putting large waste materials like broken bricks and concrete blocks into galvanized steel wire cages to create gabions. The industrial rationality of the wire cages against the warm, ruin-like nature of the infill material makes this technique applicable to entrance signage and retaining walls. Importantly, this process enables the waste material to maintain its original shape without being crushed, hence ensuring that the maximum amount of material traces is preserved.

The four methods are very different in the way they can be applied and used. The stacking technique is a simple one; it can be done quickly, and the boundary and the base can be constructed with ease, though its effectiveness in terms of sensory experience will be determined by how rich the texture of the bricks was. The vertical-laying method is the most labor-intensive, but the tactile contrast (smooth/rough, cold/hot) is the most intense. The vertical-laying method provides the highest auditory and kinesthetic effect, yet the space that is not much walked through has the lowest load-bearing capacity. The wire-cage filling technique is the best to use when there is a need to have good structural integrity as well as to preserve the materials; however, the industrial look of the wire cage may not fit in some of the old areas.

6. Overview of the case study renovation project and site survey

6.1. Site overview and design concept

There is a vacant lot in the shape of a triangle of about 150 square meters within the renewal area of Deji Alley. It was originally a collapsed courtyard, which is surrounded on three sides by ancient blue-brick walls and the ground level is around 0.6 meters below the alleyway. This lot is situated at the center of the neighborhood, where people pass through every day, but it has been left to decay and become littered with construction waste. The location was chosen as a center for renovating public space.

According to the display panels at the site and the public information, the design idea of this project is The Tactile Sense of Memory, which transforms the site from a heap of ruins into a tangible container of memory. The design keeps the historic walls on three sides of the site and uses the on-site construction waste to form four main components: a cage-filled entrance landmark wall, a memory walkway made of vertically laid roof tiles, a tactile bench made of broken ceramic mosaic, and a low wall made of dry-laid broken bricks. The design follows the principles of minimum transportation, keeping the original state, sensation first, and safe strengthening. All materials used are collected on-site without any off-site transportation; the waste materials keep the original shape after simple cleaning and passivation treatment. The construction period was from April to May 2024, and the project duration was about 4 weeks.

6.2. Field survey records

In May 2026 (after project completion), the author conducted systematic on-site observations, surveying, and documentation of the four nodes. See **Table 1**.

Table 1. Field survey records

Node name	Location and dimensions	Materials and construction	Visual impression
Cage-Filling Entrance Signage Wall	On both sides of the site entrance; 2.4 m long, 1.2 m high, and 0.5 m wide on each side	Galvanized steel wire mesh cage (50 × 50 mm mesh size, 3.5 mm wire diameter) filled with large blue bricks and concrete fragments; the front features an arrangement of smoke-stained black-spotted bricks	Sunlight casts shadows through the mesh; when a finger is inserted into the mesh, one can feel the surfaces of different materials, with distinct tactile differences
Vertically Stacked Tile Memory Path	In the center of the site, a 12-meter-long, 1.5-meter-wide curved path	Approximately 850 small blue roof tiles are vertically embedded in a coarse sand base, with 3 cm protruding above the surface; the edges are bordered with red brick fragments	While walking, the soles of the feet sense a 5–8 mm elastic give, accompanied by a faint "rustling" sound
Tactile Bench with Shattered Ceramic Mosaic	Located beneath the old wall on the north side, measuring 4.5 m long, 0.5 m wide, and 0.45 m high	The surface of the plain concrete base is embedded with broken ceramic tiles retaining their blue-and-white patterns; the edges are ground to a dull finish and coated with an epoxy resin sealer	To the touch, smooth ceramic tiles alternate with the rough base, creating rapid changes in perceived temperature
Low dry-laid brick wall	Located along the southern boundary of the site; 8 m long, 0.6 m high	Dry-laid red brick fragments without mortar, filled internally with fine-grained crushed stone, and topped with intact blue bricks	Porosity is approximately 15%, allowing for unobstructed views and air circulation; light filters through the gaps, creating dappled patterns of light and shadow

Research Summary: The four nodes employ four distinct design approaches—cage filling, vertical masonry, mosaic, and stacking—to create differentiated sensory experiences on the tactile, auditory, and visual levels, collectively demonstrating the design potential of local waste materials across multiple sensory dimensions.

6.3. Construction information and structural key points

Based on site inspections and interviews with construction workers (two masons), this study documented the following structural details: Some blue bricks in the wire-mesh-filled walls that exceeded 300 mm in size had to be broken down to less than 200 mm to fit into the wire mesh; a 5-cm-thick cement-stabilized crushed stone base was added beneath the sand layer of the tile walkway to enhance load-bearing capacity; the ceramic fragments in the broken-ceramic benches were embedded to a depth of approximately two-thirds of their thickness (about 3–4 mm), and the surface was coated with a transparent epoxy resin sealer to prevent detachment. These construction details safeguard the structural integrity and longevity of the project.

7. Effect evaluation and discussion

7.1. User feedback and effect evaluation

The author interviewed the local residents and passersby in May 2026 using semi-structured interviews. The total number of people interviewed was 15, with 9 long-term residents (those who had lived in Deji Alley for over 10 years) and 6 nearby users (residents of neighboring areas or business owners) aged between 32 and 78.

Table 2. User feedback and effect evaluation

Evaluation dimensions	Key findings	Typical feedback	Statistical data
Material recognition	The vast majority of respondents were able to accurately identify the source of the materials	Local residents identified the soot-stained bricks as having once belonged to the chimney of the Wang family's old kitchen	14/15 (93%)
Sensory comfort	The springy feel of the walkway received positive reviews, but poses safety risks for the elderly; the benches were generally recognized as cool and comfortable to sit on	Walking on the tile path is springy and enjoyable; older adults need to walk more slowly; the broken-ceramic benches feel cool to the touch and have a smooth surface	Walkway: 11/15 (73%) Benches: 14/15 (93%)
Memory-triggering effect	The memory-triggering effect was significant among original residents, but weaker among non-original residents	The sound of footsteps on the tiles reminds one of eaves; the unevenness of the brickwork brings to mind leaning against old walls; the blue-and-white patterns of the ceramic tiles resonate with memories of water jars	Long-term residents: 8/9 (89%) Non-residents: 3/6 (50%) Total: 12/15 (80%)

In general, the wastes of local origin were found to be more useful in terms of their ability to be identified and to create a memory of the waste materials used by the long-term residents. The sensory comfort was also good on the whole, though there is a need to focus on the safety of the tile walkway that is upright-laid for the elderly.

7.2. Discussion on construction feasibility and durability

Concerning the construction feasibility and durability issues that were brought up in the review, the research team has gathered the following particular data and observations based on the on-site testing and structural analysis:

The pathway was constructed in such a way that it is laid vertically and its compressive strength, as well as slip resistance, are quite high (within the first month of its completion, there were 30-50 people who passed through the site per day), and the research team has tested the friction coefficient of the tiles using a pendulum-type test. The mean value of BPN was 68 in dry state and 55 in wet state, and both values were higher than the minimum value of 45 in the Code for Design of Accessibility, which requires the surface to be non-slippery (GB 50763-2012). Nevertheless, this path can only be used in low-traffic areas within the community but cannot be used as a major street or an emergency exit.

(1) The Broken Ceramic Tile Puzzle Bench Safety

It was not until all the edges of the tiles were ground and then covered with an epoxy resin sealer that there was no sharpness in the surface. The simulated usage test (500 sit-to-stand tests, 75 kg load) revealed that there were no broken or detached tile. But, at the lowest temperature conditions (the historical low temperature in Ningbo is -5C), the epoxy resin can be brittle; hence, it is advisable to make a routine check on the sealing layer every two years.

(2) Long-term durability assessment

According to aging information on comparable traditional brick-and-tile buildings in the Ningbo region, the physical lifespan of blue bricks when subjected to normal outdoor conditions (except prolonged water immersion) can be over 50 years. Nevertheless, a portion of the blue bricks that will be utilized in this project has already developed weathering cracks and about 15 percent of the bricks have a layer of weathering more than 5 mm thick on their surfaces. In accordance with the applicable provisions on the durability of brick masonry in the Code for Design of Masonry Structures (GB 50003-2011), it is advised to introduce a

routine inspection system once every five years, which should be aimed at checking the extent of powdering in heavily weathered bricks and the rate of fragmentation of tiles, and replacing powdery materials where required.

(3) Compliance discussion

Urban public space construction acceptance is currently based on two main technical specifications, namely the Technical Specifications of Urban Road Maintenance (CJJ 36-2016) and the Specifications of Construction and Acceptance of Landscape Gardening Projects (CJJ 82-2012). Although these standards provide clear quantitative criteria of strength, levelness and durability of paving materials, they were developed with new, industrially produced materials in mind and do not cover reuse of waste materials. In Deji Alley project, structural acceptance requirements were satisfied by a composite design of recycled materials + new base materials (e.g., roof tiles + cement-stabilized crushed stone base, broken ceramics + concrete base), whereas the proportion of recycled material in the surface layer was referred to as an artistic expression instead of a structural layer, thus bypassing some compliance hurdles.

7.3. Discussion on the mechanisms linking the syntax of sensory reconstruction and place memory

Based on the above studies and analyses, this study has further explored the mechanism relating the sensory qualities of waste materials to place memory. The practice of the Deji Alley project proves that it is exactly those imperfect qualities on the surface of waste materials, such as cement paste, soot stain, moss, weathered cracks, etc., that act as the key mediators to awaken residents' place memories. Different from smooth and homogeneous new materials, these traces contain specific information about everyday life: a blue brick stained with soot may recall a family's kitchen fireplace; a moss-covered roof tile may remind one of the eaves of an old house. This association is especially strong in the tactile sense: the friction between finger and rough brick surface, the rocking sensation underfoot when stepping on an elastic tile, the change in temperature between skin and smooth, cool ceramic tile surface; these physical sensations subconsciously trigger residents' tactile memories of scenes from their previous lives.

7.4. Analysis of the mechanisms of sensory reconstruction of waste materials

The Deji Alley project demonstrates that the so-called flaws on the surface of waste materials, such as adhering mortar, soot stains, moss, and weathering cracks, are precisely what trigger place memory. Therefore, a different view of abandonment and value is formed in sensory design; instead of perceiving engineering remnants as defects to be rectified, they are recognized as materials that record the story of a building over time. Old bricks and tiles are not uniform new materials; they carry rich concrete information about life in the past, such as a soot-stained blue brick recalling a family kitchen or a moss-covered tile remembering the eaves of an old house. Thus, the waste that once had to be concealed is now a carrier of memory that can be displayed actively.

Based on the interview data in this study, tactile and auditory feedback, such as rough texture, a springy sensation underfoot and the sound of footsteps, are more strongly associated with personal memory than visual perception alone. This result provides theoretical support for Merleau-Ponty's phenomenology of the body; that is, memory is not generated by abstract ideas but by the direct engagement of the body in life. Waste materials can be felt directly through touch to create a kind of waste-feeling; thus, aesthetic judgment will be bypassed, and at a more fundamental level, people will simply experience "what it feels like".

Therefore, when using waste materials in design, the emphasis should be on the properties of the materials themselves rather than on visual appeal; the purpose is not to build beautiful environments but to create sensory memories.

The Deji Alley project is also a design solution for the idea of functional renewal. Most urban renewal efforts have focused on functional criteria, such as improving drainage efficiency, paving integrity, facility perfection, etc., and have thus created usable but unappealing spaces. Sensory reconstruction makes sensibility an object of design: the elastic flexibility of the tile walkway, the tactile quality of the broken-ceramic benches, and the dappled light filtering through the dry-stacked low walls have no practical use yet can be seen, touched, and thus remembered. Thus, the Design Logic moves from “landscape to be seen” to “environment to be experienced”, thereby creating a link between the material and the spiritual.

7.5. Four design principles for the sensory reconstruction of waste materials

Based on the above analysis, this study proposes four principles for the sensory reconstruction of waste materials:

(1) Principle 1

Priority on Preserving Traces. It is important to maintain the original traces on the surface of the waste (mortar, soot, moss, cracks) as it is not possible to erase or cover them.

(2) Principle 2

Tactile Experience Takes Precedence Over Visual Presentation. Design decisions should prioritize the tactile qualities of materials (rough/smooth, warm/cool, soft/hard) over visual effects.

(3) Principle 3

Low-Tech Adaptation. The four reconstruction methods do not need special equipment and can be used in micro-renovations of older communities with small budgets and limited construction conditions.

(4) Principle 4

Safety and durability should be considered as the primary design specifications. In addition to focusing on sensory experience, sharp edges need to be rounded off, and a periodic inspection system needs to be put in place for severely weathered parts.

8. Conclusion

This study explores the concept of local waste materials in urban renewal through the lens of sensory reconstruction, defined as a material reconstruction process grounded in tactile, auditory, and kinetic experiences. Through post-project research and analysis of the Deji Alley project, the study identifies four replicable design grammars: stacking, collage, vertical masonry, and cage-filling, and examines the tactile mechanism linking the original traces of waste materials to site memory. The three main results are shown in the literature review, field survey and case studies.

First, the original traces left by the reclaimed materials, such as mortar residue, soot stains, moss growth and weathering cracks, are special sensory resources that can effectively trigger the place memories of residents. These imperfect surfaces of new materials are not smooth and uniform; they have accumulated real-life experiences and thus carry tactile memories and emotions. Second, the four reconstruction methods are both feasible and scalable. Requiring no special equipment and executable by masonry workers with wire cages and cement mortar, they are suitable for small-scale renovation projects in older neighborhoods

with limited budgets, such as entrance signs, paving, seating, boundary features, etc. Third, the standards for judging waste-material design should prioritize sensory experience over visual appeal. The study proposes that tactile, seating, and auditory experiences should serve as the main assessment indicators, placing the user's physical engagement at the center of evaluation to promote neighborhood integration, the inheritance of historical memory, and urban intensification.

This study also has some deficiencies: severely weathered bricks may deteriorate in five to ten years and require frequent inspection; current construction standards are geared towards new materials and may not meet compliance requirements for waste-material use. In the future, three-dimensional scanning and robotic mosaic technology can be used to create more complex topological structures from waste materials, and relevant policies will also be improved.

Disclosure statement

The authors declare no conflict of interest.

References

[1] Jin J, 2026, Research on the Innovative Application of Green Energy-Saving Technologies in Modern Brick-and-Tile Architecture. Bricks and Tiles, 2026(3): 108–110.

[2] Fan T, Tang H, 2026, A Discussion on the Policy Framework and Institutional System of Urban Renewal. China Construction, 2026(6): 20–22.

[3] Tang Y, Hao T, 2026, A Study on Urban Spatial Design Under the Concept of Sustainable Development. Footwear Craftsmanship and Design, 6(6): 164–166.

[4] Li Q, Zhang Z, 2026, A Game Theory Study on the Evolution of Social Risks in Urban Renewal Contexts: A Case Study of the Old Town Renovation in District L. Research on Urban Development, 33(2): 85–91.

[5] Zhang W, Wang P, Chen Y, et al., 2026, Renovation Design of an Urban Historic District Based on Space Syntax: A Case Study of the Qianmen Area in Beijing. Buildings, 16(1): 226.

[6] Wang W, Wang Q, Jin M, 2023, Urban Renewal Design Based on Catalyst Theory: A Case Study of the Old Town Renovation in Yanjin County. Urban Renewal, 2023(2): 48–49.

[7] Wu Y, Wu A, Jiang H, et al., 2026, Analysis of Design Strategies for the Landscape Renewal of Existing Urban Bridges in the Context of Urban Renewal. Anhui Architecture, 33(1): 20–21 + 39.

[8] Liu W, 2025, A Study on the Design of Industrial Heritage Residential Area Renewal in the Context of Urban Renewal. Beauty and the Times (Urban Edition), 2025(12): 24–26.

[9] Yan J, Zhang T, 2025, Urban Renewal Design for Suzhou's Old City District Based on Socially Restorative Urbanism. Famous Cities of China, 39(10): 16–25.

[10] Qin B, Han S, Li Y, et al., 2025, Research on the Formation Mechanism of Multi-Stakeholder Collaborative Governance in the Renovation of Chinese Old Urban Residential Areas. Buildings, 15(15): 2686.

Publisher's note

Bio-Byword Scientific Publishing remains neutral with regard to jurisdictional claims in published maps and institutional affiliations.

Journal of Architectural Research and Development, 2026, Volume 10, Issue 5
https://bbwpublisher.com/journal/JARD
Online ISSN: 2208-3537
Print ISSN: 2208-3529

Research on Subway Tunnel Construction Monitoring Technology for Complex Urban Environments

Can Chen[1], Xi Ni[2]

[1]Chongqing Energy College, Chongqing 402260, China
[2]China Railway Southwest Research Institute Co., Ltd., Chengdu 610000, Sichuan, China

Copyright: © 2026 Author(s). This is an open-access article distributed under the terms of the Creative Commons Attribution License (CC BY 4.0), permitting distribution and reproduction in any medium, provided the original work is cited.

Abstract: Addressing the technical challenges of subway tunnel construction in complex urban environments—including intricate geological conditions, sensitive surrounding environments, and high safety risks—this study, based on the Phase II project of Guangzhou Metro Line 13, conducts a comprehensive investigation into the entire process of subway tunnel construction monitoring. Through systematic identification of construction risk factors under complex urban conditions, a refined risk engineering checklist is compiled, a customized monitoring system is designed, a risk identificationassessmentearly warning framework is established with operable emergency plans, standardized monitoring operation procedures are formulated, and dynamic optimization of the monitoring scheme is achieved. The research develops a set of monitoring technical systems adaptable to complex urban environments, providing a practical and feasible technical solution and engineering practice reference for subway tunnel construction monitoring under such conditions.

Keywords: Complex urban environment; Subway tunnel construction; Construction monitoring; Monitoring system design

Online publication: October 28, 2026

1. Introduction

The accelerating pace of urbanization has increasingly positioned urban rail transit as a core component of comprehensive urban transportation systems. By March 2025, 326 urban rail transit lines had been opened and operated in 54 Chinese cities, with a total operational mileage of 10,975.8 km. The Outline of the 14th FiveYear Plan and the LongRange Objectives Through 2035 explicitly sets a development target of adding 3,000 km of new urban rail transit operational mileage [1,2]. While the scale of subway tunnel construction continues to expand, construction in urban core areas is frequently plagued by safety accidents due to complex geology and sensitive surrounding environments, often resulting in multiple safety losses.

Construction monitoring serves as the core means of controlling engineering safety. Although domestic practices have progressed toward automation and informatization, incorporating technologies such as the Internet of Things, existing studies predominantly focus on single scenarios, and generalized monitoring models suffer from issues such as unreasonable resource allocation, rendering them inadequate for the demands of complex construction environments. To address this, the present study takes the Phase II project of Guangzhou Metro Line 13 as the subject, conducting a fullprocess investigation of construction monitoring technology, developing a monitoring technical system tailored to complex urban environments, overcoming the limitations of traditional models, enhancing monitoring efficiency and effectiveness, and contributing to the green, safe, and sustainable construction of rail transit.

2. Risk factor identification and checklist compilation for subway tunnel construction in complex urban environments

2.1. Project overview and complex environmental characteristics

This study is based on the Phase II project of Guangzhou Metro Line 13, selecting the Huacheng Square North Station and the section from Magang Station to Tianhe Park Station as typical research objects. The project includes complex sections such as undercrossing the Guangyuan Expressway and waterrich sand layers, presenting difficulties including complex geological conditions, sensitive surrounding environments, high construction technique requirements, and constrained working spaces, which are prone to safety risks such as structural deformation and environmental damage. The characteristics are representative of subway tunnel construction in urban settings, and the research findings can be extended to similar projects.

2.2. Systematic identification of multidimensional construction risk factors

The research systematically identifies construction risk factors from multiple dimensions. First, common risks are summarized into five major categories, including geological hazards and structural deformation. Second, the risk patterns under different construction scenarios are compared to identify scenariospecific risks such as waterrich sand layers and undercrossing of main roads. Finally, combined with the engineering investigation reports and onsite surveys, the specific risks applicable to this project are precisely identified. A systematic identification framework is ultimately established across four dimensions: engineering geology, surrounding environment, construction technology, and construction management, encompassing various specific risks including stratum settlement, building tilting, segment displacement, and untimely monitoring.

2.3. Compilation of a refined risk engineering checklist

Based on the systematic identification, this study deeply integrates macrolevel risks with the actual geological conditions, environmental factors, and construction techniques of the project, conducting customized risk analysis. Inapplicable common risks are eliminated, projectspecific risks are refined, and the source, scope of influence, triggering conditions, and severity of each risk are clearly defined. A refined risk engineering checklist is then compiled, with each risk annotated with its corresponding engineering location, type, grade, and associated factors, enabling precise positioning and systematic management of risk points. This checklist breaks through the limitations of traditional generalized approaches and serves as the core basis for subsequent monitoring design, risk early warning, and emergency response.

3. Riskoriented customized design of the monitoring system for subway tunnel construction

3.1. Determination of monitoring content and monitoring objects

Based on the refined risk project inventory as the core reference, and taking into account the construction characteristics of typical stations and sections of Phase II of Guangzhou Metro Line 13, this study carries out a riskoriented customized design of the monitoring system, achieving precise alignment between the monitoring system and construction risks. In determining the monitoring content and objects, the three key dimensions—structural deformation of the works, changes in the surrounding environment, and stress states during construction—are taken as the primary focus. Accordingly, the core monitoring items include surface heave and settlement, settlement and inclination of buildings and structures, segment displacement, settlement of underground pipelines, and support axial force. The monitoring objects are precisely targeted at the highrisk locations identified in the inventory, covering the deep foundation pit of Huacheng Square North Station, the waterrich sand layer section between Magang Station and Tianhe Park Station, the section underneath the Guangyuan Expressway, and the construction zones adjacent to important buildings, structures and underground pipelines.

3.2. Selection of monitoring instruments and accuracy specifications

The selection of monitoring instruments follows the principles of "precision, automation, and strong adaptability". Dedicated equipment is matched to different monitoring items: for example, total stations are used for surface and building settlement monitoring, crack gauges for crack observation, and axial force gauges and water level gauges for monitoring support axial force and groundwater level, respectively. At the same time, automated equipment is introduced to reduce manual intervention and improve data acquisition efficiency [3]. In accordance with the project risk control requirements and relevant standards, specific accuracy specifications for each item are established, with clear parameters such as instrument measurement error and resolution. For instance, the accuracy for surface heave and settlement monitoring is controlled within ± 2 mm, and the inclination accuracy for buildings and structures within ± 0.1‰, thereby ensuring the reliability of the monitoring data.

3.3. Dynamic design of monitoring frequency and period

The monitoring frequency and period are not based on a fixed pattern but adopt a dynamic design approach. The monitoring period is divided into three phases according to the construction schedule: the preconstruction baseline period, the construction period, and the postconstruction stabilization period. During the construction period, the frequency is adjusted according to the risk level of each work procedure. For highrisk procedures such as deep foundation pit excavation and underpassing of major roads, the frequency is set at once per day; for periods with stable procedures and lower risk, the frequency is reduced to once every three days. In parallel, a dynamic adjustment mechanism is established: when monitoring data become abnormal or a risk alert is triggered, the frequency is immediately increased to once every half day or even realtime monitoring, until the project returns to a stable state.

3.4. Monitoring control indicators and layout scheme of monitoring points

The formulation of monitoring control indicators follows relevant specifications, engineering geological conditions, and safety requirements for surrounding facilities. Based on the risk prevention and control

objectives, warning values and control values for each monitoring parameter are clearly defined. For example, the warning value for surface heave and settlement is set at +10 mm/30 mm, while the control values for building settlement are differentiated according to structure type and safety grade, thus achieving quantitative risk management for construction. The layout of monitoring points adheres to the principles of "full coverage, clear emphasis, ease of monitoring, and resistance to damage". First, a deformation monitoring network comprising reference points, working base points, and deformation monitoring points is established; then, specialized monitoring points are arranged for different monitoring items, precisely covering highrisk locations and sensitive areas. At the same time, a point inventory is compiled, specifying numbering, locations, monitoring contents and frequencies, so as to achieve standardized management of monitoring points and ensure comprehensive and accurate capture of changes in the monitored objects [4].

4. Metro tunnel construction monitoring risk early warning and emergency technology system

4.1. Risk assessment model and classification of monitoring risk levels

Based on the actual conditions of the second phase of Guangzhou Metro Line 13, this study constructed a construction risk assessment model adapted to the complex urban environment. Taking a refined risk inventory as the foundation, the model incorporates monitoring data as a core quantitative indicator, and integrates the probability of risk occurrence, the degree of hazard, and the scope of impact. Through a combination of qualitative and quantitative methods, it analyzes the deviation between monitoring data and control indicators, and quantitatively evaluates the status of each risk factor. According to the assessment results, construction monitoring risks are classified into three levels: Level I alert status (data approaching the warning value), Level II alarm status (data reaching the warning value), and Level III emergency status (data exceeding the control value), with clear criteria for determination, thereby enabling graded control of construction risks [5].

4.2. Construction of a multiindicator linkage risk early warning system

Based on the risk level classification, this study constructed a multiindicator linkage risk early warning system to overcome the limitations of singleindicator warnings. A realtime analysis mechanism for monitoring data was established to rapidly compare the data against the risk level criteria. Three levels of warning signals—yellow, orange, and red—were set to correspond to different risk levels, with clearly defined triggering conditions. Multiindicator linkage warning rules were formulated: when a single indicator reaches the warning value or when multiple related indicators exhibit anomalies, the corresponding warning is immediately triggered. Through onsite notifications and system push messages, the information is promptly delivered to relevant management personnel, ensuring efficient transmission of early warnings.

4.3. Formulation of graded prevention and control technical measures

Targeting different risk levels, this study formulated graded prevention and control technical measures to ensure precision and operability. Under the Level I yellow warning, monitoring data are reexamined, causative factors are investigated, monitoring frequency is increased, highrisk procedures are suspended, and preventive measures are implemented. Under the Level II orange warning, construction in the affected area is halted, expert evaluation is organized, and a specialized plan is developed; protective measures such as

reinforcement and support are applied to the project and surrounding environment, while realtime monitoring of risk changes is maintained. Under the Level III red warning, emergency response is immediately activated, construction personnel are evacuated, and the hazardous area is cordoned off; experts develop an emergency disposal plan, and rapid riskcontrol measures such as emergency reinforcement and drainage and pressure relief are executed.

4.4. Compilation of operational emergency response plans

Furthermore, based on the risk inventory, level classification, and graded prevention and control measures, and in combination with the construction characteristics and onsite conditions, operational emergency response plans were compiled. The plans clearly define the emergency organization structure and the responsibilities of each level and team, and standardize the complete emergency response procedures from warning trigger to project resumption. Emergency resources such as support materials and drainage equipment are preplanned, and professional rescue teams are assigned. Regular emergency drills are scheduled, and the plans are optimized based on drill results to enhance their practicality, ensuring rapid and effective response when unforeseen risks occur.

5. Standardized monitoring operations and data processing technology for metro tunnel construction

5.1. Formulation of standardized technical procedures for monitoring operations

Based on the monitoring item list, measurement point list, and onsite construction conditions, a standardized operating procedure was developed encompassing monitoring preparation, sensor installation, data acquisition, onsite recording, and data transmission [6]. During the preparation phase, instrument calibration and onsite reconnaissance are performed to ensure equipment condition and operational environment. In the installation phase, construction is carried out strictly according to the plan, with proper marking and protection of measurement points. In the acquisition phase, data are collected at the required frequency and precision to ensure their originality and accuracy. In the recording phase, detailed documentation of collected information and site conditions is made. In the transmission phase, raw data are uploaded to the management system in a timely manner for realtime storage and sharing. These standardized procedures define the operational and quality standards for each step, reducing human error and enhancing the level of standardization in monitoring operations.

5.2. Precise data acquisition and quality control for monitoring data

To ensure the precision and reliability of monitoring data, a fullprocess quality control system encompassing acquisition, transmission, and verification has been established [7]. During the acquisition phase, instruments are regularly calibrated and maintained, professional training for personnel is conducted, and automated equipment is deployed to reduce manual errors. In the transmission phase, encrypted transmission methods are employed to prevent data loss or tampering. In the verification phase, a dualpersonnel verification and multilevel review mechanism is implemented, with comparative analysis of data from the same points and onsite remeasurement for abnormal data. To address the issue of sensor drift and failure in complex environments, dualsensor redundant nodes are deployed in key areas, with regular equipment calibration and a fault early warning mechanism, thereby avoiding distortion of monitoring data.

5.3. Monitoring data processing and analysis techniques

Scientifically rigorous processing and indepth analysis are conducted on the monitoring data that have passed quality control, so as to uncover the inherent engineering patterns. The first step is data preprocessing, including elimination of outliers and imputation of missing values, to ensure data integrity and validity. Subsequently, statistical analysis and curve fitting are performed to generate spatiotemporal variation curves for each monitoring item, visually presenting the deformation patterns and development trends of the engineering structure and surrounding environment. Finally, in combination with the engineering geology and construction techniques, the causes of data variations are analyzed, the engineering stability is assessed, and potential risks are identified, providing data support for adjustment and optimization of the construction plan. Meanwhile, a monitoring data management system has been established to realize informationbased data management, supporting query, statistics, and visual display, thereby improving data processing efficiency.

5.4. Technical specifications for monitoring report compilation

Technical specifications for the compilation of monitoring reports have been formulated, clarifying the content, format, and reporting cycles. Reports are compiled in three categories: daily, phasebased, and final. Daily reports are prepared each day, reflecting the monitoring data of that day, changes, and onsite construction status. Phasebased reports are compiled at each construction milestone, summarizing monitoring data, analyzing deformation patterns, evaluating risks, and providing prevention and control recommendations. The final report, prepared upon completion of monitoring work, provides a comprehensive summary of the monitoring activities, assesses engineering stability, and offers technical recommendations. The report content is required to be comprehensive and detailed, covering key elements such as project overview, monitoring system design, operation implementation, data processing, and risk assessment, with appended data tables and variation curves, thereby providing a reliable and comprehensive basis for construction management decisionmaking.

6. Monitoring information feedback and dynamic optimization technology of monitoring schemes

6.1. Realtime feedback technical mechanism for monitoring information

A comprehensive monitoring information feedback mechanism has been established, specifying the content, procedures, recipients, and timelines of feedback, to ensure realtime and efficient information transmission. The feedback content includes monitoring data, change analysis, risk warnings, and onsite construction conditions. A threetier procedure involving “onsite monitoring personnel–technical management department–construction decisionmaking department” is adopted to ensure that data and abnormal conditions are transmitted level by level and analyzed promptly. The feedback covers relevant entities and personnel including construction management, technical staff, construction workers, and supervision units. Routine information is fed back within 24 hours, while earlywarning information is reported immediately. Additionally, a multichannel feedback network is constructed by combining online data push with offline meetings and written reports.

6.2. Technical implementation of dynamic optimization of monitoring schemes

Based on monitoring feedback results, construction progress, risk changes, and onsite conditions, the

monitoring scheme is dynamically optimized. When data indicate that deformation has stabilized and risks have decreased, the monitoring frequency is adjusted and monitoring points in lowrisk areas are reduced. When entering new construction phases, emerging new risks, or encountering abnormal data, monitoring content is supplemented, monitoring points and frequency in highrisk areas are increased, and instrument selection and accuracy are optimized. When construction conditions change, the layout of monitoring points and operational procedures are adjusted. The optimization follows the principles of "riskoriented, demandbased adjustment, and precisiondriven efficiency", adapting to the actual needs of the project.

6.3. Technical verification of the optimized monitoring scheme

Technical verification is carried out on the optimized scheme to ensure its scientific soundness and operability. The scheme is applied to the actual construction of Guangzhou Metro Line 13 Phase II. Its accuracy and effectiveness are validated by collecting data and analyzing structural and environmental changes. Expert reviews are organized to verify the scientific basis from a theoretical perspective. Further refinements are made based on onsite feedback to ensure that the scheme meets construction needs, thereby providing reliable monitoring support for subway tunnel construction.

7. Conclusions

Monitoring of subway tunnel construction in complex urban environments is a core technical means for ensuring construction safety and promoting the sustainable development of urban rail transit construction. In response to the shortcomings of traditional generic monitoring models, such as insufficient targeting and low efficiency, this study, based on the Guangzhou Metro Line 13 Phase II project, has conducted a fullprocess technical study on monitoring for subway tunnel construction, yielding a series of research outcomes. The resulting monitoring schemes, monitoring reports, and technical research reports provide feasible technical solutions and engineering practice references for subway tunnel construction monitoring in complex urban environments, and hold significant practical relevance for advancing innovation and development of construction monitoring technologies in China's subway construction sector.

Funding

Research on Monitoring Technology for Subway Tunnel Construction in Complex Urban Environments (Project No.: ZRKX202501)

Disclosure statement

The authors declare no conflict of interest.

References

[1] Guangming Online, 2025, In March This Year, 326 Urban Rail Transit Lines Were in Operation in 54 Cities Across the Country, Carrying 2.88 Billion Passenger Trips.

[2] People's Daily Online, 2021, The 14th Five-Year Plan for National Economic and Social Development of the

People's Republic of China and the Outline of Long-Term Objectives for 2035.

[3] Yuan Q, Chi G, Li X, et al., 2026, Detection, Localization, and Control Strategies for Leakage in Urban Water Supply Networks. Water Purification Technology, 45(2): 1–11 + 59.

[4] Duan G, 2025, Application of Intelligent Detection Technology in Routine Maintenance Inspection of Highway Tunnels. Transport Manager World, 2025(34): 112–114.

[5] Shi M, 2025, Brief Analysis of Monitoring and Early Warning Technology for Geological Hazards on Mountainous Expressway Slopes. China ITS Journal, 2025(S2): 302–305.

[6] Cheng Y, Wang L, Zhao P, 2023, Construction and Application of a Monitoring Management Platform for Urban Rail Transit During Construction Based on GIS + BIM Technology. Northwest Hydropower, 2023(4): 108–112 + 118.

[7] Jiang Q, 2025, Research on Multi-Source Data Fusion Monitoring Method for Equipment Status of Subway Power Supply Systems. People's Public Transport, 2025(24): 63–65.

Publisher's note

Bio-Byword Scientific Publishing remains neutral with regard to jurisdictional claims in published maps and institutional affiliations.

Journal of Architectural Research and Development, 2026, Volume 10, Issue 5
https://bbwpublisher.com/journal/JARD
Online ISSN: 2208-3537
Print ISSN: 2208-3529

Research on the Design of Central Median Opening During Expressway Reconstruction and Expansion

Miaoqian Zhou[1], Mengdie Liu[2]*

[1]Guangdong Expressway Co., Ltd., Guangzhou 510440, Guangdong, China
[2]CCCC Second expressway Consultant Co., Ltd., Wuhan 430052, Hubei, China

***Corresponding author:** Mengdie Liu, 1193570518@qq.com

Copyright: © 2026 Author(s). This is an open-access article distributed under the terms of the Creative Commons Attribution License (CC BY 4.0), permitting distribution and reproduction in any medium, provided the original work is cited.

Abstract: To achieve the objective of maintaining traffic flow while carrying out construction in highway reconstruction and expansion projects, traffic diversion is required through openings in the median for traffic maintenance. The design of these openings directly affects traffic safety and operational efficiency. Focusing on highway reconstruction and expansion projects with four lanes maintained during construction, this study considers two typical traffic transition scenarios: bidirectional traffic on both carriageways transitioning to bidirectional traffic on a single carriageway, and bidirectional traffic on the left carriageway transitioning to bidirectional traffic on the right carriageway. Median opening alignments were designed for different operating speeds. A VISSIM-based microscopic traffic simulation was then conducted to evaluate the effects of different opening lengths and alignment configurations on traffic flow from three perspectives: delay, traffic conflict rate, and speed stability. Based on the simulation results, an optimal range of median opening lengths and recommended alignment designs were proposed for four-lane traffic maintenance sections within highway construction zones.

Keywords: Expressway reconstruction and expansion; Central median opening; VISSIM; Alignment design

Online publication: Oct 16, 2026

1. Introduction

China is currently undergoing large-scale highway reconstruction and expansion. Median openings for traffic maintenance are a spatial feature unique to the construction phase of highway reconstruction and expansion projects. When one carriageway is closed during highway construction, median openings are used to divert bidirectional traffic or traffic from one carriageway onto the other carriageway, thereby enabling construction on one carriageway while maintaining traffic on the other. After vehicles pass through the work zone, traffic is guided back to the original carriageway [1–3]. If the median opening is too short, vehicles may have

insufficient turning radii, require substantial speed reductions and forced lane changes when passing through the opening. This can create a traffic bottleneck, increase traffic conflicts, and pose safety risks. Conversely, although an excessively long opening can alleviate immediate lane-changing pressure, it prolongs the duration of mixed-speed traffic and lateral interference, causing traffic to remain in an unstable weaving state over a longer distance, thereby reducing overall operational efficiency and safety. In addition, excessively long openings increase construction costs [4]. Moreover, vehicles may travel at relatively high speeds through the median opening, and loss of vehicle control can consequently result in severe traffic crashes [5].

Therefore, scientifically determining the length and alignment design of median openings for traffic maintenance is of great significance for ensuring traffic safety and operational efficiency in highway construction zones. Accordingly, this study focuses on four-lane highway reconstruction and expansion construction zones and examines the effects of median opening design on traffic operations by analyzing the macroscopic characteristics of traffic flow. The underlying mechanisms through which opening design influences traffic flow are investigated, with the aim of scientifically determining a reasonable opening design that balances safety and operational efficiency.

2. Median opening alignment design

This paper takes the centralmedian openings for fourlane trafficmaintaining expressways as the research object, targeting two typical trafficsequence conversion scenarios: conversion from twoway operation on dual carriageways to twoway operation on a single carriageway, and shift of twoway traffic from the left single carriageway to the right single carriageway. For expressways maintained with fourlane traffic during reconstruction, speedlimit schemes of 60 km/h and 80 km/h are commonly adopted for traffic preservation. In accordance with Technical Standard of Highway Engineering (JTG B012017), the alignment designs and corresponding opening lengths are derived for design speeds of 60 km/h and 80 km/h respectively. Refer **Figure 1–4**. **Table 1** and **2**.

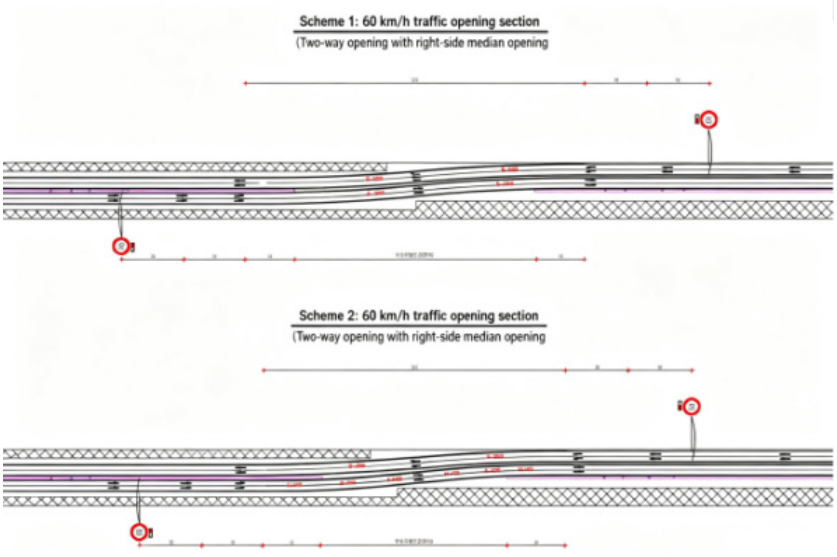

Figure 1. Alignment schemes of central median openings (design speed 60km/h, dual-carriageway to single-carriageway two-way traffic).

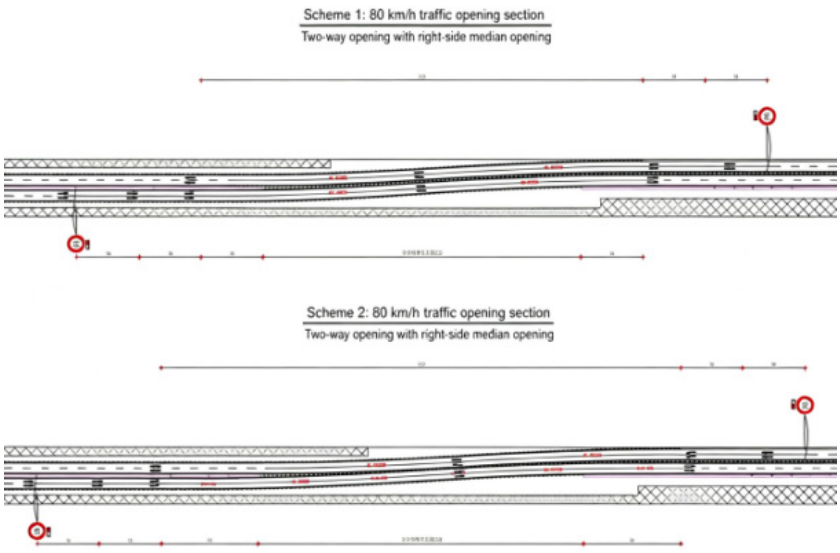

Figure 2. Alignment schemes of central median openings (design speed 80km/h, dual-carriageway to single-carriageway two-way traffic).

Table 1. Alignment design parameters of central median openings (dual-carriageway two-way to single-carriageway two-way traffic)

Design speed V (km/h)	Circular curve radius R (m)	Transition curve length Ls (m)	Hardened central median length L (m)
60	1500	—	196
60	700	50	149
80	2500	—	253
80	2300	70	260

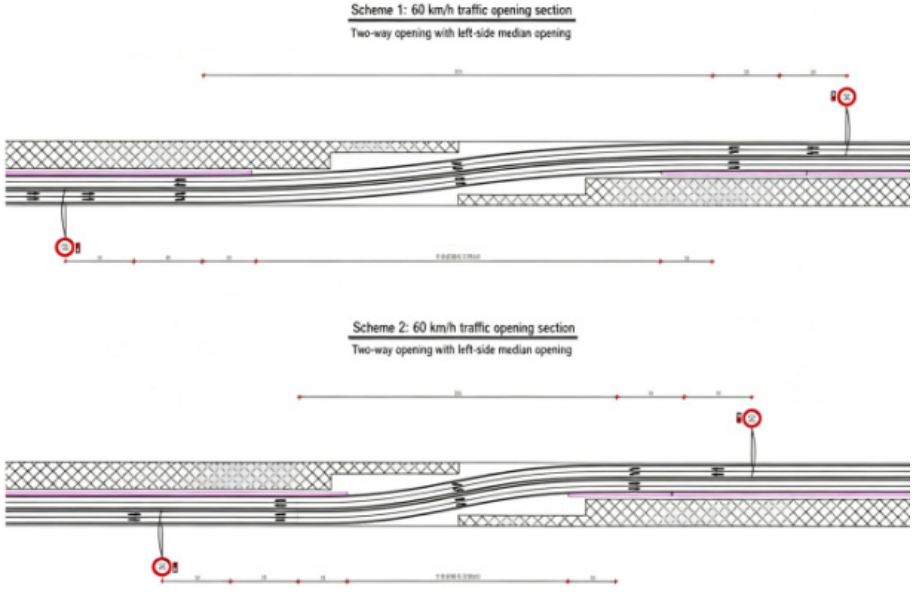

Figure 3. Alignment schemes of central median openings (design speed 60 km/h, left to right single-carriageway two-way traffic).

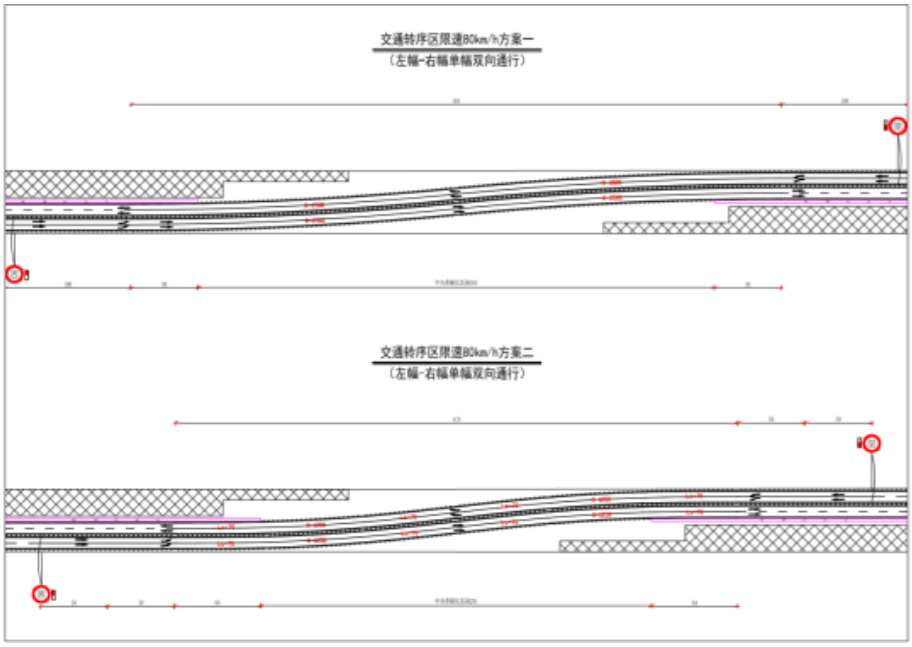

Figure 4. Alignment schemes of central median openings (design speed 80 km/h, left to right single-carriageway two-way traffic).

Table 2. Alignment design parameters of central median openings (left single-carriageway two-way to right single-carriageway two-way traffic)

Design speed V (km/h)	Circular curve radius R (m)	Transition curve length Ls (m)	Hardened central median length L (m)
60	1500	—	297
60	400	50	161
80	2500	—	384
80	1250	70	297

3.VISSIM-based traffic flow simulation analysis

3.1. Experimental design

To investigate the effects of median opening design for traffic maintenance on microscopic traffic flow, a VISSIM-based simulation experiment was developed with three factors: traffic volume, heavy-truck proportion, and median opening length. The effects of median opening design on traffic efficiency, traffic safety, and traffic stability were then analyzed [6].

According to vehicle composition data from multiple expressways in China, large buses and medium-sized vehicles account for approximately 3% and 5% of the total traffic volume, respectively, in the traffic composition of highways undergoing reconstruction and expansion. The proportions of these two vehicle types are relatively stable, and traffic management schemes in construction zones generally do not divert large buses or medium-sized vehicles. Therefore, in all scenarios considered in this study, the proportions of large buses and medium-sized vehicles were kept constant at 3% and 5%, respectively, while the proportions of heavy trucks and small vehicles were varied. The specific factor settings are presented in **Table 3**.

Table 3. Variation ranges of influencing factors

Influencing factor	Minimum value	Maximum value	Step size	Number of factor levels
Traffic volume (pcu/h)	300	1500	200	7
Heavy truck proportion (%)*	0	90	10	10
Central median opening length (m)	50	350	50	7

*Note: Heavy truck proportion refers to the percentage of heavy trucks in total PCU.

Full-factor combination tests are carried out in VISSIM. To eliminate random errors, each scheme is simulated 3 times with different random seeds, and the average value of the three simulation runs is adopted as the final result. Total simulation runs: $7 \times 10 \times 7 \times 3 = 1470$ times.

3.2. Traffic efficiency evaluation

Average travel delay is selected as the quantitative indicator to measure the influence of median opening length on traffic capacity. Simulation results show that traffic volume, heavy truck proportion and median opening length all exert significant effects on travel delay, detailed as follows:

Travel delay rises continuously with the increase of traffic volume.

Under all traffic volume conditions, the relationship between travel delay and heavy truck proportion follows a parabolic curve. Heavy trucks operate at lower speeds than other vehicle types, forcing passenger cars following behind to decelerate frequently and increasing travel delay. When heavy trucks account for an extremely high share, the number of speed reduction events decreases due to homogenized vehicle speeds, and travel delay gradually declines.

Overall, travel delay drops as the median opening length shortens. This phenomenon may be attributed to the lower speed limit at traffic conversion zones compared with regular road sections. With other conditions unchanged, average travel delay decreases as lane number increases. In addition, under certain heavy truck proportion levels, the declining trend of travel delay slows down when the opening length falls to 100–150 m (see **Table 4**, **Figure 5**).

Table 4. Three-way ANOVA results for dependent variable (travel delay)

Source of variation	Sum of squares	Degrees of freedom	Mean square	*F*-statistic	*p*-value
Traffic volume	7505	6	2502	205545	0.000
Heavy truck proportion	1449	9	161	13223	0.000
Median opening length	500	6	83	6843	0.000
Three-way interaction	901	468	3.5	284	0.000
Total	29226	1470	—	—	—

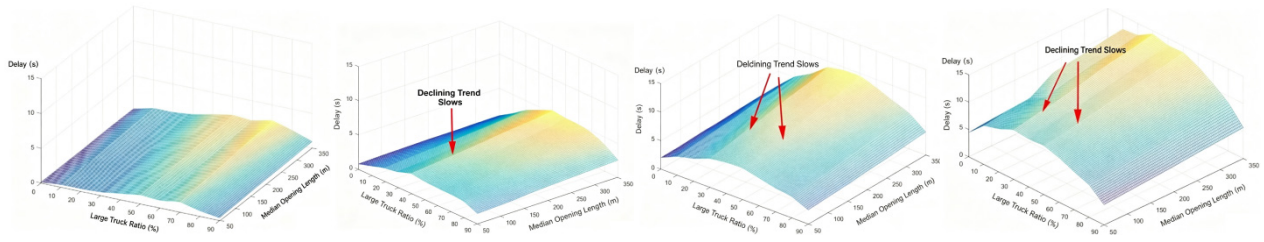

a) Traffic volume of 300 pcu/h b) Traffic volume of 700 pcu/h c) Traffic volume of 1100 pcu/h d) Traffic volume of 1500 pcu/h

Figure 5. Fitted 3D surface plot of delay versus heavyvehicle percentage and opening length under different traffic volumes.

3.3. Traffic safety evaluation

Traffic conflict rate is chosen as the core indicator to analyze the influence of median opening length on driving safety in construction zones. Trajectory (.trj) files exported from VISSIM are imported into SSAM (Surrogate Safety Assessment Model) for traffic conflict statistics and analysis. SSAM recommended thresholds are adopted: TTC = 1.5 s, PET = 5.0 s; angle thresholds for rear-end conflicts and crossing conflicts are set to 30° and 90° respectively. Key simulation conclusions are summarized below:

Traffic conflict rate is positively correlated with traffic volume; higher traffic volume leads to poorer safety performance within construction zones.

The correlation between heavy truck proportion and conflict rate is insignificant under low traffic volumes. Under high traffic volumes (1100 pcu/h, 1500 pcu/h), traffic conflict rate first rises then falls as heavy truck proportion increases, peaking at 10%. Heavy trucks have poor dynamic performance and lower operating speeds, widening speed differences between vehicle types and triggering more traffic conflicts. When heavy trucks dominate traffic flow, speed differences shrink and total vehicle count drops, reducing conflict probability after the peak point. At fixed traffic volume, median openings of 100–150 m produce markedly lower conflict rates and better safety performance under high traffic volume and 10% heavy truck proportion (**Figure 6**). Openings shorter than 50 m force sharp vehicle deceleration, creating a large speed differential with upstream traffic and raising conflict risks; overlong openings extend the mixing zone of fast passenger cars and slow heavy trucks, degrading safety. (**Table 5**)

Table 5. Three-way ANOVA results for dependent variable (traffic conflict rate)

Source of variation	Sum of squares	Degrees of freedom	Mean square	*F*-statistic	*p*-value
Traffic volume	0.638	6	0.106	41397.135	0.000
Heavy truck proportion	0.144	9	0.016	6251.365	0.000
Median opening length	0.001	6	0.000	78.103	0.000
Three-way interaction	0.329	468	0.001	274.202	0.000
Total	1.841	1470	—	—	—

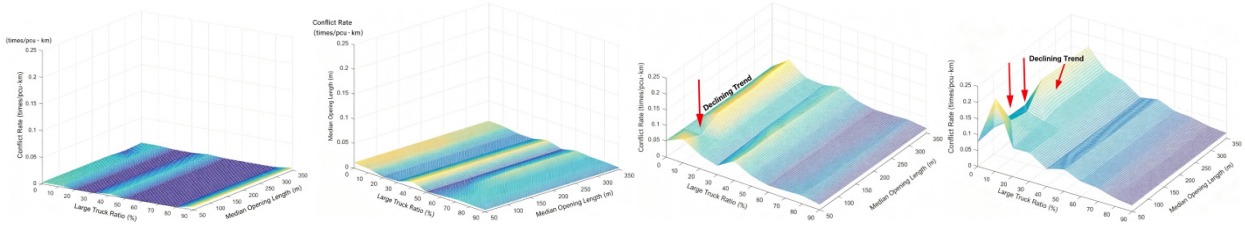

a) Traffic volume of 300 pcu/h b) Traffic volume of 700 pcu/h c) Traffic volume of 1100 pcu/h d) Traffic volume of 1500 pcu/h

Figure 6. Fitted 3D surface plot of conflict rate versus heavyvehicle percentage and opening length under various traffic volumes.

3.4. Traffic stability evaluation

Traffic stability reflects the anti-interference resilience and evolution law of traffic flow in restricted road space. Test analysis is conducted for typical combinations of traffic volume and heavy truck proportion, as listed in **Table 6**.

Table 6. Typical combinations of traffic volume and heavy truck proportion

Combination No.	1	2	3	4	5	6	7	8	9
Traffic volume (pcu/h)	300 (Low)	900 (Medium)	1500 (High)	300 (Low)	900 (Medium)	1500 (High)	300 (Low)	900 (Medium)	1500 (High)
Heavy truck proportion (%)	10 (Low)	10 (Low)	10 (Low)	40 (Medium)	40 (Medium)	40 (Medium)	80 (High)	80 (High)	80 (High)

Average speed curves at each observation point under different median opening lengths are plotted for low traffic + low heavy truck ratio, low traffic + high heavy truck ratio, medium traffic + medium heavy truck ratio and high traffic + high heavy truck ratio (**Figure 7** and **Table 7**).

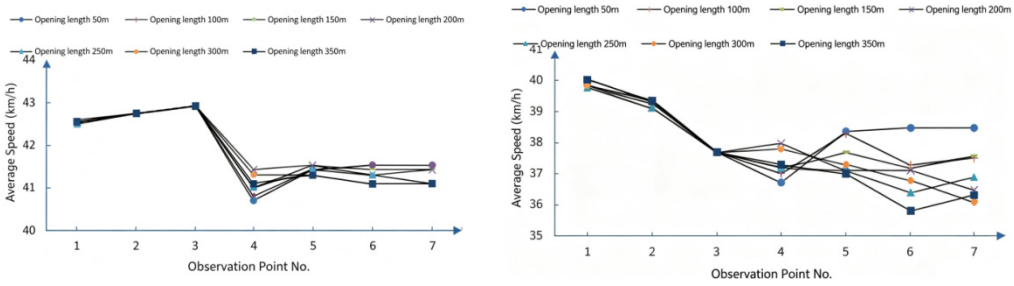

a) 300 pcu/h with heavyvehicle percentage of 10% (comb 1) b) 900 pcu/h with heavyvehicle percentage of 40% (comb 5)

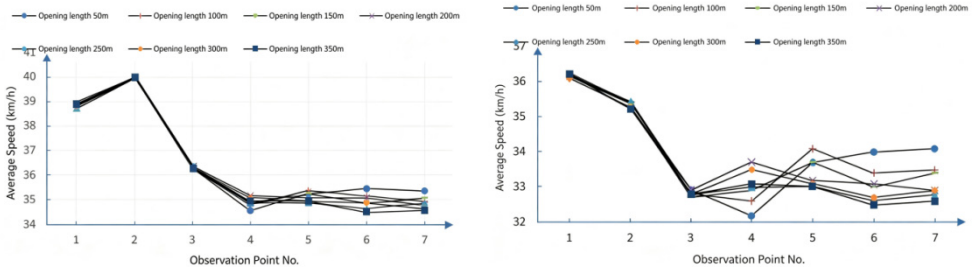

c) 300 pcu/h with heavyvehicle percentage of 80% (comb 7) d) 1500 pcu/h with heavyvehicle percentage of 80% (comb 9)

Figure 7. Schematic diagram of average speed variation at each observation point under different opening lengths.

Table 7. Standard deviation of operating speed for all combinations & opening lengths

Opening length (m)	Comb.1	Comb.2	Comb.3	Comb.4	Comb.5	Comb.6	Comb.7	Comb.8	Comb.9
50	0.83	0.77	1.04	1.05	1.11	1.51	2.06	1.13	1.36
100	0.81	0.73	1.11	1.05	1.04	1.34	2.02	1.09	1.31
150	0.78	0.77	1.11	1.04	1.02	1.46	2.11	1.17	1.34
200	0.72	0.66	0.91	1.08	1.28	1.54	2.10	1.21	1.37
250	0.83	0.76	0.94	1.14	1.23	1.40	2.14	1.34	1.46
300	0.83	0.74	0.93	1.11	1.34	1.51	2.14	1.36	1.36
350	0.86	0.82	1.02	1.15	1.54	1.61	2.23	1.47	1.47

Under low traffic volumes, speed fluctuations at observation points show minor differences across all opening lengths. As traffic volume rises, opening length exerts a prominent influence on speed variation. Standard deviation analysis of speeds at all observation points yields the following conclusions:

For low heavy truck proportions (Combination 1–3), the 200 m opening length delivers optimal traffic stability. For medium heavy truck proportions (Combination 5–6) and high heavy truck proportions

(Combination 7–9), opening lengths of 100–150 m achieve superior speed stability.

4.Conclusions

From the perspectives of engineering economy and vehicle driving stability, when the proportion of smallsized vehicles is high, the median opening for traffic maintenance may be appropriately lengthened. It is recommended to adopt a transition curve combined with a smallradius circular curve in alignment design. This can satisfy vehicle driving requirements while reducing construction workload. In contrast, when heavy vehicles account for a large proportion during maintenance construction, the mediandivider opening alignment is suggested to be designed directly with a largeradius circular curve.

Considering traffic efficiency, traffic safety, and traffic stability, the recommended length of the mediandivider opening for twoway fourlane traffic maintenance in work zones is 150–200 m.

Disclosure statement

The authors declare no conflict of interest.

References

[1] Shao C, Ma S, Luo K, et al., 2020, Study on the Length of Median Opening in Expressway Reconstruction and Extension Work Zones. In CICTP 2020, 1233–1245.

[2] Mohanty M, Dey P, 2022, Operational Effects of U-Turns at Median Opening. Transportation Letters, 14(6): 565–577.

[3] Ran J, Zhan S, Lei Z, et al., 2025, Optimal Opening Length of Median Transition Sections of Expressway Reconstruction and Expansion Based on Multidimensional Evaluation Indicators. In Fifth International Conference on Intelligent Traffic Systems and Smart City (ITSSC 2025). SPIE, 13792: 632–640.

[4] Ma S, Hu J, Wang R, et al., 2023, Study on the Median Opening Length of a Freeway Work Zone Based on a Naturalistic Driving Experiment. Applied Sciences, 13(2): 851.

[5] Tian W, Li Z, Hao J, et al., 2024, Method for Determining Median Opening Length in Multi-Lane Conversion of Expressway Renovation and Expansion Projects. In Seventh International Conference on Traffic Engineering and Transportation System (ICTETS 2023). SPIE, 13064: 346–355.

[6] Chen C, Bo Y, 2026, Research on the Reasonable Length of the Median Opening for Five-Lane Traffic Flow During the Reconstruction and Expansion of Expressways//International Conference on Artificial Intelligence and Autonomous Transportation. Springer, Singapore, 103–119.

Publisher's note

Bio-Byword Scientific Publishing remains neutral with regard to jurisdictional claims in published maps and institutional affiliations.

Journal of Architectural Research and Developmentn, 2026, Volume 10, Issue 5
https://bbwpublisher.com/journal/JARD
Online ISSN: 2208-3537
Print ISSN: 2208-3529

Study on Seepage and Deformation Responses during Tunnel Excavation and the Influence of Support Parameters

Xizhen Wang

School of Civil Engineering, Shijiazhuang Tiedao University, Shijiazhuang 050043, Hebei, China

Copyright: © 2026 Author(s). This is an open-access article distributed under the terms of the Creative Commons Attribution License (CC BY 4.0), permitting distribution and reproduction in any medium, provided the original work is cited.

Abstract: To investigate the evolution characteristics of groundwater seepage and surrounding rock deformation during tunnel excavation and the effectiveness of support control, a steady-state seepage model and an elastoplastic mechanical model were developed for a deep-buried circular tunnel. The spatial distributions of the seepage and displacement fields and their responses to construction steps under the bench excavation method were analyzed, and the effects of the thickness, elastic modulus, and permeability coefficient of the primary support and grouting ring were examined. The results indicate that after excavation, groundwater converges toward the tunnel cavity and tunnel face, while the surrounding rock deforms toward the excavated space; the more significant responses are mainly concentrated around the tunnel periphery and near the tunnel face. As the excavation face approaches and passes the studied section, the peripheral displacement and outflow change rapidly and then gradually stabilize. Increasing the thickness of the primary support and grouting ring reduces the peripheral displacement and water inflow, but the incremental control effect diminishes with increasing thickness. Increasing the elastic modulus of the primary support and grouting reinforcement zone is beneficial for controlling surrounding rock deformation, whereas reducing their permeability coefficients can effectively decrease tunnel water inflow. When the water-blocking capacity of the primary support is enhanced, the external water pressure on the lining increases; when the water-blocking capacity of the grouting ring is enhanced, the external water pressure on the lining decreases. These results can provide a reference for selecting support and grouting parameters for tunnels in water-rich surrounding rock.

Keywords: Tunnel engineering; Steady-state seepage; Surrounding rock deformation; Primary support; Grouting reinforcement

Online publication: Oct 13, 2026

1. Introduction

Excavation of a tunnel in water-rich surrounding rock simultaneously alters the stress state of the ground and the groundwater drainage conditions. After the surrounding rock is unloaded, stress redistribution and

deformation occur around the tunnel periphery, while groundwater converges toward the newly formed drainage boundary. Water inflow not only increases the burden of construction drainage but may also affect the stability of the surrounding rock and the forces acting on the support structures. Therefore, understanding the spatial distribution and evolution characteristics of seepage and deformation during excavation, and clarifying the control effects of support and grouting measures, constitute an important basis for selecting tunnel construction parameters.

With respect to the mechanical and permeability characteristics of rock masses under unloading conditions, previous studies have conducted triaxial tests on limestone, dolomite, and sandstone, revealing the relationships between fracture opening, damage development, and permeability variation [1–3]. Unloading tests on sandstone and marble indicate that the unloading path and initial stress conditions affect rock deformation and mechanical parameters; seepage studies on fractured rock masses have further analyzed the evolution characteristics of flow channels during unloading [4–7]. At the tunnel scale, the surrounding rock conditions, support performance, and groundwater boundary jointly govern the response around the tunnel, and primary support and grouting reinforcement are important measures for controlling deformation and water inflow [8–10].

Primary support shares the surrounding rock load by constraining peripheral deformation, whereas grouting provides reinforcement and water-blocking effects by improving the mechanical properties and reducing the permeability of the surrounding rock. The thickness and material properties of these two measures directly affect their control effectiveness, and their effects also vary with the advancement of the tunnel face and the installation of support. An integrated analysis of the construction process and support parameters is helpful for identifying the key response locations, control timing, and parameter variation patterns.

This study focuses on a deep-buried circular tunnel and establishes a staged steady-state seepage model and an elastoplastic mechanical model. First, the spatial distributions of seepage and displacement induced by bench excavation are analyzed. Subsequently, the variations in the response of a typical section with construction steps are compared. Finally, the effects of the thickness, stiffness, and permeability of the primary support and grouting ring are investigated, and the control patterns of these two measures on surrounding rock deformation, water inflow, and external water pressure on the lining are summarized.

2. Numerical model and calculation cases

2.1. Model and construction process

The tunnel has an excavation radius of 8 m and a burial depth of 300 m. It is constructed using the bench excavation method, with a round length of 2 m per cycle and a bench spacing of 4 m between the upper and lower benches. In the construction process analysis, the primary support consists of 0.25 m thick C25 shotcrete and lags the excavation by one cycle. The crown, haunch, and invert are selected as monitoring locations. The response to construction steps is analyzed at a section 10 m from the tunnel portal, while the influence of support parameters is analyzed at a section in the middle of the tunnel.

Mechanical analysis was performed using FLAC3D. The model dimensions in the transverse, vertical, and longitudinal directions were 200, 200, and 50 m, respectively. The surrounding rock and grouting reinforcement zone were modeled using the Mohr–Coulomb constitutive model, while the support and lining were simulated using solid elements. The bottom boundary of the model was constrained in all three

displacement directions, and the four lateral boundaries were constrained in the normal direction. For the construction process case, the lateral pressure coefficient was 1.2, and an equivalent load of 4.6 MPa was applied at the top; for the support parameter case, the lateral pressure coefficient was 1.1, and the equivalent top load was 4.0 MPa. These equivalent top loads correspond to the self-weight of the 200 m overlying strata above the model.

Seepage analysis was performed using MIDAS. The construction process model has dimensions of 1600 m × 600 m × 50 m, while a longitudinal thickness of 1 m is adopted for the support parameter analysis. The bottom boundary of the model is impermeable, the left and right lateral boundaries are prescribed with a total head of 300 m, the exposed excavation surfaces are set as zero-pressure-head boundaries, and the support and lining are assigned finite permeability coefficients. As the bench advances, the excavation and support domains are updated sequentially, and the steady-state seepage field is solved for each construction stage.

2.2. Material parameters and variable settings

The surrounding rock and support parameters were selected according to relevant specifications and the literature, and the main values are listed in **Table 1** [8–10]. The construction process analysis and the support parameter analysis adopted their respective baseline cases, and within each parameter group, the model boundaries, construction method, and other material parameters were kept consistent. In the support parameter analysis, the secondary lining is 0.30 m thick and lags 10 m behind the primary support in the mechanical construction simulation.

Table 1. Material parameters of surrounding rock and support

Working conditions and materials	E/GPa	c/MPa	φ/(°)	γ/(kN/m³)	ν	k/(m/s)
Construction process surrounding rock	1.3	0.25	22	23	0.35	1×10^{-5}
Construction process primary support	28	1.5	50	24	0.18	9.26×10^{-10}
Parameter analysis surrounding rock	1.3	0.25	27	20	0.24	1×10^{-6}
Parameter analysis primary support	28	—	—	24	0.18	1×10^{-8}
Parameter analysis secondary lining	30	—	—	25	0.20	1×10^{-10}
Parameter analysis grouting ring	6.4	0.85	45	26	0.25	1×10^{-7}

Note: E, elastic modulus; c, cohesion; φ, internal friction angle; γ, unit weight; ν, Poisson's ratio; k, permeability coefficient.

In the thickness analysis, the primary support thicknesses were set to 0.10, 0.15, 0.20, 0.30, and 0.50 m, and the grouting ring thicknesses were set to 1, 3, 5, 7, and 9 m. In the stiffness analysis, the elastic modulus of the primary support was set to 15, 20, 24, 28, 35, 50, 60, and 70 GPa, and that of the grouting reinforcement zone was set to 1, 2, 3, 5, 7, and 10 GPa.

In the permeability analysis, the permeability coefficient ratio of adjacent materials was adopted as the variable. In the primary support analysis, the permeability coefficient of the grouting ring was fixed at $k_g = 1 \times 10^{-7}$ m/s, and the primary support permeability coefficient kl was varied such that kg/kl was set to 2, 4, 8, 12, 20, 100, and 200. In the grouting ring analysis, the permeability coefficient of the surrounding rock was fixed at $k_r = 1 \times 10^{-6}$ m/s, and k_r/k_g was set to the same sequence. For both groups, the grouting

ring thickness, primary support thickness, and secondary lining thickness were 3 m, 0.25 m, and 0.30 m, respectively, and the secondary lining permeability coefficient was 1×10^{-10} m/s.

3. Seepage and deformation responses during excavation

3.1. Spatial distributions of seepage and displacement fields

Before excavation, the pore water pressure increased with depth, reaching approximately 2.94 MPa at the tunnel location. After excavation, a low-pore-pressure zone formed around the tunnel periphery, and the pore water pressure gradually recovered from the tunnel wall toward the deeper surrounding rock. In the cross-section, groundwater converged toward the tunnel cavity, with a relatively high seepage velocity near the tunnel wall; in the longitudinal direction, the low-pore-pressure zone advanced with the tunnel face, and water flow concentrated near the tunnel face and the bench interface. The surrounding rock deformation was also mainly distributed around the tunnel periphery and near the tunnel face, decreasing with increasing distance from the excavation boundary.

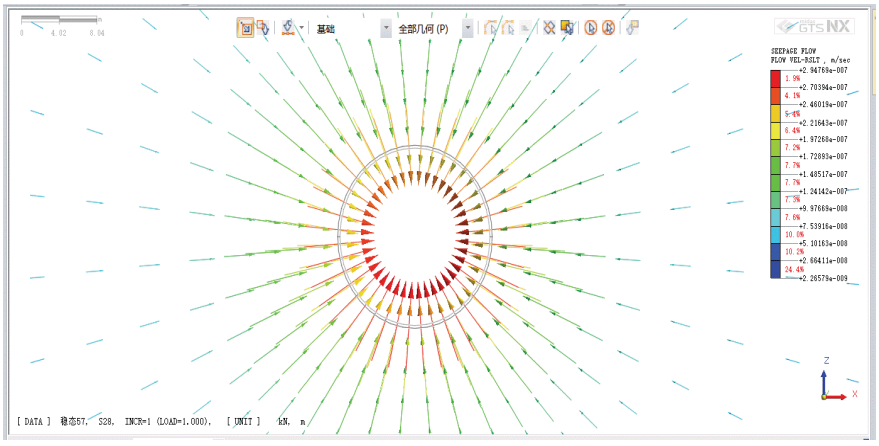

(a) Seepage vectors

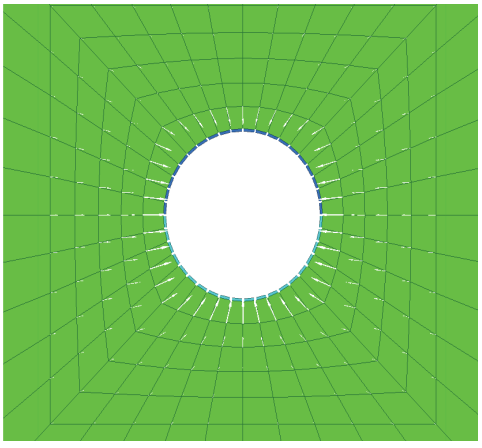

(b) Displacement vectors

Figure 1. Distributions of seepage and displacement in the cross-section after tunnel breakthrough: (a) Seepage Vectors; (b) Displacement Vectors.

Figure 1 indicates that after tunnel breakthrough, groundwater generally enters the tunnel cavity along

the normal direction to the tunnel wall, while the surrounding rock converges inward, with the response relatively concentrated near the invert. During upper bench excavation, the crown and the region near the bench are first disturbed; after lower bench excavation, the response extends to the lower surrounding rock. The longitudinal displacement of the surrounding rock increases as the tunnel face approaches, and face extrusion is pronounced, reflecting the spatial effect of excavation unloading.

3.2. Response of a typical section to construction steps

To analyze the evolution characteristics of seepage and deformation at a typical section during tunnel excavation, a section located 10 m from the tunnel portal was selected. The outflow per unit length and displacement at the crown, haunch, and invert were extracted, and their variation patterns with construction steps were compared. The results are shown in **Figure 2**.

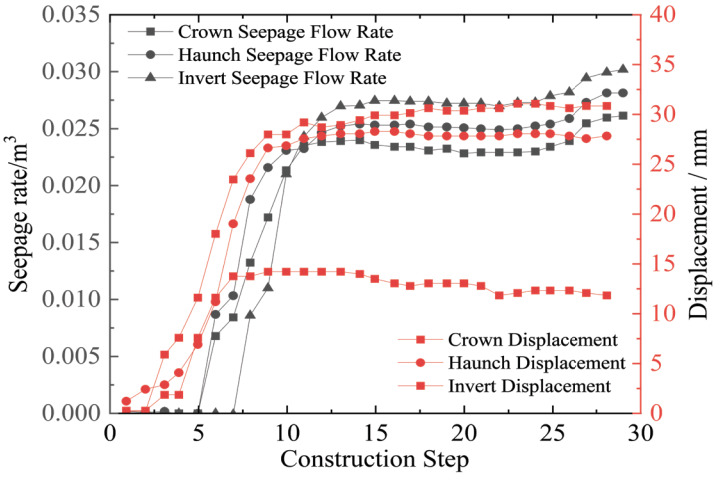

Figure 2. Response of the section 10 m from the tunnel portal to construction steps.

As shown in **Figure 2**, after the studied section is exposed, the outflow at the tunnel wall increases rapidly and then gradually stabilizes with excavation advancement and support installation. The outflow is largest at the invert, followed by the haunch, and smallest at the crown. The surrounding rock displacement begins to develop before the tunnel face reaches the section, accelerates when excavation approaches the studied section, and slows after the tunnel face moves away. The crown exhibits settlement, the haunches converge inward, and the invert experiences heave. Both types of response change markedly near the passage of the excavation through the section, indicating that timely support installation plays an important role in controlling deformation and outflow during this stage.

4. Influence of support thickness on seepage and deformation

4.1. Primary support thickness

As the primary support thickness increases, the displacement amplitudes at all monitoring points gradually decrease, and crown settlement, haunch convergence, and invert heave are all controlled, as shown in **Figure 3**.

When the thickness is relatively small, the displacement change induced by thickening is more pronounced; once the thickness reaches approximately 0.30 m, the curves gradually level off. A thicker primary support enhances the overall stiffness and constraint capacity of the structure around the tunnel, enabling it to effectively share the surrounding rock load and thereby reduce subsequent deformation.

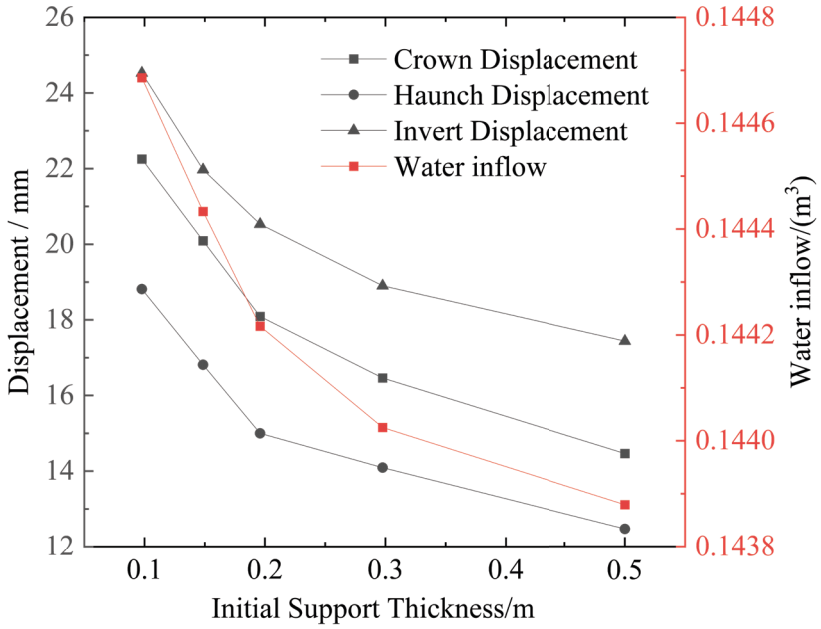

Figure 3. Influence of primary support thickness on the response around the tunnel.

The water inflow around the tunnel decreases with increasing primary support thickness, while the magnitude of this decrease gradually diminishes as shown in **Figure 3**. Thickening the low-permeability primary support lengthens the seepage path through the support layer and increases its hydraulic resistance. Within the calculation range of this group, the variation in water inflow is relatively gentle, indicating that under the given surrounding rock, grouting ring, and lining conditions, the water-control benefit of merely increasing the primary support thickness is limited. Meanwhile, increasing the primary support thickness raises the external water pressure on the lining to some extent, reflecting the redistribution of hydraulic head after the water-blocking effect of the support layer is enhanced.

4.2. Grouting ring thickness

When the grouting ring thickness increases from 1 m to 9 m, the displacement amplitudes around the tunnel decrease overall, as shown in **Figure 4**. At relatively small thicknesses, enlarging the reinforcement zone noticeably improves the confinement around the tunnel; as the thickness continues to increase, the displacement curves gradually level off. Grouting reinforcement enhances the overall bearing capacity of the rock mass within a certain range around the tunnel, allowing the excavation load to be shared by the reinforcement zone and the external surrounding rock.

Water inflow continuously decreases with the thickening of the grouting ring and gradually exhibits a leveling-off trend, as shown in **Figure 4**. Under the same material permeability coefficient, enlarging the grouting zone increases the hydraulic head loss before groundwater reaches the support structure.

Correspondingly, the external water pressure on the lining also decreases as the grouting ring thickness increases. Compared with thickening the primary support, the grouting ring forms a water-blocking zone outside the structure, thereby simultaneously reducing the water inflow into the tunnel and lowering the external water pressure on the lining.

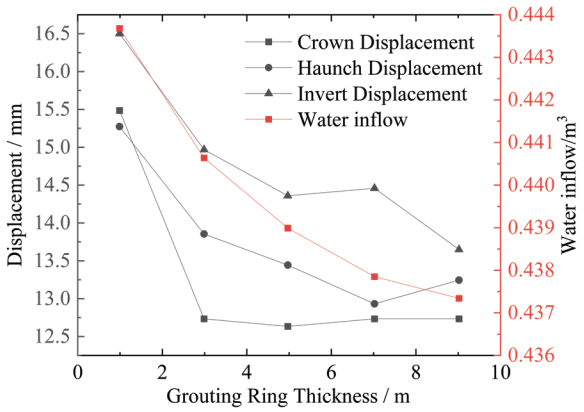

Figure 4. Influence of grouting ring thickness on the response around the tunnel.

5. Influence of material properties on seepage and deformation

5.1. Elastic moduli of primary support and grouting reinforcement zone

As the elastic modulus of the primary support increases, crown settlement, haunch convergence, and invert heave all decrease, and the mechanical response of the lining is correspondingly reduced. When the primary support stiffness is relatively low, increasing the elastic modulus markedly enhances confinement around the tunnel; as the stiffness continues to increase, the reduction in displacement gradually diminishes. A similar trend is observed when the elastic modulus of the grouting reinforcement zone is increased from 1 GPa to 10 GPa, indicating that improving the mechanical properties of the reinforcement zone is beneficial for restricting deformation around the tunnel and reducing the loads borne by subsequent support structures.

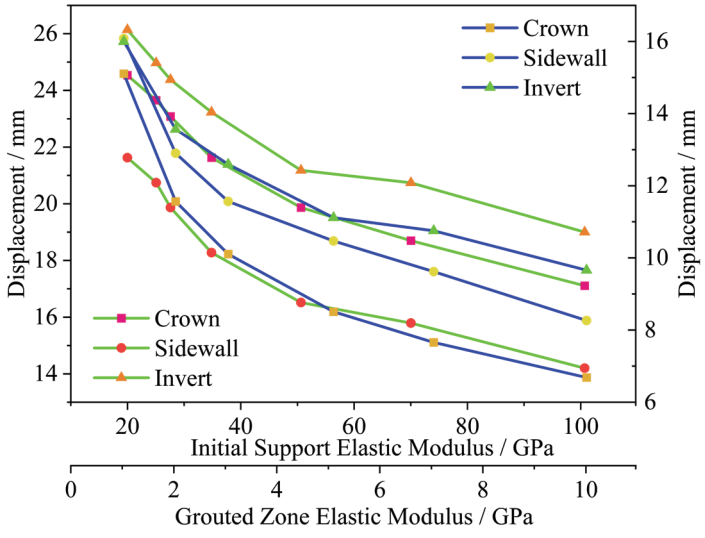

Figure 5. Influence of elastic moduli of the primary support and grouting reinforcement zone on tunnel peripheral displacement.

5.2. Primary support permeability coefficient

With the permeability coefficient of the grouting ring fixed, an increase in k_g/k_l indicates a decrease in the permeability coefficient of the primary support. As shown in **Figure 6**, as this ratio increases from 2 to 200, the water inflow around the tunnel first decreases rapidly and then gradually levels off. At relatively small ratios, changes in the primary support permeability noticeably alter the water inflow into the tunnel; as the ratio increases, the incremental effect of further reducing the primary support permeability coefficient diminishes. The external water pressure on the lining increases with increasing ratio, indicating that enhanced water-blocking by the primary support is accompanied by an increase in water pressure outside the structure.

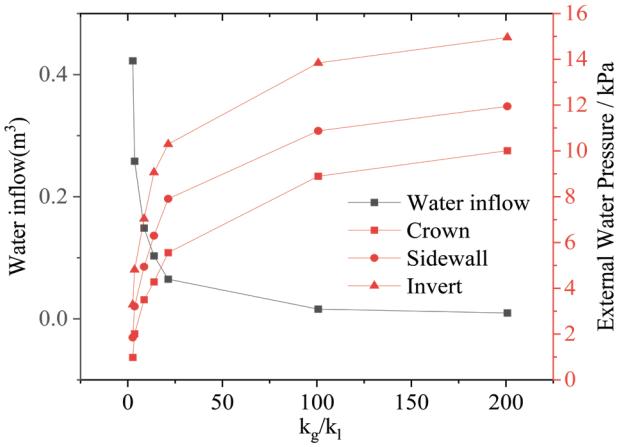

Figure 6. Influence of primary support and grouting ring permeability on water inflow and external water pressure on the lining.

5.3. Grouting ring permeability coefficient

When the permeability coefficient of the surrounding rock is fixed, an increase in k_r/k_g indicates a decrease in the permeability of the grouting ring. As shown in **Figure 7**, the water inflow decreases rapidly with increasing ratio and then transitions to a gradual decline; the external water pressure on the lining decreases synchronously. A low-permeability grouting ring causes more hydraulic head loss to occur outside the support structure, reducing both the amount of water flowing toward the tunnel cavity and the water pressure acting on the outer side of the lining. Both measures have water-control effects; however, the grouting ring can reduce the external water pressure while decreasing water inflow, and its effect is clearly different from that of the primary support.

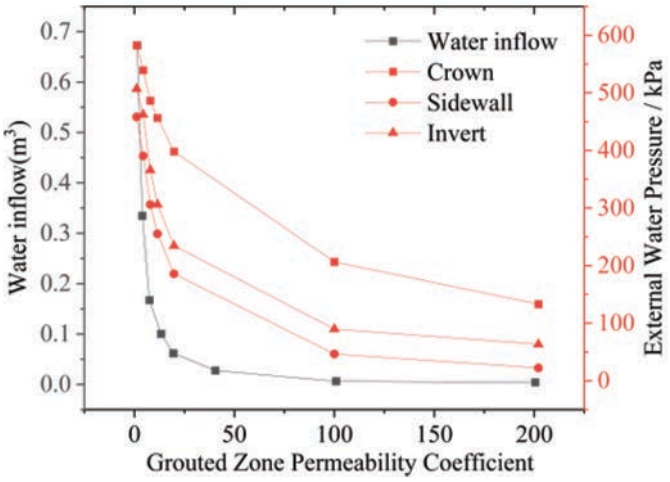

Figure 7. Influence of primary support and grouting ring permeability on water inflow and external water pressure on the lining.

6. Conclusions

(1) After bench excavation, groundwater converges toward the tunnel cavity and tunnel face, while the surrounding rock deforms toward the excavated space, with more pronounced responses concentrated around the tunnel periphery and near the tunnel face. The responses change markedly as the tunnel face approaches and passes the studied section, and then gradually stabilize with support installation and as the excavation face moves away.

(2) Increasing the thickness of the primary support and grouting ring can reduce the peripheral displacement and water inflow, and the incremental control effect gradually diminishes as the thickness increases. Increasing the elastic modulus of the primary support and grouting reinforcement zone can further restrict the deformation of the surrounding rock, and this effect also tends to level off gradually.

(3) Reducing the permeability coefficients of both the primary support and the grouting ring can decrease tunnel water inflow. When the water-blocking capacity of the primary support is enhanced, the external water pressure on the lining increases, whereas when the water-blocking capacity of the grouting ring is enhanced, the external water pressure decreases. The selection of support and grouting parameters should comprehensively account for deformation control, water inflow control, and structural water pressure.

Disclosure statement

The author declares no conflict of interest.

References

[1] Liu H, Liu J, Zhang Y, et al., 2020, Experimental Study on the Mechanical Properties of Fractured Limestone Under Unloading Confining Pressure Damage. Water Power, 46(3): 28–32 + 60.

[2] Li K, Yang B, Qin Q, 2019, Experimental Study on Unloading Damage and Permeability of Dolomite Based on Nuclear Magnetic Resonance Technique. Chinese Journal of Rock Mechanics and Engineering, 38(S2):

3493–3502.

[3] Wang R, Xu B, Xu W, et al., 2019, Experimental Research of the Influence of Different Unloading Stress Paths on Permeability Evolution of Sandstone. Chinese Journal of Rock Mechanics and Engineering, 38(3): 467–475.

[4] Wang R, Li J, Jiang Y, et al., 2010, Experimental Study of Influence of Excavation Unloading on Mechanical Properties of Sandstone. Rock and Soil Mechanics, 31(S1): 156–162 + 206.

[5] Li H, Xia C, Yan Z, et al., 2007, Study on Marble Unloading Mechanical Properties of Jinping Hydropower Station Under High Geostress Conditions. Chinese Journal of Rock Mechanics and Engineering, 26(10): 2104–2109.

[6] Liu X, Lin Y, Kong J, 2007, Study of Hydro-Mechanical Coupling of Fractured Rock Masses Considering Unloading Effect. Rock and Soil Mechanics, 28(S1): 192–196.

[7] Liang N, Liu X, Ai W, et al., 2011, Experiment Study on the Permeability of Fractured Rock Under Unloading. China Civil Engineering Journal, 44(1): 88–92.

[8] Code for Design of Railway Tunnel: TB 10003—2016, 2016, Beijing: China Railway Publishing House.

[9] Liu Z, 2015, Study on Mechanism and Control Technology of Interaction Between Fractured Rock Mass Tunnel and Groundwater Environment, thesis, Beijing Jiaotong University.

[10] Zhang H, 2014, Seepage Analysis of Groundwater and Study on Treatment Measures of Pouring Water in WuDuxi Highway Tunnel, thesis, Chang'an University.

Publisher's note

Bio-Byword Scientific Publishing remains neutral with regard to jurisdictional claims in published maps and institutional affiliations.

Journal of Architectural Research and Developmentn, 2026, Volume 10, Issue 5
https://bbwpublisher.com/journal/JARD
Online ISSN: 2208-3537
Print ISSN: 2208-3529

Soundscape Evaluation and Optimization Strategies for an Urban Riverside Wetland Park in Arid Northwest China: A Case Study of Yintan Wetland Park, Lanzhou

Yang Chao

School of Architecture and Urban Planning, Lanzhou Jiaotong University, Lanzhou 730000, Gansu, China

Copyright: © 2026 Author(s). This is an open-access article distributed under the terms of the Creative Commons Attribution License (CC BY 4.0), permitting distribution and reproduction in any medium, provided the original work is cited.

Abstract: Urban wetland parks in arid regions are simultaneously exposed to ecologically valuable natural sounds and urban acoustic disturbances, yet their soundscape dynamics remain less documented than those of parks in humid regions. This study evaluates the soundscape of Yintan Wetland Park in Lanzhou, a riverside wetland on the Yellow River, by integrating field sound-level measurements, a sound-source inventory, a questionnaire survey, and GIS-based ordinary Kriging interpolation. Twenty-eight accessible measurement locations were surveyed in May 2025 during three periods (08:00–09:00, 12:00–13:00, and 19:00–20:00), and 76 valid questionnaires were obtained. A total of 24 typical sound sources were identified; natural sounds, human-activity sounds, and mechanical/traffic sounds accounted for 38%, 32%, and 30%, respectively. Mean A-weighted sound levels across the 28 locations were 54.04 dB(A) in the morning, 51.71 dB(A) at noon, and 54.25 dB(A) in the evening. Higher levels were concentrated along the northern traffic edge and at localized evening activity nodes, whereas areas with more continuous water and vegetation generally exhibited lower levels. The park-wide mean of the point-based representative values was 53.33 dB(A), corresponding to a mean study-specific relative noise index (PN) of 0.71. Visitors showed stronger preferences for birdsong, rustling foliage, and water sounds, and weaker preferences for construction, motor-vehicle, and broadcast sounds. Based on the combined physical and perceptual evidence, the study proposes traffic-edge buffering, conservation of natural-sound core areas, temporal-spatial management of activity nodes, context-sensitive integration of cultural sounds, and long-term acoustic monitoring. The findings provide planning and management implications for riverside wetland parks in arid Northwest China.

Keywords: A-weighted sound level; Arid region; Kriging interpolation; Soundscape; Urban wetland park; Visitor perception

Online publication: Oct 13, 2026

1. Introduction

Soundscape research focuses on how people perceive, interpret, and experience acoustic environments in

context, thereby linking physical acoustic conditions, spatial characteristics, and human responses [1–3]. Unlike environmental acoustics approaches that are primarily oriented toward noise control, soundscape studies also consider the meaning and appropriateness of different sound sources—including natural sounds, human activities, and mechanical or traffic sounds—within a specific place. Urban parks, waterfront green spaces, and wetland parks simultaneously support ecological conservation, recreation, and cultural interpretation; consequently, their acoustic environments are often characterized by multiple overlapping sound sources, pronounced temporal variability, and spatial heterogeneity. Evaluating such environments therefore benefits from combining objective measurements with perceptual assessment.

The Yellow River waterfront in Lanzhou forms a representative urban ecological corridor in arid Northwest China. Yintan Wetland Park, located on the north bank of the river, contains wetlands, open water, reed communities, urban roads, residential areas, and recreational facilities within a relatively compact spatial system. The park retains natural sounds such as flowing water, birdsong, and wind-driven vegetation, while also receiving persistent inputs from road traffic, visitor activity, and localized sound-amplification devices. Previous research has addressed soundscape perception, soundwalk methods, and soundscape evaluation in urban parks, wetland parks, and related recreational landscapes [4–9]. However, the composition, spatial differentiation, and user perception of soundscapes in large-river wetland parks in the arid Northwest remain comparatively underexplored. In practice, landscape design and management also tend to prioritize visual qualities over auditory experience, while acoustic management is often treated as post-hoc noise reduction rather than being coordinated with habitat conservation, recreational zoning, and place-based cultural expression.

Against this background, this study investigates Yintan Wetland Park through an analytical sequence of sound-source composition, spatial sound-level distribution, visitor perception, and planning response. The objectives are to: (1) identify the major sound sources and characterize their composition; (2) reveal spatial differences in A-weighted sound levels through multi-period field measurements and GIS interpolation; (3) describe visitor preferences for typical sound sources and their perceived congruence with the environment; and (4) identify priority intervention areas using a study-specific relative noise index and translate the combined physical and perceptual evidence into soundscape optimization strategies. Because the dataset is based on short-duration measurements at representative periods, the results are interpreted as comparative soundscape evidence rather than as a statutory environmental-noise compliance assessment.

2. Study area and methods

2.1. Study area

Yintan Wetland Park is located on the north bank of the Yellow River in Anning District, Lanzhou, and covers approximately 32.86 ha [10]. The park comprises open water, riparian flats, reed and wetland vegetation communities, pedestrian paths, and recreational nodes. Its surroundings include North Binhe Road, Yintan Yellow River Bridge, residential districts, and public activity spaces. The acoustic setting varies markedly across the park: areas close to the river, water bodies, and dense vegetation are dominated by flowing water, birdsong, and vegetation sounds; locations near roads and entrances are more strongly affected by traffic; and several plazas and recreational nodes are influenced by crowd activity and amplified sound during particular periods.

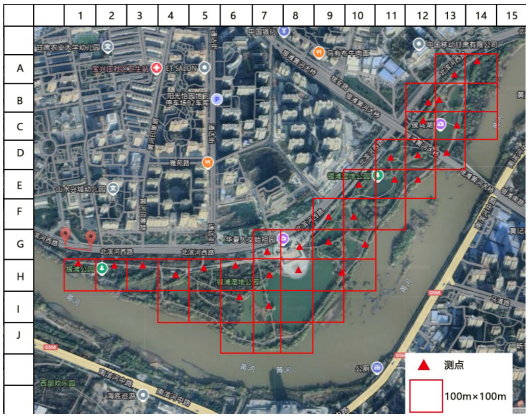

Figure 1. Sampling grid and distribution of sound-level measurement points in Yintan Wetland Park.

2.2. Sound-level measurements and spatial analysis

Field measurements were conducted with a TES-1350A sound level meter using A-weighting, with terminology referenced to the national sound-level-meter specification [11]. Measurement locations were arranged with reference to a 100 m × 100 m grid and adjusted according to the accessibility of roads, paths, and major landscape nodes; a total of 28 accessible locations were included in the final dataset. The survey was undertaken in May 2025 on both working and non-working days. At each location, measurements were collected during the morning (08:00–09:00), noon (12:00–13:00), and evening (19:00–20:00). Each measurement lasted 5 min with a sampling interval of 30 s. The instrument was positioned approximately 1.5 m above ground, and measurements were preferentially carried out under precipitation-free conditions with wind speeds not exceeding 3 m/s. Geographic coordinates were recorded in the WGS84 coordinate system.

Coordinates and A-weighted sound-level data for the three periods were imported into ArcGIS 10.8.1. Ordinary Kriging was used to interpolate continuous spatial surfaces for the study area. The interpolation maps were used to compare relative spatial patterns among areas and survey periods. They were not used to substitute for long-term monitoring or statutory assessment under environmental acoustic functional zoning and related standards [12,13].

2.3. Sound-source survey and questionnaire survey

Recognizable sound sources were recorded during field reconnaissance and grouped, according to source origin, into three study-specific categories: natural sounds, human-activity sounds, and mechanical/traffic sounds. This classification was adopted to describe the local soundscape composition and should not be interpreted as a formal source taxonomy prescribed by ISO 12913-1; the standard primarily establishes the definition of soundscape and its contextual perceptual framework [2].

The questionnaire survey was also conducted in May 2025. A total of 100 questionnaires were distributed to park visitors, nearby residents, and other users, of which 76 were valid, corresponding to a valid-response rate of 76%. A five-point Likert scale was used to assess preference for typical sound sources, perceived congruence between the soundscape and the surrounding environment, perceived disturbance from traffic and broadcast sounds, and recognition of sounds with local cultural characteristics. Because complete respondent-level records were unavailable for the present analysis, the questionnaire results are reported using descriptive statistics only; inferential tests, correlation coefficients, and regression estimates are therefore not presented.

2.4. Study-specific relative noise index

To compare the relative acoustic condition of the measurement locations, this study adopts a study-specific relative noise index (PN) as an internal comparative metric. Because the available data consist of short-duration measurements from three representative periods, the arithmetic mean of the three measured A-weighted sound levels was calculated as the representative value for each location. PN was calculated by dividing the representative A-weighted sound level at each location by 75 dB(A), which served as the reference value for this analysis. PN is used only for internal comparison among locations in this study and is not a statutory exceedance criterion. The classification scheme is shown in **Table 1**. Grades in the point-level results were assigned from unrounded PN values; displayed PN values are rounded to two decimal places.

Table 1. Classification of the study-specific relative noise index (PN)

Grade	Assessment	PN range	Representative sound-level range [dB(A)]
I	Very good	< 0.60	< 45.0
II	Good	0.60 to < 0.67	45.0 to < 50.25
III	Moderate	0.67 to < 0.75	50.25 to < 56.25
IV	Relatively poor	0.75–1.00	56.25–75.0
V	Poor	> 1.00	> 75.0

3. Results and analysis

3.1. Soundscape composition

The field survey identified 24 typical sound sources. By source origin, natural sounds accounted for 38%, human-activity sounds for 32%, and mechanical/traffic sounds for 30%. Natural sounds included egret calls, sounds from flocks of ruddy shelducks, frog calls, cicadas, insects in reed beds, Yellow River flow, reed rustling, and willow rustling. Human-activity sounds included quiet conversation, children playing, camera shutters, footsteps, and sounds generated by use of the wooden boardwalk. Mechanical/traffic sounds included motor vehicles along North Binhe Road and Yintan Yellow River Bridge, shared-bicycle notification sounds, broadcast/public-address sound, and drone noise. Overall, the park retains a diverse natural-sound resource, while traffic edges and several activity nodes interrupt the continuity of the natural soundscape. See **Table 2**.

Table 2. Typical sound sources identified in Yintan Wetland Park

Primary category	Secondary category	Typical sound sources
Natural sounds	Biological sounds	Egret calls; ruddy shelduck flock sounds; frog calls; cicadas; insects in reed beds
Natural sounds	Geophysical sounds	Yellow River flow; reed rustling; willow rustling
Human-activity sounds	Visitor activity	Quiet conversation; children playing; camera shutters; footsteps
Human-activity sounds	Facility-use sounds	Creaking of the wooden boardwalk and related use sounds
Mechanical/traffic sounds	Traffic and notification sounds	Motor vehicles; shared-bicycle notification sounds
Mechanical/traffic sounds	Equipment sounds	Broadcast/public-address sound; drone noise

3.2. Spatiotemporal distribution of A-weighted sound levels

Mean A-weighted sound levels across the 28 measurement locations differed among the three survey periods:

54.04 dB(A) in the morning, 51.71 dB(A) at noon, and 54.25 dB(A) in the evening. The noon period had the lowest overall mean, whereas localized evening activities produced several pronounced high-level locations. The measured ranges were 42–68 dB(A) in the morning, 42–66 dB(A) at noon, and 46–70 dB(A) in the evening.

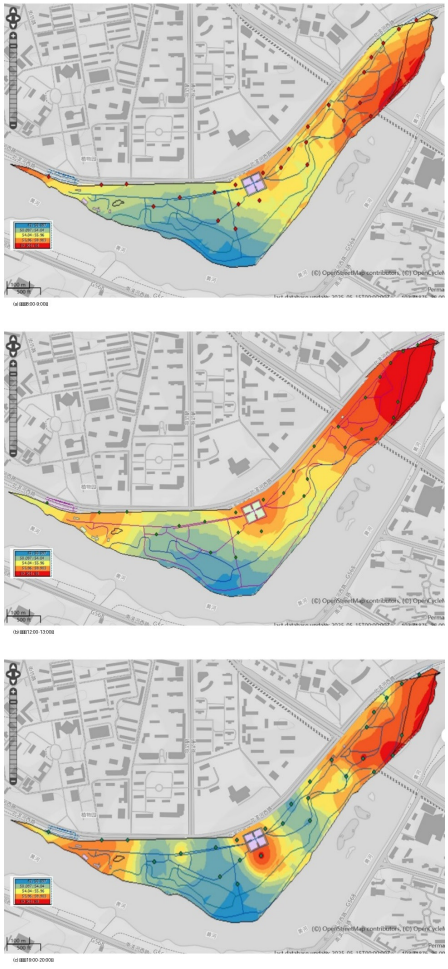

Figure 2. Spatial distribution of A-weighted sound levels in Yintan Wetland Park during (a) morning (08:00–09:00), (b) noon (12:00–13:00), and (c) evening (19:00–20:00).

Spatially, the northern and northeastern parts of the park adjacent to urban roads and the bridge consistently exhibited higher sound levels during all three periods, indicating that traffic is a relatively stable external acoustic disturbance. Interior areas closer to water bodies, denser vegetation, and less accessible spaces generally showed lower sound levels, where natural sounds were more readily perceptible. The highest morning value was 68 dB(A) and occurred near the traffic edge. The maximum decreased to 66 dB(A) at noon, while localized activity spaces reached 70 dB(A) in the evening. These patterns indicate that the park acoustic environment is shaped jointly by a stable traffic background and time-dependent recreational activity.

3.3. Characteristics of the relative noise index

The park-wide mean of the point-based representative sound levels was 53.33 dB(A), corresponding to a mean PN of 0.71 and Grade III under the study-specific classification. Among the 28 locations, 2 were

classified as Grade I, 5 as Grade II, 13 as Grade III, and 8 as Grade IV; no Grade V location was recorded. Grade IV locations were concentrated along traffic edges and at several nodes with pronounced activity-related disturbance, demonstrating that acoustic pressure is spatially clustered rather than uniformly distributed across the park.

For representative landscape areas recorded in the site survey, location 8H in Shizu Garden had a three-period mean of 61.67 dB(A) and a PN of approximately 0.82 (Grade IV). Location 13C near Migratory Bird Lake had a mean of 56.67 dB(A) and a PN of approximately 0.76 (Grade IV). By comparison, location 10G near Yuyue Lake had a mean of 48.00 dB(A) and a PN of 0.64 (Grade II), while location 6I near Waterfowl Lake had a mean of 45.33 dB(A) and a PN of approximately 0.60 (Grade II). These representative areas therefore span Grades II to IV, further illustrating the pronounced spatial heterogeneity of the park.

3.4. Visitor perception and integrated physical–perceptual analysis

The 76 valid questionnaires showed clear differences in visitor responses to sound sources. The five most preferred sound types were birdsong (4.15), wind in foliage (4.10), water waves (4.00), frog calls (3.85), and goose/duck calls (3.70). The least preferred sounds were construction activity (1.78), motor vehicles (2.05), and broadcast/public-address sound (2.20). These descriptive results indicate that natural sounds contribute positively to wetland recreation, whereas persistent or abrupt mechanical, traffic, and amplified sounds are more likely to be experienced negatively.

Comparison of the spatial sound-level patterns with the questionnaire results reveals a consistent directional relationship between the objective and subjective evidence. Traffic edges and localized amplified-activity areas appeared as high-level zones in the measurements, while motor-vehicle and broadcast sounds received low preference scores. Conversely, areas with more continuous water and vegetation generally had lower measured sound levels, and natural sounds such as birdsong, water, and wind-driven foliage received higher preference scores. Because complete individual-level questionnaire data and respondent-to-location matching are unavailable, this study does not infer statistical relationships such as a significant correlation between A-weighted sound level and preference, nor does it estimate a fixed change in preference for a specified increase in sound level. The results are therefore interpreted as descriptive convergence between physical and perceptual evidence.

4. Soundscape planning and optimization strategies

The combined findings suggest that soundscape improvement should not rely on uniform noise reduction across the entire park. Instead, design and management responses should correspond to the distinct acoustic roles of traffic edges, natural-sound cores, high-activity nodes, and culturally expressive spaces. The following strategies translate the measured spatial patterns and visitor perceptions into site-specific planning actions.

4.1. Establish acoustic buffers along traffic edges

Persistent traffic background sound along North Binhe Road and Yintan Yellow River Bridge indicates that the northern park edge should be prioritized for continuous multi-layered vegetation and microtopographic buffering. Existing locally adapted species such as tamarisk, reeds, and willows can be organized in combined tree–shrub–herb and wetland-plant layers to strengthen spatial enclosure and visual screening. Where hydrological and spatial conditions permit, gentle berms, low mounds, or sunken spaces may be used to increase propagation distance and provide additional separation from traffic. These measures should

be integrated with ecological-restoration objectives and should avoid high-maintenance or poorly adapted planting introduced solely for acoustic purposes [14].

4.2. Conserve low-level natural-sound core areas

In areas such as Waterfowl Lake and Yuyue Lake, where natural-sound resources are comparatively rich, management should shift from adding new sounds to protecting the audibility of existing ecological sounds. High-level facilities should be restricted, drone use and portable amplification should be controlled, and nighttime lighting and circulation routes should be managed to reduce disturbance to bird habitat and acoustically tranquil wetland areas. Birdwatching platforms, boardwalks, and pause points should be located where visitors can perceive water sounds, birdsong, and vegetation sounds without intruding into core habitats, allowing natural sound to function as an integral component of the recreational experience.

4.3. Apply temporal and spatial management to high-activity nodes

Shizu Garden, park entrances, and other activity-intensive nodes exhibit time-dependent increases in sound level. At these locations, activity scheduling, volume limits for amplified sound, and spatial zoning can reduce acoustic spillover into adjacent wetland areas. Fitness plazas and group-activity spaces should be separated from quiet recreation areas by adequate distance and vegetated buffers, while signage can define nighttime quiet periods. Temporal zoning, spatial separation, and directional control of sound are more compatible with everyday community use than blanket prohibition and can better balance recreational demand with wetland soundscape conservation.

4.4. Integrate place-specific cultural sounds with restraint

Yellow River culture can be interpreted acoustically through elements associated with waterwheels, local customs, and memories of riverside life, but cultural soundscape interventions should avoid becoming new sources of repetitive mechanical or broadcast disturbance. Priority should be given to authentic environmental sounds, small interactive sound installations, or low-volume, time-limited interpretive elements. These should be coordinated with water, vegetation, pedestrian routes, and interpretive systems so that cultural sound enriches place experience rather than functioning as continuous background noise.

4.5. Establish dynamic monitoring and feedback

Representative long-term monitoring locations should be established at traffic edges, core wetland habitats, major activity nodes, and quiet-experience areas to record seasonal and diurnal changes in A-weighted sound levels and dominant sound sources. Park managers can combine acoustic monitoring with visitor feedback, bird activity, and patterns of spatial use to create a recurring cycle of monitoring, identification, adjustment, and verification. Future studies should incorporate standardized soundwalks, event-based sound-source annotation, and perceptual survey procedures recommended in the ISO 12913 series to improve comparability across seasons and across parks.

5. Conclusions

Yintan Wetland Park contains a diverse soundscape in which 24 typical sound sources were identified. Natural sounds, human-activity sounds, and mechanical/traffic sounds accounted for 38%, 32%, and 30%, respectively. Natural sounds represent an important ecological and experiential asset, while road traffic and

localized amplified activities form the principal acoustic disturbances.

The 28 valid measurement locations exhibited marked spatiotemporal differences. Mean A-weighted sound levels were 54.04 dB(A) in the morning, 51.71 dB(A) at noon, and 54.25 dB(A) in the evening. Higher values were concentrated along traffic edges and at localized evening activity nodes, whereas areas with more continuous water and vegetation were generally quieter. The park-wide mean representative level was 53.33 dB(A), with a mean PN of 0.71. Twenty-one of the 28 locations fell within Grades III and IV, indicating that targeted treatment of traffic edges and activity nodes is more appropriate than uniform intervention across the park.

Visitors expressed stronger preferences for birdsong, wind in foliage, and water sounds, while construction, motor-vehicle, and broadcast sounds received lower ratings. Integrating the objective and subjective findings supports a soundscape optimization framework centered on traffic-edge buffering, conservation of natural-sound cores, temporal-spatial management of activity areas, restrained integration of cultural sounds, and dynamic monitoring. The study is limited by short-duration measurements, a single-season survey, and the absence of complete individual-level questionnaire data and respondent–location matching. Future research should therefore employ multi-season continuous monitoring, standardized soundwalk protocols, and respondent-level statistical analysis to test the observed physical–perceptual relationships more rigorously.

Disclosure statement

The author declares no conflict of interest.

References

[1] Schafer R, 1977, The Tuning of the World. New York: Knopf.

[2] International Organization for Standardization (ISO), 2014, ISO 12913-1:2014 Acoustics—Soundscape—Part 1: Definition and Conceptual Framework. Geneva: ISO.

[3] Axelsson Ö, Nilsson M, Berglund B, 2010, A Principal Components Model of Soundscape Perception. Journal of the Acoustical Society of America, 128(5): 2836–2846.

[4] Kang J, Schulte-Fortkamp B, 2016, Soundscape and the Built Environment. Boca Raton: CRC Press.

[5] Wang D, 2018, Soundscape Evaluation and Design Methods for Xixi National Wetland Park, thesis, Zhejiang Gongshang University.

[6] Zhao J, Yang S, Zhang L, 2017, Effects of Soundscape on Visual Aesthetic Perception. Urban Problems, 2017(4): 41–46 + 51.

[7] Lee H, Lim K, Garg S, 2019, A Case Study of Recording Soundwalk of Fushimi Inari Shrine in Kyoto, Japan Using Smartphone. International Journal of Environmental Science and Technology, 16: 1555–1564.

[8] Li J, 2019, Soundscape Evaluation of Riverside Parks in Shenyang, thesis, Shenyang Agricultural University.

[9] Wang L, Zhang H, Lu L, et al., 2014, Visitor Perceived Value in Wetland Parks: A Comparison of Xixi and Qinhu. Tourism Tribune, 29(6): 87–96.

[10] Yang X, Wang Y, 2025, Usage Conditions and Optimization Strategies of Lanzhou Yintan Wetland Park. Co-Operative Economy & Science, 2025(5): 179–182.

[11] General Administration of Quality Supervision, Inspection and Quarantine of the People's Republic of China, Standardization Administration of China, 2010, GB/T 3785.1—2010 Electroacoustics—Sound Level Meters—

Part 1: Specifications. Beijing: Standards Press of China.

[12] Ministry of Ecology and Environment of the People's Republic of China, General Administration of Quality Supervision, Inspection and Quarantine of the People's Republic of China, 2008, GB 3096—2008 Environmental Quality Standard for Noise. Beijing: China Environmental Science Press.

[13] General Administration of Quality Supervision, Inspection and Quarantine of the People's Republic of China, Standardization Administration of China, 2014, GB/T 15190—2014 Technical Specifications for Environmental Noise Functional Zoning. Beijing: Standards Press of China.

[14] Ding S, 2018, Landscape Planning for Urban Riverbanks Oriented Toward Ecological Restoration: A Case Study of the Comprehensive Landscape Improvement Plan for Both Banks of the Hun River in Shenyang. Urban Housing, 25(11): 78–80.

Publisher's note

Bio-Byword Scientific Publishing remains neutral with regard to jurisdictional claims in published maps and institutional affiliations.

Appendix A. A-Weighted Sound-Level Measurements

Table A1. Raw summary of A-weighted sound-level measurements for the three survey periods

Point	Longitude	Latitude	Morning [dB(A)]	Noon [dB(A)]	Evening [dB(A)]
1H	103.7089995	36.0857941	54	45	51
2H	103.7039508	36.0856968	56	55	58
3H	103.7056395	36.0856517	52	50	55
4H	103.7065911	36.0850722	46	42	46
5H	103.7089995	36.0856524	52	50	54
6H	103.7075479	36.0855072	48	46	48
6I	103.7095423	36.0846109	46	42	48
7G	103.7103111	36.0858711	55	52	55
7H	103.7105476	36.0852384	55	46	50
7I	103.7107733	36.0842631	42	44	46
8G	103.7123806	36.0860171	60	56	54
8H	103.7119451	36.0855569	62	58	65
9F	103.7134825	36.0874972	50	48	48
9G	103.7133158	36.0864391	55	50	51
10E	103.7145467	36.0880710	56	48	53
10F	103.7142779	36.0872728	56	50	54
10G	103.7143048	36.0865531	50	45	49
11D	103.7161591	36.0896687	54	58	56
11E	103.7158957	36.0882028	55	46	51
12B	103.7176076	36.0912726	58	60	57
12C	103.7171104	36.0906130	50	54	55
12D	103.7168766	36.0896219	64	60	64

Point	Longitude	Latitude	Morning [dB(A)]	Noon [dB(A)]	Evening [dB(A)]
12E	103.7162988	36.0890575	52	50	54
13A	103.7181423	36.0918694	54	56	58
13B	103.7180133	36.0914921	54	54	52
13C	103.7171104	36.0906130	56	55	59
13D	103.7158062	36.0897507	68	66	70
14A	103.7190291	36.0925382	53	62	58

Appendix B. Representative Sound Levels and PN Values

Table B1. Representative sound levels and study-specific relative noise index (PN) by measurement location

Point	Longitude	Latitude	Representative level [dB(A)]	PN	Grade
1H	103.7089995	36.0857941	50.00	0.67	II
2H	103.7039508	36.0856968	56.33	0.75	IV
3H	103.7056395	36.0856517	52.33	0.70	III
4H	103.7065911	36.0850722	44.67	0.60	I
5H	103.7089995	36.0856524	52.00	0.69	III
6H	103.7075479	36.0855072	47.33	0.63	II
6I	103.7095423	36.0846109	45.33	0.60	II
7G	103.7103111	36.0858711	54.00	0.72	III
7H	103.7105476	36.0852384	50.33	0.67	III
7I	103.7107733	36.0842631	44.00	0.59	I
8G	103.7123806	36.0860171	56.67	0.76	IV
8H	103.7119451	36.0855569	61.67	0.82	IV
9F	103.7134825	36.0874972	48.67	0.65	II
9G	103.7133158	36.0864391	52.00	0.69	III
10E	103.7145467	36.0880710	52.33	0.70	III
10F	103.7142779	36.0872728	53.33	0.71	III
10G	103.7143048	36.0865531	48.00	0.64	II
11D	103.7161591	36.0896687	56.00	0.75	III
11E	103.7158957	36.0882028	50.67	0.68	III
12B	103.7176076	36.0912726	58.33	0.78	IV
12C	103.7171104	36.0906130	53.00	0.71	III
12D	103.7168766	36.0896219	62.67	0.84	IV
12E	103.7162988	36.0890575	52.00	0.69	III
13A	103.7181423	36.0918694	56.00	0.75	III
13B	103.7180133	36.0914921	53.33	0.71	III
13C	103.7171104	36.0906130	56.67	0.76	IV
13D	103.7158062	36.0897507	68.00	0.91	IV
14A	103.7190291	36.0925382	57.67	0.77	IV
Mean			53.33	0.71	III

Journal of Architectural Research and Developmentn, 2026, Volume 10, Issue 5
https://bbwpublisher.com/journal/JARD
Online ISSN: 2208-3537
Print ISSN: 2208-3529

Soundscape Creation of the Lanzhou Yellow River Waterwheel Garden from the Perspective of Historical Soundscape Restoration

Yichao Sun

School of Architecture and Urban Planning, Lanzhou Jiaotong University, Lanzhou 730070, Gansu, China

Copyright: © 2026 Author(s). This is an open-access article distributed under the terms of the Creative Commons Attribution License (CC BY 4.0), permitting distribution and reproduction in any medium, provided the original work is cited.

Abstract: Against the backdrop of rapid urbanization, the protection of heritage soundscapes faces severe challenges. As a typical water-conservancy heritage site in northwestern China, the Lanzhou Yellow River Waterwheel Garden has witnessed a decline in place recognition as historical sound sources—such as the mechanical sounds of waterwheels and boatmen's work chants—have disappeared, and the sonic symbols that carry collective memory now confront a crisis of rupture. Current research on heritage soundscapes remains limited by insufficient attention to the cultural value of historical soundscapes and an overreliance on physical noise reduction in conservation methods. Taking the Lanzhou Yellow River Waterwheel Garden as its research object, this study employs documentary archaeology, oral history interviews, and acoustic measurement to uncover the elements of its historical soundscape and to diagnose the underlying causes of soundscape rupture, including the erasure of soundscapes in the physical environment, intergenerational gaps in cultural memory, and the absence of authenticity-maintenance mechanisms. The study proposes site-specific soundscape creation strategies and constructs a "soundscape–memory–space" model through low-tech interventions such as mortise-and-tenon transmission devices, pebble wind-chime arrays, and interactive soundscape node designs, thereby achieving the cultural translation of the historical soundscape and the restoration of the genius loci. This research offers a new pathway for the soundscape conservation of industrial heritage and provides a reference for the living inheritance of water-conservancy heritage in the Yellow River Basin.

Keywords: Soundscape creation; Yellow River Waterwheel Garden; Heritage conservation; Cultural memory; Low-tech intervention; Spatial narrative

Online publication: Oct 13, 2026

1. Introduction

As an important dimension of human environmental perception, the soundscape—a concept proposed in the 1960s—refers to "the acoustic environment as perceived, experienced, or understood by an individual, group, or community in a given context" [1]. In recent years, soundscape research has evolved from a purely acoustic discipline into an interdisciplinary field integrating architecture, anthropology, and environmental

psychology [2]. Against the backdrop of rapid urbanization, the soundscape conservation of historic spaces faces severe challenges. As a typical water-conservancy heritage site in northwestern China, the Lanzhou Yellow River Waterwheel Garden possesses historical soundscapes of pronounced regional character, such as the "creaking of waterwheels" and "raftmen's work chants", which are not only living testimonies of regional culture but also acoustic expressions of the symbiotic "human–water–technology" relationship [3]. However, with the encroachment of modern traffic noise and the decline of traditional cultural practices, the traditional soundscapes of the Yellow River Waterwheel Garden—the core carrier of Lanzhou's reputation as the "City of Waterwheels"—including the mechanical sounds of the waterwheels, the flow of the Yellow River, and folk antiphonal singing, are fading and have led to a decline in place recognition. These sonic symbols bearing collective memory now face a crisis of rupture.

The main limitations of current research on heritage soundscapes are as follows. First, most studies focus on optimizing the contemporary acoustic environment and pay insufficient attention to the cultural value of historical soundscapes [4]. Second, conservation methods for heritage and historical soundscapes tend to rely heavily on physical noise reduction, lacking an organic integration of technical measures with cultural narrative. This research gap leaves places such as the Yellow River Waterwheel Garden—which combine industrial heritage value with ecological landscape value—trapped in a dilemma of "prioritizing the material over the immaterial" in soundscape conservation and creation.

From the perspective of historical sound restoration, and guided by Norberg-Schulz's theory of genius loci and UNESCO's Convention for the Safeguarding of the Intangible Cultural Heritage, this paper constructs a systematic framework for soundscape creation in the Lanzhou Yellow River Waterwheel Garden [5,6]. The study addresses three core questions:

(1) How to uncover the historical soundscape elements of the Waterwheel Garden through documentary archaeology and oral history;
(2) How the modern noise environment affects the perception and transmission of historical soundscapes; and
(3) How restoration strategies can achieve the cultural translation of historical soundscapes. By integrating methods such as soundscape archaeology, acoustic measurement, and participatory design, this study aims to explore a new pathway for the soundscape conservation of industrial heritage.

2. Research object

This study takes the Yellow River Waterwheel Garden section in Chengguan District, Lanzhou, as its research object, focusing on the distinctive historical sonic environment formed by the waterwheel irrigation system since the Ming and Qing dynasties and on its contemporary rupture. The Waterwheel Garden is located in the western section of Binhe Road in Lanzhou, adjacent to Zhongshan Bridge to the east, the "Mother of the Yellow River" sculpture to the west, facing Baitashan (White Pagoda Hill) Park to the north and Baiyun (White Cloud) Temple to the south, making it an important node of the Yellow River Scenic Corridor. The history of the Lanzhou Waterwheel Garden can be traced back to the Jiajing reign of the Ming dynasty (1556), when Duan Xu, a jinshi degree holder from Lanzhou, created the waterwheel by adapting the noria (bamboo-tube waterwheel) technology of Yunnan. Drawing on the hydrological characteristics of the Yellow River, Duan Xu refined the design, and the first waterwheel was erected on the north bank of the Yellow River outside Guangwu Gate for farmland irrigation, giving rise to the place name "Waterwheel Garden". By the late Qing dynasty, waterwheels stood in large numbers along both banks of the Yellow River, reaching 157 wheels; at their peak in 1952, the number increased to 252 wheels, irrigating an area of 100,000 mu

(approximately 6,667 hectares), which earned Lanzhou the reputation of the "City of Waterwheels". After the 1950s, electric irrigation gradually replaced the traditional waterwheels, and the waterwheels disappeared. In 1994, to protect the cultural heritage, the Lanzhou municipal government rebuilt the Waterwheel Garden in the western section of Binhe Road and restored a pair of antique waterwheels. As shown in Figure 1, creating a cultural landscape integrating exhibition, tourism, and education. As the largest and most complete traditional waterwheel settlement extant in northwestern China, this riverside site not only carries the material production memory of "the creaking of waterwheels answered by the chorus of work chants" but also embodies the technical wisdom and ecological philosophy of "the joint force of nature and humankind" in the agrarian civilization of the Yellow River.

The existing waterwheel in the garden measures 16.5 m in diameter and is composed of a wooden mortise-and-tenon structure fastened without a single iron nail, demonstrating the exquisiteness of traditional craftsmanship. Its operation relies on the kinetic force of the Yellow River's flow: during high-water seasons it is driven naturally, while in low-water seasons water is diverted and impounded by cofferdams; the buckets scoop up water and channel it through wooden troughs into the farmland, with a single wheel capable of irrigating up to 300 mu (20 hectares) per day. The functional zoning of the Waterwheel Garden comprises three main parts. The core exhibition area, centered on the twin waterwheels and supplemented by facilities such as a water-powered mill and cofferdams, reproduces the traditional irrigation scene. The cultural experience area includes a teahouse, a photography studio, and a folk-custom museum, enhancing the interactivity of visits through folk activities. The ecological landscape area consists of silt-deposited alluvial islands along the Yellow River and willow-shaded flats, complemented by landscape trails; the sections adjacent to urban traffic are planted with native vegetation such as Chinese willow (*Salix matsudana*) and tamarisk, forming a natural soundscape buffer zone.

By excavating the immaterial historical soundscape, this study addresses issues such as the coverage of historical sounds by traffic noise in contemporary urbanization and the cognitive gap regarding soundscapes among younger generations, exploring the feasibility of restoring the genius loci through low-tech soundscape installations. This study not only opens a new dimension for the living conservation of heritage but also constitutes a site-specific experiment in the revitalization of Lanzhou's heritage.



Figure 1. Actual shooting of waterwheels in Lanzhou Waterwheel Garden.

3. Research methods

3.1. Documentary archaeology and oral history interviews

Historical records of the Waterwheel Garden's soundscape from the Ming and Qing dynasties to the Republican period were sorted out through ancient texts such as the *Annals of Lanzhou Prefecture* and the *Illustrated Investigation of Yellow River Water Transport*, from which core soundscape symbols—including "the creaking of waterwheels", "raftmen's work chants", and "market clapper sounds"—were extracted [7,8]. Questionnaires were administered to randomly selected elderly Lanzhou residents to record the keywords of their soundscape memories. Interviews were conducted with intangible cultural heritage inheritors of high professional competence and relevant professionals to collect their opinions on the effectiveness of soundscape creation strategies, from the perspective of historical sound restoration, in the living transmission of traditional skills.

3.2. Stratified questionnaire survey on restoration effectiveness

Questionnaires were designed for different groups, including elderly Lanzhou residents and tourists, to investigate issues such as the historical authenticity of the soundscape, from the initial extraction of soundscape elements to the evaluation of post-creation outcomes.

4. Composition and rupture of the historical soundscape of the waterwheel garden

4.1. Excavating historical soundscape elements

Historical soundscape elements mainly comprise material sound sources and symbolic soundscapes. Material sound sources include, but are not limited to, the creaking of Ming-Qing waterwheels, boatmen's work chants at the ferry, and the human voices of the market; symbolic soundscapes refer to the sounds of bells and drums in sacrificial activities and the sounds of festival folk customs.

Material sound sources are centered on the mechanical sounds of the waterwheel, whose acoustic characteristics can be deduced from ancient texts and physical remains. The *Annals of Lanzhou Prefecture* (Water Conservancy Section) records that "the water impels the wheel, and its creaking never ceases day or night" [7]. Combined with the illustrated descriptions of wooden waterwheel construction in *Tiangong Kaiwu*, it is inferred that the gear-meshing sounds are concentrated in the 200–500 Hz frequency range, with sound pressure levels of approximately 65–72 dB(A) [9].

Boatmen's work chants at the ferry constitute another core soundscape element. Described in the *History of Yellow River Water Transport* as "voices that pierce the turbid waves and harmonize with the water's rhythm", spectrographic analysis of extant recordings of Tao River work chants shows that their fundamental frequency remains stable at 220 Hz ±10%, and their rhythmic patterns are positively correlated with variations in the flow velocity of the Yellow River [10].

Market human voices map spatial vitality through soundscape density. The acoustic scene recorded in the Qing-dynasty *Annals of Gaolan County* as "the clamorous cries of peddlers and laborers" can be spatially reconstructed using the density of shop distribution at the historical wharf site (approximately 12 shops per 100 m) and a sound pressure level attenuation model (6 dB per 10 m) [3].

In addition to the element extraction from the literature, the questionnaire survey of Lanzhou residents also showed that the sound of the Yellow River's flow (75%), the sound of waterwheel operation (81%), and boatmen's work chants (48%) are widely recognized as the core soundscape symbols of Lanzhou's Yellow

River culture.

Because the constitution of symbolic soundscapes is closely tied to the local folk-cultural system, and because the Waterwheel Garden as the research object possesses prominent material sound-source characteristics, this study does not discuss symbolic soundscapes in detail.

4.2. The underlying causes of soundscape rupture

The soundscape rupture of the Lanzhou Yellow River Waterwheel Garden results from multiple dimensions of influence, as manifested in the following

4.2.1. The erasure of soundscapes in the physical environment

As the core element of the historical soundscape, the authenticity of the waterwheel's mechanical sound has been severely compromised by the cessation of the waterwheels. According to field measurements conducted in 2023, the equivalent sound level of the extant antique waterwheel is only 52.1 dB(A), a 24% reduction from the 68.5 dB(A) documented in historical records. Traffic noise from North Binhe Road (peak 79.5 dB(A)) exerts a significant masking effect in the 500–1000 Hz frequency band, which will inevitably reduce tourists' accuracy in recognizing the waterwheel sound. The impact of traffic noise was also prominent in the questionnaire survey: 75% of respondents were deeply impressed by traffic noise, and 61% mentioned the clamor of visitors, further corroborating the masking effect of North Binhe Road traffic noise (peak 79.5 dB(A)) and visitor activity sounds (peak 68.5 dB(A)) on the historical soundscape.

Meanwhile, the alienation of the spatial structure of the soundscape has exacerbated this phenomenon: the current layout of the riverside trails diverts the visitor route 200 m away from the axis of the historical wharf, breaking the interconnected soundscape system of waterwheel sounds and work chants and making it difficult for visitors to experience a complete and authentic soundscape during their tour.

4.2.2. Intergenerational gaps in cultural memory

In the oral history interviews, the recognition accuracy of historical soundscapes among the group aged over 70 (82%) was significantly higher than that of younger groups (17%). The questionnaire survey further verified this disparity: among respondents over 51, 68% could clearly describe the historical soundscape features of the Waterwheel Garden, whereas only 12% of the 18–30 age group chose "fairly familiar". The intergenerational gap is especially evident in the recognition of "boatmen's work chants" (82% in the older group vs. 23% in the younger group), reflecting the rupture of the traditional soundscape memory chain.

4.2.3. The absence of authenticity-maintenance mechanisms

Soundscape conservation lacks an interdisciplinary coordination mechanism. Existing restoration strategies rely mostly on single technical measures such as noise barriers (with a noise reduction of 4.2 dB) and audio playback, neglecting the cultural-contextual associations of soundscape elements. The value of the historical soundscape lies not only in the transmission of physical sound waves but also in its social function as a "cultural resonator": the intensity variations of sacrificial drum-and-music sounds (from 58 dB(A) at the opening of rituals to 82 dB(A) at their climax) correspond to the ebb and flow of collective emotion, and the spatiotemporal distribution of the market soundscape (with a peak sound pressure level of 68 dB(A) at the *chen* hour, i.e., 7:00–9:00 a.m.) reflects the exchange networks of agrarian society [11]. When modern

interventions strip away these associative dimensions, the soundscape degenerates into a museumified sound specimen, losing its agency to activate collective memory.

5. Soundscape creation strategies based on the regeneration of waterwheel power

5.1. The site-specificity of soundscape creation

The site-specificity of soundscape creation is mainly manifested in the following aspects.

(1) Minimal intervention

The purely mechanical transmission structure of the traditional waterwheel is retained, and the soundscape installations are driven through reversible mortise-and-tenon connections, ensuring that all restoration measures are reversible and non-destructive to the heritage itself [12].

(2) Material authenticity

Local materials such as Yellow River pebbles (10–20 cm in particle size), rammed earth (red clay with an 18% moisture content), and elm wood (density 0.68 g/cm³) are adopted to form a material dialogue with the texture of the historic environment, avoiding the erosion of the site's historicity by modern materials [13].

(3) Living transmission

Oral history collection and audio archiving are carried out with the extant inheritors of boatmen's work chants; the recording process follows the ethical norms of the *Convention for the Safeguarding of the Intangible Cultural Heritage* and preserves the socio-contextual information of the soundscape (e.g., the usage scenarios of the chants and the roles of participants) [6]. A blockchain-based soundscape database is established to achieve tamper-proof storage of cultural memory, providing sustainable resources for dynamic conservation [14].

In response to the traffic noise problem raised by 75% of respondents, the restoration strategy prioritizes Chinese willow belts and soundscape zoning design over fully enclosed noise barriers, so as to preserve the openness of the site and its compatibility with the historic fabric.

5.2. Cultural memory-based translation of soundscape symbols

The restoration of the Waterwheel Garden's soundscape should take the "authenticity" and "integrity" of cultural heritage as its core principles [15]. In terms of translation strategy, the principle of "low-tech intervention" is adopted: modified waterwheel mechanisms can drive wooden clappers, using traditional mortise-and-tenon craftsmanship to simulate the historical percussive rhythms, thereby avoiding the damage that electrical systems would cause to the integrity of the heritage itself. Meanwhile, arrays of Yellow River pebble wind chime metaphorically evoke hydrological rhythms, and the random colliding sounds of natural materials awaken the agrarian civilization's perception of time, elevating soundscape restoration from a technical issue to the reproduction of cultural meaning [16].

5.3. Spatial narrative and the revitalization of heritage value

The spatial organization of the soundscape should respond to the genius loci of the Waterwheel Garden as an industrial heritage site [17]. Along the historical axis of the waterwheels, a three-tier narrative sequence of "production–ecology–faith" is constructed. In the production zone, the mechanical sounds of the waterwheels form the core, while Chinese willow belts—plants documented in historical records as windbreaks and sand stabilizers—create a soundscape buffer zone, sustaining the traditional "waterwheel–vegetation" ecological

association while reducing noise. In the ecological zone, the superimposition of pebble wind chimes and the sound of the Yellow River's flow reconstructs a dynamic "soundscape–nature" dialogue. In the faith zone, interactive installations such as pedal-triggered chant players activate the ritual soundscape, with their spatial positioning strictly following the positional coordinates of the historical wharf site, ensuring the spatial isomorphism between soundscape events and material remains [2]. This linear narrative is not merely a reproduction of historical functions; through visitors' participatory experience, it realizes the "embodied transmission" of cultural heritage—by designing correlations between bodily actions and soundscape responses, such as sound pressure levels increasing with the number of participants, abstract cultural memory is transformed into perceptible place-based practice [18].

The questionnaire survey showed that 68% of respondents supported recreating the historical soundscape through soundscape installations, and the preference rate for interactive installations among the 18–30 age group reached 82%. On this basis, a "soundscape–memory–space" model—embodied in a "soundscape memory cabin at the waterwheel viewing platform"—can be designed to activate the soundscape. It employs mortise-and-tenon interactive installations (72% support) combined with visual symbols (58%) to enhance visitors' experience, effectively helping younger generations associate bodily memory with soundscape impressions.

6. Conclusion and outlook

This study systematically explored the compositional characteristics, the underlying causes of rupture, and the restoration strategies of the historical soundscape of the Lanzhou Yellow River Waterwheel Garden. The findings reveal that the historical soundscape system of the Waterwheel Garden faces multiple challenges, including traffic noise masking, intergenerational cognitive gaps, and the absence of authenticity-maintenance mechanisms. Through site-specific soundscape creation strategies—including mortise-and-tenon transmission devices, pebble wind-chime arrays, and interactive soundscape node designs—the feasibility of "low-tech intervention" in industrial heritage conservation has been verified. The "soundscape–memory–space" model constructed in this study provides a new paradigm for historical soundscape restoration that carries both academic value and practical significance.

Future research will be deepened in the following aspects. First, data dimensions will be expanded by incorporating EEG technology and seasonal acoustic monitoring to enhance research depth. Second, the ArcGIS platform will be introduced: spatial analysis tools will be used to quantify the distribution characteristics of the soundscape, a spatiotemporal soundscape database will be established, spatial interpolation will be applied to generate noise contour maps for the precise identification of soundscape rupture zones, and historical map registration will be combined to achieve the visualized presentation of soundscape change. Subsequent research will further improve the precision of soundscape restoration proposals and provide more scientific technical support for the conservation of water-conservancy heritage in the Yellow River Basin.

The theoretical framework and methods of this study can be extended to the conservation of other water-conservancy heritage in the Yellow River Basin, offering an important reference for the living inheritance of cultural heritage amid rapid urbanization. Soundscape restoration is not merely a technical practice but a cultural reconstruction process that reconnects the past and the present through the medium of sound; its social value and humanistic connotations call for continued exploration through interdisciplinary collaboration.

Disclosure statement

The author declares no conflict of interest.

References

[1] Schafer R, 1996, The Soundscape: Our Sonic Environment and the Tuning of the World. Zhurnal Vyssh Nervnoi Datel Nosti Imeni I P Pavlova, 38(3): 569–570.

[2] Meng X, Wu X, 2024, Soundscape Evaluation and Design Strategies for Parks Along Urban Railway Corridors: A Case Study of the Beijing Central Urban Section of the Beijing–Qinhuangdao Railway. Applied Acoustics, 43(4): 900–911.

[3] Li B, 2008, A Historical-Geographical Study of the Waterwheel Culture in Lanzhou. Dunhuang Research, 2008(4): 78–84.

[4] Kang J, Li G, 2015, A Review of Soundscape Research in Urban Public Spaces. Architectural Journal, 2015(S1): 1–6.

[5] Norberg-Schulz C, 1980, Genius Loci: Towards a Phenomenology of Architecture. New York: Rizzoli.

[6] UNESCO, 2003, Convention for the Safeguarding of the Intangible Cultural Heritage.

[7] Editorial Committee of the Collection of Chinese Local Gazetteers, 2009, Collection of Chinese Local Gazetteers: Prefecture and County Gazetteers of Gansu (Volume 1): Lanzhou Prefecture Gazetteer of the Daoguang Reign. Beijing: National Library of China Publishing House.

[8] Anon, An Illustrated Study of Water Transport on the Yellow River. Hand-Painted Manuscript of the Qing Dynasty.

[9] Kang J, Zhang X, 2021, Archaeology and Reconstruction of Traditional Chinese Mechanical Soundscapes. Architectural Journal, 2021(3): 45–51.

[10] Zhou J, 1995, Collection of Chinese Folk Songs: Gansu Volume. Beijing: China ISBN Center: 203–205.

[11] Wu S, 2000, Principles of Architectural Acoustics Design. Beijing: China Architecture & Building Press: 67–69.

[12] ICOMOS China, 2015, Principles for the Conservation of Heritage Sites in China.

[13] Wang S, 2012, Fictional City. Beijing: SDX Joint Publishing Company.

[14] UNESCO, 2021, Recommendation on Historic Urban Landscape.

[15] ICOMOS, 1964, Venice Charter.

[16] Connerton P, 1989, How Societies Remember. Cambridge: Cambridge University Press.

[17] Norberg-Schulz C, 1980, Genius Loci: Towards a Phenomenology of Architecture. New York: Rizzoli.

[18] Pallasmaa J, 2005, The Eyes of the Skin: Architecture and the Senses. London: Wiley.

Appendix: Survey Questionnaire

(1) Your age: □ Under 18□ 18–30□ 31–50□ Over 51

(2) Your relationship with the Lanzhou Waterwheel Garden: □ Local resident□ Tourist□ Researcher/Student□ Other

(3) Are you aware of the historical sounds that once existed in the Waterwheel Garden (e.g., boatmen's work chants, the sound of the water-powered mill)? □ Completely unaware□ Vaguely heard of□ Fairly familiar□ Very familiar

(4) Which of the following sounds do you think best represent Lanzhou's Yellow River culture? (Multiple

choice) □ Sound of the Yellow River's flow□ Sound of waterwheel operation□ Traditional folk songs/ work chants□ Market voices□ Sacrificial bell and drum sounds□ Other_____

(5) Which sounds in the current environment of the Waterwheel Garden impress you most? (Multiple choice) □ Traffic noise□ Visitor clamor□ Natural flowing water□ Modern music broadcasting□ Almost no particular impression

(6) Do you think the sounds in the current environment help you understand the waterwheel culture? □ Not at all□ Not really□ Neutral□ Somewhat□ Very much

(7) If the historical soundscape were recreated through installations (e.g., waterwheel-driven wooden clappers simulating the rhythm of work chants), how would you evaluate such designs? □ Enhances historical immersion□ Interferes with the current environment□ Neither here nor there□ Other_____

(8) In what form would you prefer the soundscape installations to appear? (Multiple choice) □ Interactive installations (e.g., pedal-triggered sounds) □ Background soundscape (continuously playing historical sounds) □ Combined with visual symbols (e.g., modified waterwheel components) □ Other_____

(For elderly Lanzhou residents)

(9) Are you satisfied with the sound environment of the Waterwheel Garden after restoration? □ Very satisfied (faithfully restores the historical atmosphere and evokes strong memories)□ Satisfied (the historical soundscape is perceptible, but some details are insufficient)□ Neutral (improved but below expectations)□ Dissatisfied (differs greatly from the sound environment in my memory)□ Other suggesti ons:_____

(For relevant intangible cultural heritage inheritors)

(10) How effective do you think the soundscape restoration project is for the living transmission of traditional skills? □ Very effective (the soundscape accurately translates the culture of the craft and draws the attention of younger generations)□ Effective (some soundscape symbols match the characteristics of the craft, but details need to be deepened)□ Neutral (formalistic presentation that fails to reflect the core value of the craft)□ Ineffective (the soundscape design is disconnected from the culture of the craft)□ Other suggestions:_____

Integrated Services Platform of International Scientific Cooperation

Innoscience Research (Malaysia), which is global market oriented, was founded in 2016.Innoscience Research focuses on services based on scientific research. By cooperating with universities and scientific institutes all over the world, it performs medical researches to benefit human beings and promotes the interdisciplinary and international exchanges among researchers.

Innoscience Research covers biology, chemistry, physics and many other disciplines. It mainly focuses on the improvement of human health. It aims to promote the cooperation, exploration and exchange among researchers from different countries. By establishing platforms, Innoscience integrates the demands from different fields to realize the combination of clinical research and basic research and to accelerate and deepen the international scientific cooperation.

Cooperation Mode



Clinical Workers



In-service Doctors



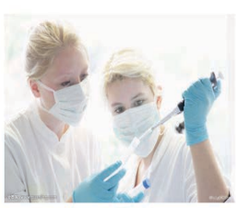

Foreign Researchers

China Collaborators



Oversea Collaborators



Hospital



University



Scientific institutions

Our Journals



The *Journal of Architectural Research and Development* is an international peer-reviewed and open access journal which is devoted to establish a bridge between theory and practice in the fields of architectural and design research, urban planning and built environment research.

Topics covered but not limited to:

- Architectural design
- Architectural technology, including new technologies and energy saving technologies
- Architectural practice
- Urban planning
- Impacts of architecture on environment

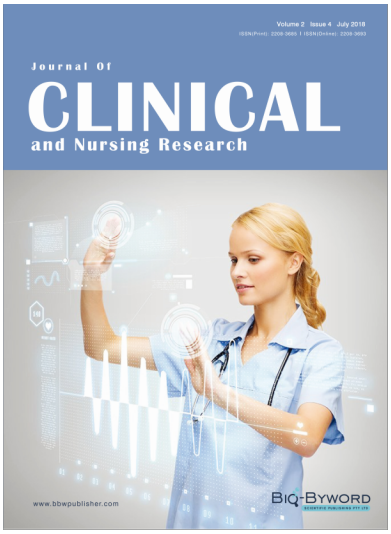

Journal of Clinical and Nursing Research (JCNR) is an international, peer reviewed and open access journal that seeks to promote the development and exchange of knowledge which is directly relevant to all clinical and nursing research and practice. Articles which explore the meaning, prevention, treatment, outcome and impact of a high standard clinical and nursing practice and discipline are encouraged to be submitted as original article, review, case report, short communication and letters.

Topics covered by not limited to:

- Development of clinical and nursing research, evaluation, evidence-based practice and scientific enquiry
- Patients and family experiences of health care
- Clinical and nursing research to enhance patient safety and reduce harm to patients
- Ethics
- Clinical and Nursing history
- Medicine



Journal of Electronic Research and Application is an international, peer-reviewed and open access journal which publishes original articles, reviews, short communications, case studies and letters in the field of electronic research and application.

Topics covered but not limited to:

- Automation
- Circuit Analysis and Application
- Electric and Electronic Measurement Systems
- Electrical Engineering
- Electronic Materials
- Electronics and Communications Engineering
- Power Systems and Power Electronics
- Signal Processing
- Telecommunications Engineering
- Wireless and Mobile Communication